الجمهورية الجزائرية الديمقراطية الشعبية
République Algérienne Démocratique et Populaire
وزارة التعليم العالي و البحث العلمي
Ministère de l'Enseignement Supérieur et de la Recherche Scientifique

Université Mohamed Khider – Biskra
Faculté des Sciences et de la Technologie
Département : Génie Mécanique
Ref : ……

جامـعة محمد خيضر - بسكرة
كليـة العلـوم والتكنـولوجيا
قسم : الهندسة الميكـانيكية
المرجع : .....

Thèse Présentée en vue de l'obtention du diplôme de

Doctorat LMD en Génie Mécanique

Spécialité : Construction Mécanique

Évaluation du confort thermique dans des constructions isolées thermiquement par différents types de matériaux

Présentée par :

Houssam eddine BENCHOUIA

Soutenue publiquement le 06/06/2024

Pr. Noureddine Moummi	**Professeur**	**Président**	**Université de Biskra**
Pr. Belhi GUERIRA	**Professeur**	**Rapporteur**	**Université de Biskra**
Pr. Noureddine Belghar	**Professeur**	**Examinateur**	**Université de Khenchela**
Dr. Youcef DJEBLOUN	**MCA**	**Examinateur**	**Université de Biskra**
Dr. Hefaidh HADEF	**MCA**	**Examinateur**	**Université de Biskra**

People's Democratic Republic of Algeria
Ministry of Higher Education and Scientific Research
Mohamed Khider University of Biskra
Faculty of Sciences and Thechnology
Department of Mechanical Engineering

Order Number: .....

Devant le jury composé de :

THESIS

In Candidacy for the Degree of

DOCTOR 3rd CYCLE IN MECHANICAL ENGINEERING

Option: Mechanical construction

TITLE

Evaluation of thermal comfort in constructions thermally insulated by different types of materials

Presented by **Houssam Eddine BENCHOUIA**

Defended on: 06/06/2024

In front of the jury composed of:

Pr. Noureddine Moummi	**Professor**	**Presedent**	**Université de Biskra**
Pr. Belhi GUERIRA	**Professor**	**Supervisor**	**Université de Biskra**
Pr. Noureddine Belghar	**Professor**	**Examiner**	**Université de Khenchela**
Dr. Youcef DJEBLOUN	**MCA**	**Examiner**	**Université de Biskra**
Dr. Hefaidh HADEF	**MCA**	**Examiner**	**Université de Biskra**

ACKNOWLEDGMENTS

This research was conducted in the mechanical engineering laboratory (LGM) at the University of Mohamed Khider-Biskra. I want to thank all those who contributed to the success of this thesis.

First, I would like to thank my thesis supervisor, Pr. Belhi GUERIRA, for welcoming me into his team and supporting me in completing this thesis. I benefitted from a serious, attentive, and humorous supervisor. I'm very grateful to him for trusting me and allowing me to complete this thesis peacefully.

I want to express my gratitude to Pr. Cristina TEDESCHI was often available to listen and discuss with me and welcomed me into her laboratory during my Erasmus stay in Italy.

Many thanks to Pr. Lakhdar SEDIRA and Dr. Hamida BOUSSEHEL, for their advice and comments, made me think and progress in many aspects. Working with them was a pleasure, and I benefited greatly from their advice.

My thanks also go to Pr. Noureddine MOUMMI, who did me the honor of chairing my thesis jury, and Pr. Noureddine BELGHAR, Dr.Youcef DJEBLOUN and Dr. Hefaidh HADEF, thank you for agreeing to participate in the jury and suggesting many tips and avenues of thought.

I want to thank the staff of the LGM and the Technological Hall at the University of Biskra, the CNERIB, and the PTAPC EL HADJEB laboratories, who enabled me to carry out the experimental part of this thesis under excellent conditions.

I take this opportunity to express my heartfelt thanks to the most precious people dear to me, my mother and father, for their generosity and everything they have given me.

I want to express my sympathy and affection to my family (BENCHOUIA and BENZINE) and friends. I want to thank all those who came to my defense and helped prepare the reception, especially Youcef and Idriss.

To the spirit of my uncles Abd Hamid and Lazhari...

ABSTRACT

This study aims to develop and characterize innovative biocomposite materials using waste plant compounds and commonly found wastes in Algeria for effective thermal insulation in civil and mechanical engineering applications. The goal is to create materials with mechanical and thermo-physical properties equal to or surpassing those of traditional construction materials, thereby reducing environmental impact and construction costs while promoting sustainable waste management practices.

In the first place, Date palm leaflet waste (DPF) is used as reinforcement, and melting polystyrene (PS) is used as a matrix. Three categories of fibers, untreated fiber (UDPF), alkalinized fiber (ADPF), and benzoylated fiber (BDPF), are employed to create samples with fillers of 10%, 20%, and 30% (by weight). The composites were produced using the melt-mixing method and hot compression molding. In this study, various morphological, mechanical, and thermophysical tests were conducted on the composites to assess their potential as thermal insulators. The bulk density, pore size, and distribution of the fibers and composite were assessed using the Mercury Intrusion Pore Measurement method (MIP). Tensile and three-point bending tests were performed using a traction machine type INSTRON 5969. The thermal conductivity was measured using a CT-meter device. Results show that Alkalinization and benzoylation treatments improved the interfacial interaction between the hydrophilic fibers and the hydrophobic polystyrene, as confirmed by SEM and FTIR analyses. XRD studies indicated the highest crystallinity index for ADPF. The results of PS-DPF composites demonstrated satisfactory tensile and flexural strength of 14–44 MPa, The chemical treatments enhanced strength while slightly decreasing modulus (2.9–5.9 GPa). Thermogravimetric analysis revealed increased thermal stability for composites with 30% untreated and treated fibers. These composites exhibited low thermal conductivity (0.118–0.141 W/ (m.K)) and decreased bulk density after incorporation fibers (860 -980 kg/m3). Replacing one-third of conventional building materials with PS-DPF composites showed a reduction in thermal conductivity by up to 50%, highlighting their potential in thermal insulation applications.

The second research endeavor explores the valorization of common wastes—date palm petiole fibers (DPP) and expanded polystyrene waste (EPS)—to elaborate a gypsum plaster hybrid biocomposite. Hand-made samples with varying DPP mass loadings (0%, 5%, 10%, and 15%), EPS mass ratios (0.3%), or both were examined through morphological, mechanical, and thermophysical tests. Despite a reduction in mechanical properties, the hybrid biocomposites exhibited lower thermal conductivity of 0.2645-0.425 W/ (m.K) and bulk density of 852-977 kg/m3 compared to neat gypsum plaster (NGP). The study positions gypsum plaster reinforced with DPP, EPS, or both as a potential alternative to traditional insulation materials, offering a sustainable solution for construction purposes.

Keywords: biocomposite material, Date palm waste, Polystyrene, Gypsum plaster, Mechanical properties, Thermophysical properties, Insulating materials.

RÉSUMÉ

Cette étude vise à développer et à caractériser des matériaux biocomposites innovants utilisant des composés de déchets végétaux et des déchets couramment trouvés en Algérie pour une isolation thermique efficace dans les applications de génie civil et mécanique. L'objectif est de créer des matériaux ayant des propriétés mécaniques et thermophysiques égales ou supérieures à celles des matériaux de construction traditionnels, réduisant ainsi l'impact sur l'environnement et les coûts de construction tout en promouvant des pratiques de gestion durable des déchets.

En premier lieu, les déchets de feuillets de palmier dattier ont utilisés comme renfort, et le polystyrène fondu (PS) comme matrice. Trois catégories de fibres, les fibres non traitées (UDPF), les fibres alcalinisées (ADPF) et les fibres benzoylées (BDPF), sont utilisées pour fabriquer des échantillons avec des charges de 10 %, 20 % et 30 % (en poids). Les composites ont été produits en utilisant la méthode de mélange par fusion et le moulage par compression à chaud. Dans cette étude, divers tests morphologiques, mécaniques et thermophysiques ont été effectués sur les composites afin d'évaluer leur potentiel en tant qu'isolants thermiques. La densité apparente, la taille et la distribution des pores des fibres et du composite ont été évaluées à l'aide de la méthode de mesure des pores par intrusion de mercure (MIP). Des essais de traction et de flexion en trois points ont été réalisés à l'aide d'une machine de traction de type INSTRON 5969. La conductivité thermique a été mesurée à l'aide d'un appareil CT-meter. Les résultats montrent que les traitements d'alcalinisation et de benzoylation améliorent l'interaction interfaciale entre les fibres hydrophiles et le polystyrène hydrophobe, comme le confirment les analyses MEB et FTIR. Les études XRD ont indiqué l'indice de cristallinité le plus élevé pour l'ADPF. Les résultats des composites PS-DPF ont montré une résistance à la traction et à la flexion satisfaisante de 14-44 MPa, les traitements chimiques améliorant la résistance tout en diminuant légèrement le module d'élasticité (2,9-5,9 GPa). L'analyse thermogravimétrique a révélé une stabilité thermique accrue pour le composite contenant 30 % de fibres non traitées et traitées. Ces composites présentent une faible conductivité thermique (0,118-0,141 W/(m.K)) et une densité apparente réduite après l'incorporation de fibres (860 - 980 kg/m^3). Le remplacement d'un tiers des matériaux de construction conventionnels par des composites PS-DPF a montré une réduction de la conductivité thermique allant jusqu'à 50 %, soulignant leur potentiel dans les applications d'isolation thermique.

Le deuxième matériau étudié explore la valorisation de déchets communs - fibres de pétiole de palmier dattier (DPP) et déchets de polystyrène expansé (EPS) - pour créer un biocomposite hybride à base de plâtre. Des échantillons fabriqués à la main avec différentes charges massiques de DPP (0 %, 5 %, 10 % et 15 %), de ratio massique constant d'EPS (0,3 %) ou les deux ont été examinés par des tests morphologiques, mécaniques et thermophysiques. Malgré une réduction des propriétés mécaniques, les biocomposites hybrides ont présenté une conductivité thermique inférieure de 0,2645-0,425 W/(m.K) et une densité apparente de 852-977 kg/m^3 par rapport au plâtre de gypse pur (NGP). L'étude positionne le plâtre renforcé avec de la DPP, du EPS ou les deux comme une alternative potentielle aux matériaux d'isolation traditionnels, offrant une solution durable pour la construction.

Mots-clés : matériaux biocomposites, déchets de palmier dattier, polystyrène, plâtre de gypse, propriétés mécaniques, propriétés thermophysiques, matériaux d'isolation.

ملخص

تهدف هذه الدراسة إلى تطوير وتوصيف مواد مركبة حيوية مبتكرة باستخدام مركبات نفايات النباتات والنفايات الشائعة في الجزائر للعزل الحراري الفعال في تطبيقات الهندسة المدنية والميكانيكية. والهدف هو إنشاء مواد ذات خواص ميكانيكية وفيزيائية حرارية تساوي أو تتفوق على مواد البناء التقليدية، وبالتالي تقليل الأثر البيئي وتكاليف البناء مع تعزيز ممارسات الإدارة المستدامة للنفايات.

في المقام الأول، يتم استخدام مخلفات و أوراق النخيل (DPF) كتعزيز، ويستخدم البوليسترين الذائب (PS) كمصفوفة. يتم استخدام ثلاث فئات من الألياف، الألياف غير المعالجة (UDPF) ، والألياف المعالجة بكالور الصوديوم (ADPF)، والألياف المعالجة بكلوريد البنزويل (BDPF)، لإنشاء عينات تحتوي على نسبة كتلية 10%، و20%، و30%. تم إنتاج المواد المركبة باستخدام طريقة الخلط الذائب والقولبة بالضغط الساخن. في هذه الدراسة، تم إجراء العديد من الاختبارات المورفولوجية والميكانيكية والفيزيائية على المواد المركبة لتقييم إمكاناتها كعوازل حرارية. تم تقييم الكثافة وحجم المسامات للمواد المركبة وتوزيع الألياف باستخدام طريقة قياس المسامات المتسللة بالزئبق . (MIP) تم إجراء اختبارات الشد والانحناء البسيط باستخدام آلة الشد INSTRON 5969 .وتم قياس التوصيل الحراري باستخدام جهاز CT-meter. أظهرت النتائج أن المعالجة بكلور الصوديوم و بكلوريد البنزويل تحسنت وكان التجانس جيدا من تلحم البيني بين الألياف المحبة للماء والبوليسترين النافر للماء، كما أكدته ذلك تحليلات SEM و FTIR. أشارت دراسات XRD إلى أعلى مؤشر تبلور لـ ADPF. أظهرت نتائج مركبات PS-DPF قوة شد وانحناء بسيط مرضية تبلغ 44 MPa -14، عززت المعالجات الكيميائية القوة مع تقليل المعامل قليلاً(2.9 GPa-5.9). أظهر التحليل الحراري الوزني استقرارًا حراريًا متزايدًا للمركب الذي يحتوي على 30٪ من الألياف غير المعالجة والمعالجة. أظهرت هذه المركبات موصلية حرارية منخفضة ((0.118-0.141 W/ (m.K)) وانخفاض الكثافة الظاهرية بعد دمج الألياف (kg/m^3 980- 860). أظهر استبدال ثلث مواد البناء التقليدية بمركبات PS-DPF انخفاضًا في التوصيل الحراري بنسبة تصل إلى 50%، مما يسلط الضوء على إمكاناتها في تطبيقات العزل الحراري.

يستكشف المسعى البحثي الثاني تثمين النفايات الشائعة - ألياف سويقات نخيل التمر (DPP) ونفايات البوليسترين الممدد (EPS) - لتطوير مركب حيوي هجين من الجبس الجبس. تم فحص عينات مصنوعة يدويًا بأحمال كتلة DPP متفاوتة (0%، 5%، 10%، و15%)، ونسب كتليه ثابتة EPS (0.3%)، أو كليهما من خلال الاختبارات المورفولوجية والميكانيكية والفيزيائية الحرارية. على الرغم من الانخفاض في الخواص الميكانيكية، أظهرت المركبات الحيوية الهجينة موصلية حرارية أقل تبلغ ((0.2645-0.425 W/ (m.K)) وكثافة كبيرة (kg/m^3 852-977) مقارنة بالجص الجبسي النقي(NGP) . تضع الدراسة الجبس المعزز بألياف بـ DPP أو EPS أو كليهما كبديل محتمل لمواد العزل التقليدية، مما يوفر حلاً مستدامًا لأغراض البناء.

الكلمات المفتاحية: المواد المركبة الحيوية، مخلفات النخيل، البوليسترين، الجبس المعزز بألياف ، الخواص الميكانيكية، الخواص الفيزيائية الحرارية، المواد العازلة.

TABLE OF CONTENTS

Chapter II. BIBLIOGRAPHIC REMINDER

CHAPTER III. MATERIALS AND METHODS

CHAPTER IV: RESULTS AND DISCUSSION

LIST OF FIGURES

CHAPTER I

CHAPTER III

CHAPTER IV

LIST OF TABLES

CHAPTER I

CHAPTER III

CHAPTER VI

NOMENCLATURE

EPS	Expandable Polystyrene
CFC	Chlorofluoro carbon gas
DPF	Date Palm Fiber
UDPF	Untreated Date Palm Fiber
ADPF	Alkali Date Palm Fiber
BDPF	Benzoylated Date Palm Fiber
VPS	Virgin Polystyrene (without fibers)
PS-DPF	Date palm fiber reinforced Polystyrene composites
PS-UDPF	Untreatead Date palm fiber reinforced Polystyrene composites
PS-10%UDPF	10%Untreatead Date palm fiber reinforced Polystyrene composites
PS-20%UDPF	20%Untreatead Date palm fiber reinforced Polystyrene composites
PS-30%UDPF	30%Untreatead Date palm fiber reinforced Polystyrene composites
PS-10%ADPF	10%Alkali Date palm fiber reinforced Polystyrene composites
PS-20%ADPF	20%Alkali Date palm fiber reinforced Polystyrene composites
PS-30%ADPF	30%Alkali Date palm fiber reinforced Polystyrene composites
PS-10%BDPF	10%Benzoylated Date palm fiber reinforced Polystyrene composites
PS-20%BDPF	20%Benzoylated Date palm fiber reinforced Polystyrene composites
PS-30%BDPF	30%Benzoylated Date palm fiber reinforced Polystyrene composites
W_{DPP}	Weight ratio of DPP (%)
m_{DPP}	Mass of DPP [kg]
m_{EPS}	Mass of EPS [kg]
W_{EPS}	Weight ratio of EPS (%)
m_{G}	Gypsum plaster mass [kg]
NG	Neat Gypsum

G-EPS	Gypsum plaster reinforced with EPS
G-EPS-5F	Gypsum plaster reinforced with EPS and 5% Fiber (DPP)
G-EPS-10F	Gypsum plaster reinforced with EPS and 10% Fiber (DPP)
G-EPS-15F	Gypsum plaster reinforced with EPS and 15% Fiber (DPP)
G-5F	Gypsum reinforced with 5% fiber
G-10F	Gypsum reinforced with 10% fiber
G-15F	Gypsum reinforced with 15% fiber
DPP	Date Palm Petiole
A_{cryst}	Area under the crystalline peaks [A.U]
A_{amorph}	Area under the amorph peaks [A.U]
X_{Cryst}	Degree of crystallinity (%)
FTIR	Fourier transform infrared spectroscopy
XRD	X-ray diffraction
I_c	Crystallinity Index
I002	The counter reading at peak intensity close to 22˚(cts)
Iam	The counter reading at peak intensity close to 18˚.
2θ	Diffraction angle (˚)
SEM	Scanning Electron Microscopy
Cr	Crystallinity percentage (%)
TGA	Thermogravimetric analysis
DTGA	Derivative thermogravimetric analysis
MIP	Mercury Intrusion Porosimetry
γ	Mercury's surface tension [N/m]
d	Diameter of the intruding pore[μm]
θ	Contact angle between mercury and the pore wall

P	Pressure exerted [Pa]
m_c	Mass of composite [kg]
v_c	Volume composite [m^3]
ρ	Bulk density [$kg.m^{-3}$]
λ	Thermal conductivity [$W.\ m^{-1}\ K^{-1}$]
ρ_c	Volumetric thermal capacity [$KJ.m^{-3}.K^{-1}$]
α	Thermal diffusivity [$m^2.s^{-1}$]
wt	Weight percentages (%)
DZD	Algerian Dinar

GENERAL INTRODUCTION

GENERAL INTRODUCTION

Due to the inadequate insulation properties of most building materials, there has been a significant rise in worldwide energy consumption in the residential [1]. Moreover, the manufacturing of traditional materials like cement, bricks, and steel gives rise to a multitude of environmental problems, including contamination of the air, water, and land [2]. According to the International Institute of Refrigeration in Paris (IIF/IIR), around 15% of global electricity production is dedicated to refrigeration and air-conditioning. Additionally, air-conditioning systems are estimated to contribute to 45% of energy consumption in residential and commercial buildings. Insulating materials have a crucial role in designing and constructing energy-efficient buildings [3]. Hence, using sustainable and biodegradable bio-based materials to create more valuable environmentally friendly chemicals and bio-based commodities has motivated many researchers to explore the feasibility of employing natural fibers as strengthening materials for eco-friendly biocomposites [4].

Vegetal fibers, used alone or as additives in composite construction materials, are becoming increasingly popular due to their advantages. These advantages include their easy availability, low cost, capacity to decompose naturally, renewable nature, widespread availability, lack of hazardous properties, and absence of pollution-causing characteristics [5]. Moreover, the reduced density of natural fibers renders them viable substitutes for specific synthetic fibers such as glass, carbon, and aramid fibers [6]. While it is often observed that incorporating natural fibers into polymer matrices tends to reduce their mechanical strength, there are exceptions to this trend [7].

The properties of natural composites are determined by the matrix, fibers, and the bonding between them [8]. The adhesion between the reinforcing fibers and the matrix greatly influences a composite material's overall mechanical and physical properties. Several research have investigated this subject. Employ many chemical methodologies, including alkaline and silane treatments, Graft Copolymerization, Acetylation, benzoylation, and peroxide treatments, to enhance the adhesion between the matrix and reinforcement [9].

It is essential to acknowledge the significance of date palm fibers (DPF) as a type of natural fiber, given the large amounts produced and discarded worldwide. Using this organic fiber as a primary material would enhance the utilization of renewable natural resources [10].

Polystyrene (PS) is frequently used in the electronics, food packaging, and kitchen appliance sectors due to its outstanding dielectric properties and dependable dimensional stability [11]. Furthermore, it is commonly used as a thermal insulator [2]. Significant amounts of polystyrene trash are produced in both domestic and industrial environments. Despite being non-biodegradable, the production, utilization, and disposal of polystyrene have a harmful effect on the environment. Consequently, scientists have investigated alternative uses for polystyrene, such as using it as a compound to advance composite materials [12].

Gypsum plasters are commonly used in building construction due to their efficient production method, wide availability, and cost-efficiency. Moreover, gypsum can undergo several recycling cycles with the implementation of an appropriate technique [13]. Nevertheless, plaster has several disadvantages, such as its intrinsic fragility, limited ability to resist cracking, and unsuitability for external plaster applications due to its incapacity to endure moist conditions.

In these environmental, economic, and innovation contexts, the present work aims to elaborate and characterize two new biocomposite materials to serve as effective thermal insulation for structures and building construction. The materials developed are based on waste (date palm fibers) distributed within a polystyrene matrix in the first material and in a gypsum matrix in the second material, considering different parameters such as fiber ratio and chemical treatment. This biocomposite's morphological, thermo-physical, and mechanical properties are obtained by experimental analysis.

The primary concern of this work is whether these new biocomposites will satisfy the technical and economic requirements for their use in thermal insulation in construction buildings.

For a detailed and in-depth study of this issue, this manuscript is subdivided into four chapters:

This thesis's first chapter presents a few definitions concerning composite materials, encompassing classifications, historical evolution, and utilization, limiting ourselves to natural fiber-reinforced composites. Then, we will focus on date palm wood, presenting its composition, morphology, Distribution, and summary of the mechanical and physical characteristics of palm wood. Finally, this chapter ended with a general discussion on building insulation and thermal comfort.

In the second chapter, we will present some of the work carried out on composite materials based on the utilization of polystyrene, gypsum, and date palm fibers, which are the principal compounds used in our work.

In the third chapter, we present the materials used, the experimental protocols, and the processes used to produce the two studied biocomposite materials (the first is the date palm leaflets fiber reinforced polystyrene, and the second is biocomposite based on gypsum, expanded polystyrene waste, and/ or date palm petiole fiber) we will also present the deferent morphological, mechanical and thermo physical proprieties tests conducted on the elaborated samples.

The fourth chapter will discuss the results obtained from the various tests carried out on the studied composite material, and we will compare our results with those found in the literature.

Based on this work, an overall view will be proposed in the general conclusion to highlight the main advances of this work as well as the prospects of the study.

CHAPTER I. GENERAL ON COMPOSITE MATERIAL AND THERMAL INSULATION MATERIAL

Introduction

In the opening chapter of this study, we delve into the fundamental aspects of composite materials and thermal insulation. Composite materials, composed of distinct phases, offer superior performance by combining different materials. We explore the types of reinforcement fibers, including natural and synthetic varieties, and the essential components of fiber structure. The chapter also discusses methods for enhancing adhesion between the matrix and reinforcement. Moving to thermal insulation, we examine its critical role in maintaining human comfort in built environments. Various insulation materials are discussed, highlighting their characteristics and applications. This chapter sets the stage for a deeper exploration of these crucial materials in subsequent sections.

A. Composite material

I.1. Introduction to composites

Composites are material systems consisting of many phases created by combining different materials to attain enhanced features and performance that the individual components cannot accomplish. A composite material's achievement necessitates combining at least two components, namely the reinforcement and the matrix [14] (Figure I. 1). The amalgamation of these two distinct phases gives rise to a third phase called the interface or interphase. This set's characteristics are contingent upon its constituents' attributes, geometric distribution, relative quantities, and ability to adhere to one another [15]. Typically, reinforcement imparts mechanical strength to the material, while the matrix facilitates the transmission of external loads to the reinforcement across the contact. The matrix further safeguards the reinforcement against external aggressions and occasionally establishes the upper limit of temperature that the material can withstand for practical application [16].

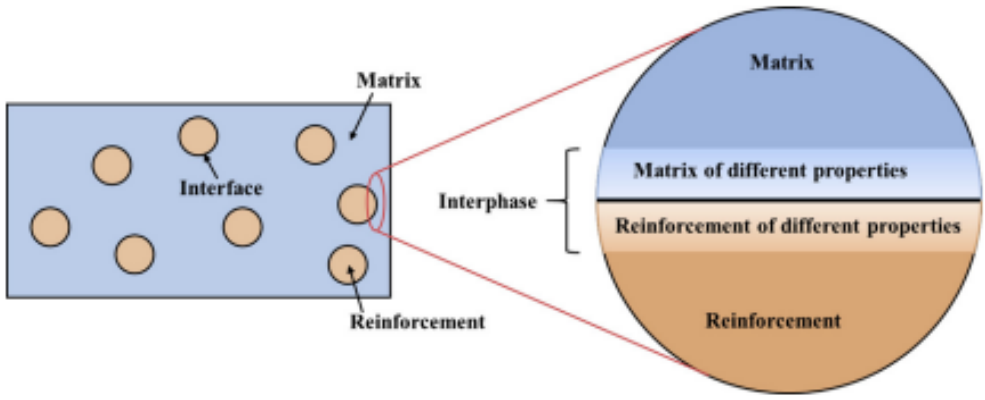

Figure I. 1. Constituent phases of a composite material [18]

I.2. Interface

The interface can be described as the intricate region of transition between the reinforcing phase and the matrix (Figure I. 1). This interface enables the transmission of load from the matrix to the fibers, facilitated by strain compatibility between the two components [17]. In the event of the interface's early failure, the matrix's deformation or strain is incongruent with that of the fiber, leading to the inability to transfer load from the weaker matrix to the more robust fiber component. Put otherwise, it is not possible to attain the reinforcing effect of fibers on a polymer substrate.

Hence, strain compatibility at the interface is crucial in ensuring the structural integrity of fiber-reinforced polymer materials. However, achieving strain compatibility becomes challenging in stressed and/or hostile environmental conditions due to the disparities in mechanical properties (such as elastic modulus) and physical properties (such as the swelling ratio) of fibers, and the matrix is a significant factor to consider.

Stress concentration is more prone to occur at the interface than in the fibers or matrix, resulting in a higher likelihood of microcrack formation between the fiber and matrix. The load-carrying capacity of the composite material decreases as the microcracks propagate. A thorough examination of the interfacial characteristics between the fibers and matrix is essential to utilize this material effectively. In addition, the interface between the fiber and matrix is of utmost importance in determining the mechanical properties of fiber-reinforced polymers (FRP) for extended periods, particularly when exposed to harsh environmental conditions[18].

I.2.1. Mechanism of the interface

As depicted in Figure 1, at the macroscopic level, the interface refers to the shared boundary between the reinforcement, which consists of fibers in a composite material, and the polymer matrix. At the micro-scale, the "boundary" referred to is a transition region known as the interphase, which possesses a limited volume extending zone. This region's chemical, physical, and mechanical characteristics exhibit continuous or stepwise variations from the reinforcement to the matrix materials. Based on interphase, a composite fiber can be subdivided into two distinct components. A component within the structure does not come into touch with the matrix and retains the inherent qualities of the original fibers. The matrix impacts the remaining fiber portion, resulting in altered properties compared to the original Fiber [6].

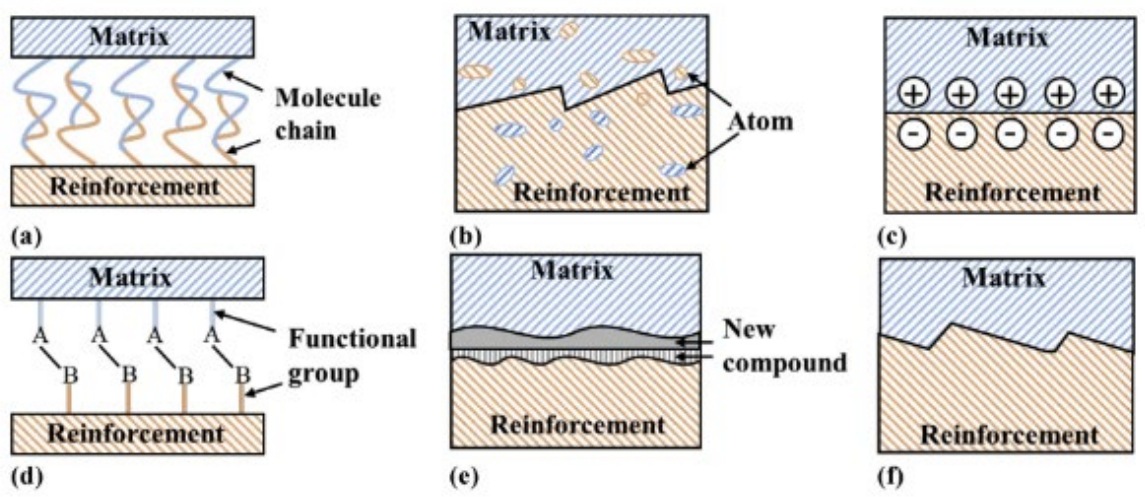

Figure I. 2. Interfacial bonding resulting from (a) molecular entanglement; (b) inter-diffusion of elements; (c) electrostatic attraction; (d) chemical reaction between groups on reinforcement and matrix surfaces; (e) chemical reaction forming a new compound, especially in metal matrix composite (MMC); and (f) mechanical interlocking [18].

Composite materials create interfaces through several mechanisms, such as physical attraction, molecular entanglement, inter-diffusion, electrostatic attraction, chemical bonding, reaction bonding, and mechanical bonding, as depicted in Figure I. 2. Additionally, low energy forces like hydrogen bonding and van der Waals forces exist. Before the reinforcement and matrix contact each other during interfacial bonding, physical attractions such as electrostatic attraction and physical attraction between electrically neutral entities may occur. After reinforcement and matrix contact, molecule entanglement and inter diffusion begin. The final connection between reinforcements and matrix is achieved through processes functioning independently or jointly. Individual bonding processes are presented in Figure I. 2[20].

I.2.2. Failure modes

According to the failure location, the failure modes of the interface can be classified into three types (Figure I. 3): Depending on the bond strength, critical strength of the filaments, and shear strength of the polymer matrix, these failure modes can occur singly or simultaneously. Due to the incompatibility between the unprocessed date palm fiber (hydrophilic) and polyurethane matrix (hydrophobic), the only failure mode observed during the single fiber pull-out test was debonding failure at the fiber-matrix interface, as reported by Oushabi et al.[21].

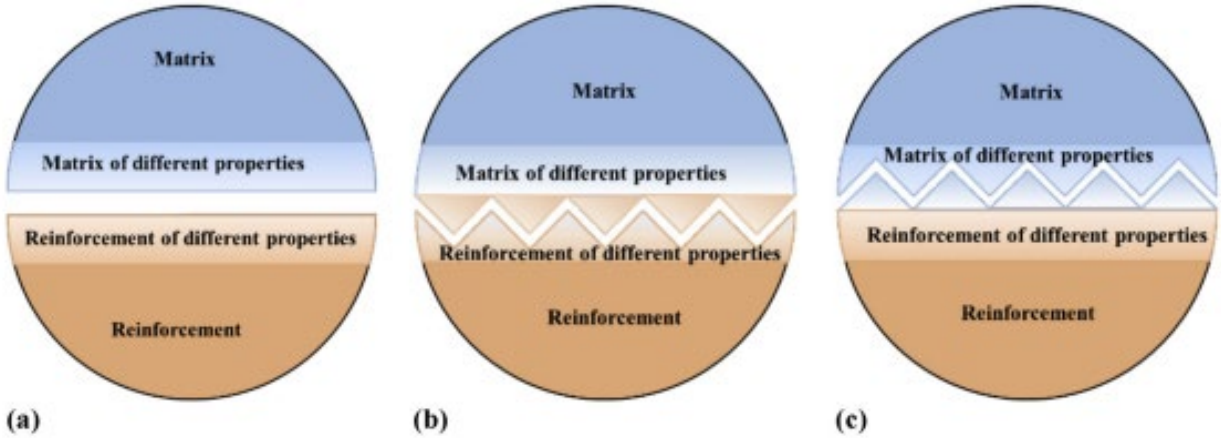

Figure I. 3. Failure modes of the interphase: (a) debonding, (b) reinforcement failure, and (c) matrix failure[18].

When the unprocessed date palm fiber was treated with 5 wt% NaOH, more matrix was attached to the fiber surface. This phenomenon was attributed to alkali treatment exposing hydroxyl groups on the fiber's surface [21]. Therefore, the matrix's polymer chains can establish chemical bonds with the fiber surface, enhancing the bond's strength. Liu et al.[22] Debonding and matrix failures with varying moisture contents were also observed at the epoxy matrix and palm fiber interfaces.

The debonding failure occurred when the moisture content of palm fibers was 328%. The water at the fiber/matrix interface diminished the mechanical interlocking between the fiber and matrix. However, as the moisture content decreased, the bond strength between the palm fiber and the epoxy increased, and the failure occurred at their interface and/or matrix.

I.3. Reinforcement

I.3.1. Classification

Using fiber-reinforced composites commonly involves incorporating natural and synthetic fibers as conventional fiber materials. As depicted in Figure I. 4, natural fibers can be classified into three main categories: plant-based, animal-based, and mineral-based. Synthetic fibers can be categorized into two main groups: organic fibers and inorganic fibers [23], [16].

Because our thesis is based on natural fibers, which are date palm fibers common from plants, we will be interested in plant-based fibers.

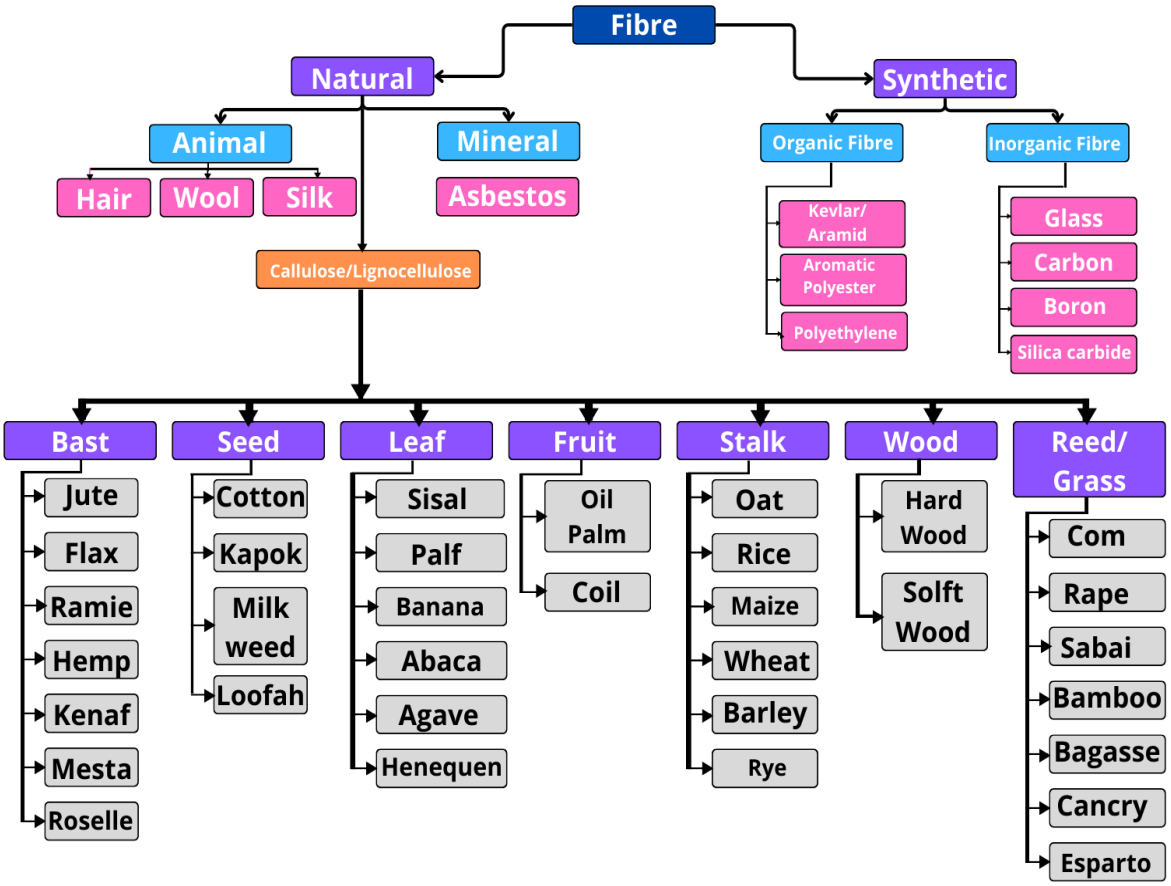

Figure I. 4. Classification of commonly encountered types of reinforcements [16]

I.3.2. Natural Fiber

Natural fibers come from plants, animals, or minerals. Plant fibers are mostly cellulose, a complex carbohydrate, while animal fibers like hair, silk, and wool are proteins. Plant fibers include Bast (stem or soft sclerenchyma), leaf or hard fibers, seed, fruit, wood, cereal straw, and other grass fibers. Figure I. 4 shows a schematic of fiber classification.

I.3.3. Plant fibers

Plant fibers are typically categorized based on the specific plant parts from which the fibers are harvested. Therefore, the fibers can be primarily classified into four distinct types, namely seed fibers, leaf fibers, bast fibers, and fruit fibers. Furthermore, it is worth noting that plant fibers, such as straw fibers derived from corn, rice, and wheat, grass fibers obtained from bagasse and bamboo, as well as wood fibers sourced from both softwood and hardwood, hold significant significance within the textile and composite business [24].

I.3.4. Plant fiber compounds

Botanical types are the most common classification for natural fibers. Lignocellulosic fibers consist of α-cellulose, hemicelluloses, and lignin. Additionally, lignocellulosic fibers contain a small amount of pectin, waxes, and water-soluble compounds [25]. Figure I.5 and Figure I.6 show the basic chemical structures of cellulose, hemicelluloses, lignin, and pectin. The chemical composition of several lignocellulosic fibers is shown in Table 1. The composition and architecture of lignocellulose fibers vary due to plant species, age, climate, and soil conditions.

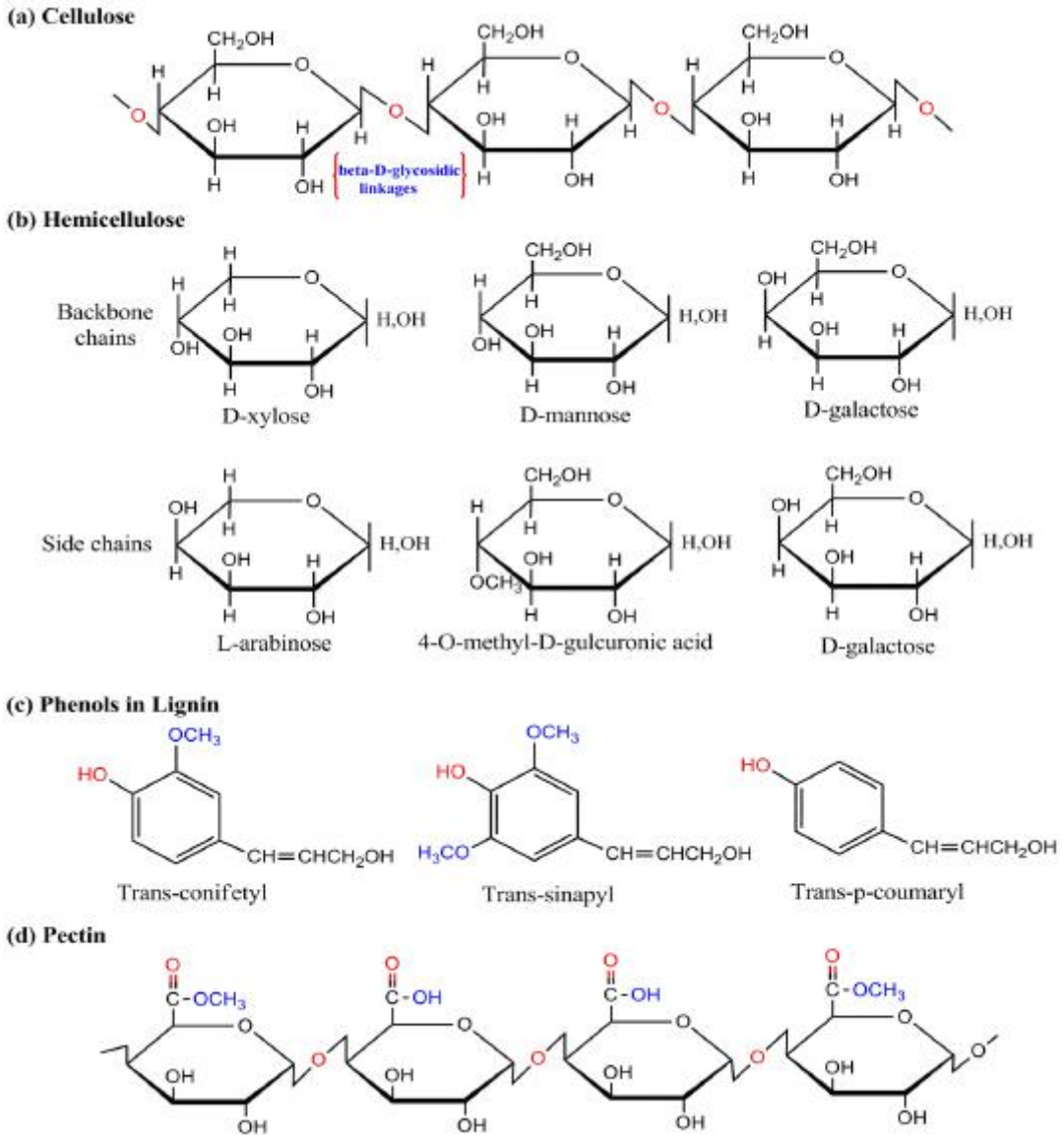

Figure I. 5. Chemical composition of plant fibers[25]

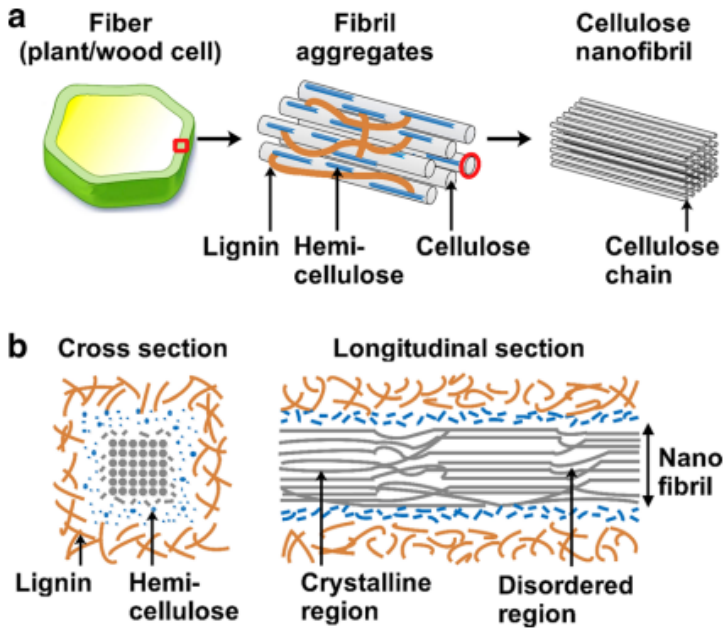

Figure I. 6. An illustration depicting the microstructure of a cellulosic fiber. a Plant/wood fiber, fibril aggregate, and nanofibril (consisting of cellulose chains) accompanied by lignin and hemicellulose. b Cross section and longitudinal section illustrating cry[27]

I.3.4.1. Cellulose

Cellulose $(C_6H_{12}O_5)_n$ is classified as an organic compound, specifically a polysaccharide, composed of a linear arrangement of numerous β(1→4) linked D-glucose units, ranging from several hundred to over ten thousand in number (its structure showed in Figure I. 5) It is the primary structural constituent of the cellular walls in green plants and numerous species of algae. Cellulose, the predominant organic polymer found in abundance on Earth, confers plants with structural rigidity and resilience to compression. Cellulosic plant fibers typically exhibit a notable capacity for moisture absorption and a limited degree of dimensional stability due to their tendency to expand upon exposure to water; it is found in diverse industrial application products such as paper, textiles, and biocompatible and biodegradable materials[26].

I.3.4.2. Hemicellulose

The second most abundant organic substance, after cellulose, has 2.6 times more moisture than lignin. Hemicellulose is a diverse collection of non-cellulosic polysaccharides that coexist with cellulose and lignin within the cell walls of plants. In contrast to cellulose, hemicelluloses possess a disordered and branched molecular arrangement. Hemicelluloses, consisting of diverse sugar monomers, including glucose, mannose, galactose, xylose, and

arabinose, exhibit greater susceptibility to hydrolysis than cellulose. They link cellulose fibers together and connect them to lignin, thereby contributing to the pliability of the plant cell wall[27].

I.3.4.3. Lignin

Lignin is a biochemically derived substance that enhances the structural integrity of plants. Moreover, it is worth noting that this particular biopolymer, which possesses an aromatic molecular structure and establishes ester linkages with hemicellulose, ranks as the second most abundant biopolymer, following cellulose. Lignin molecules are composed of three primary precursors that serve as active functional groups, specifically coniferyl alcohol (G), p-coumaryl alcohol (H), and synapyl alcohol (S). The hydrophobic lignin system couples a separate network and stiffens plant cellulose/hemicellulose[28].

I.3.4.4. Pectin

Pectins exhibit high hydrophilicity due to the carboxylic acid groups they contain[29]. The pectins, lignin, and hemicellulose bind individual fibers and can be readily hydrolyzed under elevated temperatures (Figure I.5).

I.3.4.5. Waxes

Waxes are constituents of the fiber matrix that can be extracted using organic solvents. The substance consists of various alcohol compounds that exhibit insolubility in water and certain acids[30].

I.3.5. Surface modification

Given the hydrophilic nature of fibers, it is typically observed that they do not exhibit strong adhesion with polymer matrices. Various surface modification methodologies have been employed to address this issue. These alterations not only enhance the ability of the polymer matrices to be wetted but also decrease the level of moisture absorption. Additionally, they can occasionally confer distinctive characteristics and facilitate the manufacturing process. Surface modification commonly encompasses four primary methods: chemical, physical, and mechanical methods (such as rolling and swaging).

I.3.5.1. Physical alteration of natural fibers

Physical methods include corona discharge, steam explosion, high-energy ray radiation, and autoclave treatments. Physic-chemical methods combine physical and chemical processes. These methods reduce the hydrophilic/hydrophobic difference between the fiber and matrix to improve adhesion [102]. Physical treatments are the most eco-friendly. Plasma treatment changes fiber and polymeric surfaces' chemical and physical properties while preserving

their structures and properties [106]. Plasma treatment increases film surface hydrophilicity and adhesion by forming polar groups. Thus, adding hydrophilic antimicrobial substances to treated films can improve their properties.[31].

I.3.5.2. Chemical processing of natural fibers

Chemical modifications were implemented on natural fibers to enhance the adhesion between the matrix and the fibers[32]. Certain chemical modifications have the potential to result in a decrease in the moisture absorption properties of natural fibers and their composites.

The majority of chemical modifications applied to natural fibers encompass various processes such as silanization, alkalization (also known as mercerization), acetylation, cyanoethylation, benzoylation, isocyanate, dewaxing, esterification, etherification, and graft copolymerization [33].

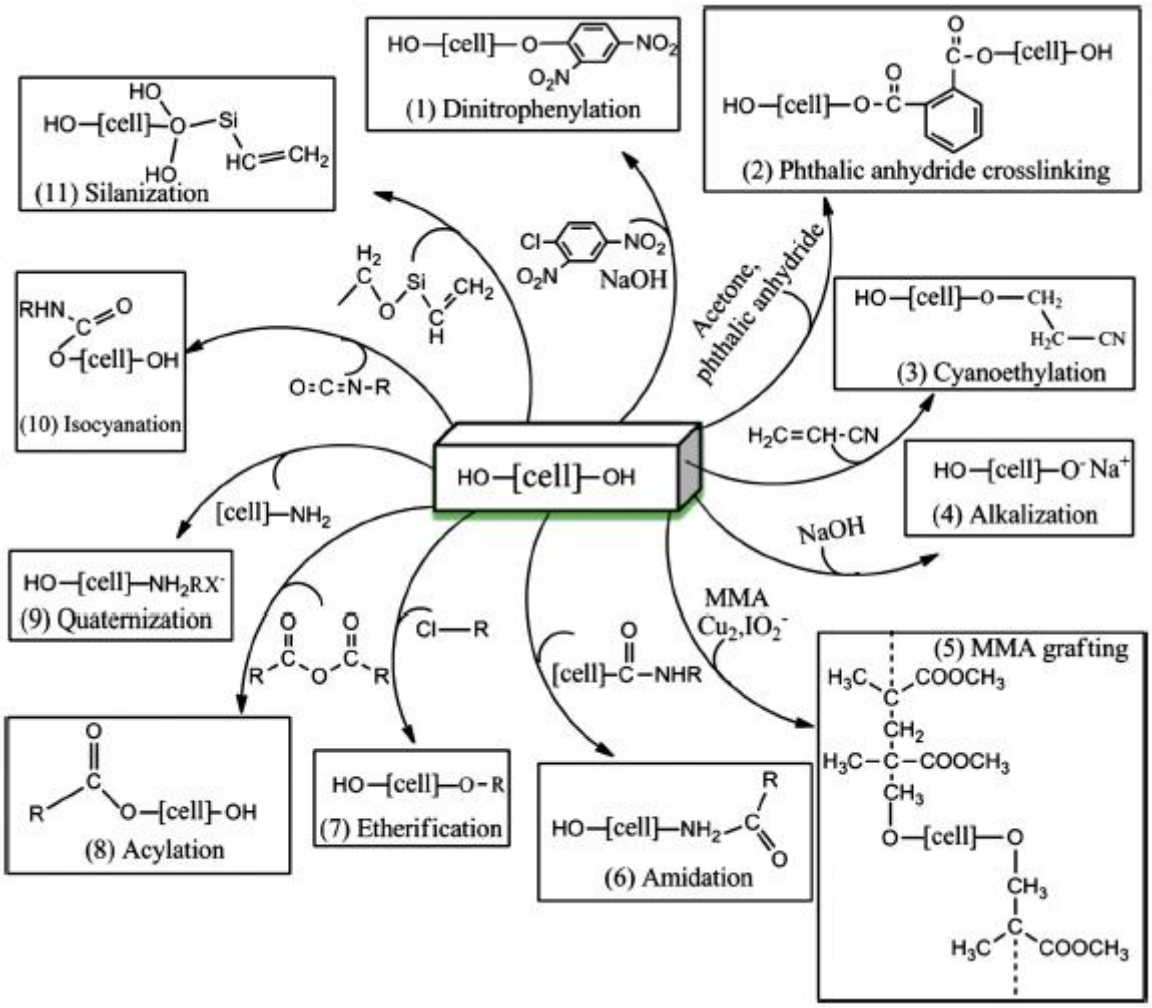

Figure I. 7. schematic presentations of some chemical surface modification methods on natural fiber

Additional modifications of natural fibers can be achieved through various processes such as crosslinking with formaldehyde, p-phenylenediamine, and phthalic anhydride, as well as nitration, dinitrophenylation, and transesterification[34] .

The chemical composition of these substances enables them to react with the surface of the fiber, forming chemical bonds that establish a connection between the fiber and the matrix. Scheme I.7 illustrates schematic representations of several surface chemical modifications applied to natural fibers.

I.3.6. Advantages and disadvantages of plant fibers

Plant fibers play a significant role in the building industry as bio-based materials, offering considerable potential for addressing the challenges posed by climate change on our planet. Plant fibers' commendable thermal insulating properties substantiate their potential as viable alternatives to conventional insulation materials with lower environmental sustainability. The significance of recognizing the value of plant fibers in tropical climates lies in their diverse abundance, as they provide the potential to address contemporary climate concerns, particularly within the building industry. The utilization of unprocessed natural fibers, namely those derived from plants, presents some drawbacks that impose constraints on their applicability unless they undergo enhancements. The abovementioned drawbacks could be attributed to these substances' hydrophilic properties and limited thermal stability [35]. We have referred to relevant scholarly sources that outline the primary benefits and drawbacks associated with plant fibers (Table I.1). Several works have been identified for citation in this context, including [36], [37], and [38].

I.3.7. Classification of composites based on the reinforcement form.

Figure I.8 depicts the composite material's categorization based on the reinforcements' configuration. The subject matter can be categorized into three distinct families. A composite material can be classified as a fiber composite when its reinforcing consists of continuous (long fibers) or discontinuous (chopped, short fibers). A particulate composite refers to a composite material whereby the reinforcing takes the form of discrete particles[39].

The "structural" family, the third in this classification, is a combination of the "particle-reinforced" and "fiber-reinforced" families.These initial two families are distinguished by the reinforcement's form factor L/d, where L is its length and d is its diameter [40].

Table I. 1. The advantages and disadvantages of plant-based fibers.

Advantages	Disadvantages
• renewable, biodegradable resource • lightweight (low density) • abandoned in nature • low environmental impact and low energy consumption in manufacturing • good regulator of internal humidity in the building • low-cost price • non-abrasive for tools • no co2 emission, it absorbs the co2 emitted by quotidian activities • non-toxic (no skin irritation when fibers are handled) • important specific mechanical properties (rigidity and resistance) • good thermal, acoustic, and electrical insulators	• poor adhesion to polymers • request control for industrial application • low long-term durability • wide variety of properties for the same species depending on climate, plant age, composition, and sampling position • susceptible to microbial attack (rodents) and fire • fibers discontinuity • dimensional variability (swelling or shrinkage) • anistropic fibers • quality variation depending on plant growth location and metrological conditions • high water absorption capacity or humidity • high water absorption capacity or humidity • low thermal resistance (200 to 230 ˚C)

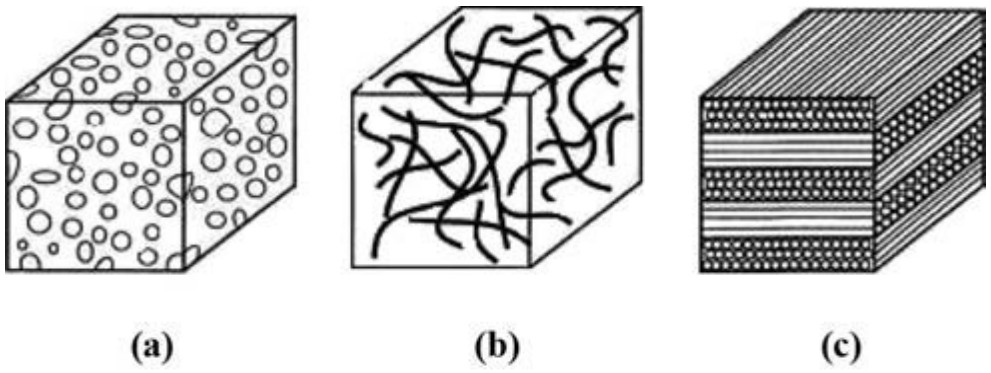

Figure I. 8. Reinforcement geometry for composite materials: (a) particulate composites, (b) fiber composites, and (c) laminated composites

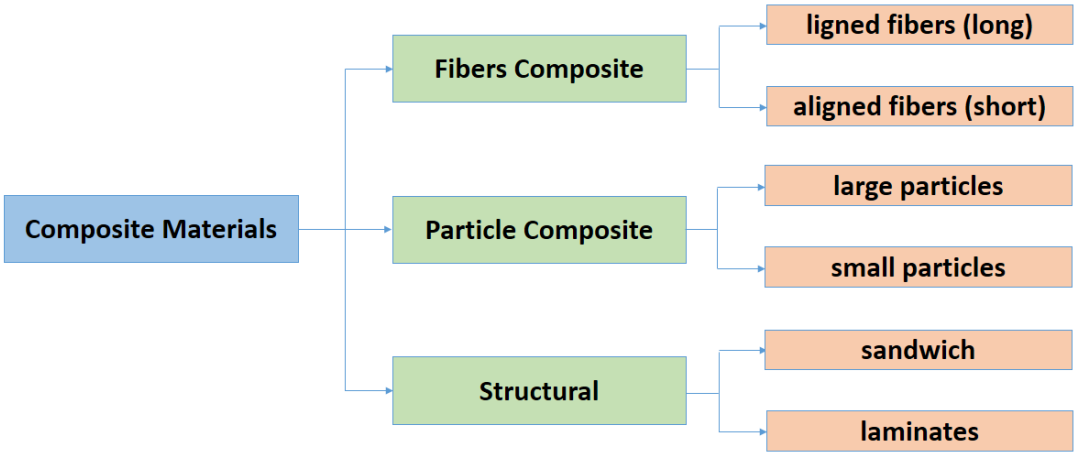

Figure I. 9. Classification of composites based on the reinforcement form.

I.4. Matrix

The primary function of the matrix is to establish a connection between the reinforcing fibers, facilitate the distribution of external forces, impart chemical resistance to the structure, and determine the desired form of the end product. Fiber-reinforced composites can be categorized into four distinct groups based on their matrices: metal matrix composites (MMCs), ceramic matrix composites (CMCs), carbon/carbon composites (C/C), and polymer matrix composites (PMCs) or polymeric composites[41] (Figure I. 10.).

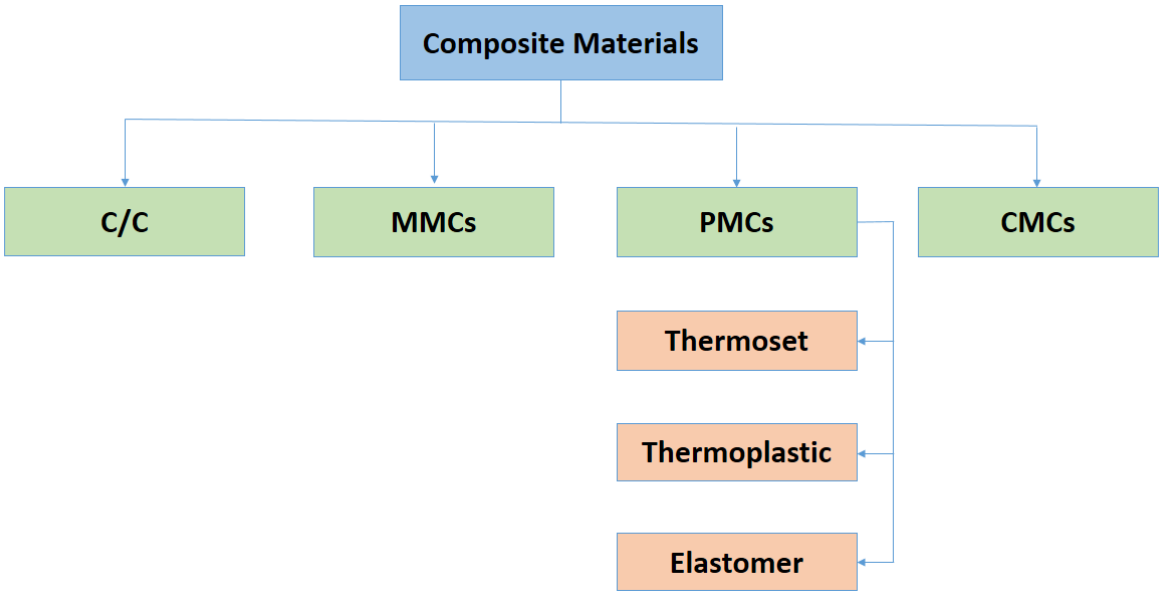

Figure I. 10. Classification of composites based on Matrix

I.5. Classification of composites based on Matrix

I.5.1. Polymer matrix composite

Polymer matrix composites (PMCs) are differentiated from other composites primarily due to their lightweight nature. Furthermore, PMCs can be further categorized into thermoset, thermoplastic, and elastomeric composites. Thermosets are characterized by crosslinked polymer chains during curing, forming a rigid final product with limited or no reshaping ability. In contrast to thermosets, thermoplastics possess the unique characteristic of being capable of undergoing reheating and subsequent remelting [42] Table I. 2.

Table I. 2. comparison between thermosets and thermoplastics [49]

Thermosets	Thermoplastics
To produce parts, cold material is injected into an extremely heated mold.	Parts are produced by melting plastic and injecting it into a mold.
Form an irreversible chemical bond	(100% reversible because no chemical bonding occurs during the procedure)
Not capable of molding or reshaping	Recyclable and susceptible to molding
Comparatively hard to finish on the outside	The surface finishes produced by injection molding with thermoplastics are flexible, precise, and aesthetically appealing.
Thermoset injection molding does not require intense heat and pressure, unlike thermoplastic injection molding.	High heat and pressure are necessary for thermoplastic injection molding.
Produced mainly by condensation polymerization.	primarily produced through supplemental polymerization
Products manufactured by thermosetting injection molding include: Handles, insulation, computer and television elements,.etc.	The following are examples of products manufactured by thermoplastic injection molding: Vacuum cleaners, kettles, toasters, toys, machine screws, gear wheels.etc
The manufacturing procedure includes compression, transfer, and casting.	The manufacturing process consists of injection molding, extrusion, and blast molding.
Drawbacks, including: • Recycling presents problems • Volatile organic compound (VOC) emissions are emitted.	There are several drawbacks associated with this, including: • Costly • The substance has the potential to undergo a phase transition into a liquid state when exposed to elevated temperatures. • Developing a prototype has challenges.

This property enables them to be reshaped into novel forms, thereby facilitating a broader scope of recycling opportunities in comparison to thermosets. One notable advantage of thermosets is their ability to maintain structural rigidity even when exposed to elevated temperatures. Common examples of thermosetting polymer matrices include polyester, vinyl ester, epoxy, phenolic, cyanate ester, polyurethane, polyimide, and bismaleimide [43]

In contrast, several thermoplastic polymer matrices are commonly encountered in various applications. These include polyamide, polyethylene, polypropylene, PEEK, thermoplastic polyimide, thermoplastic polyurethane, polycarbonate, PLA, polysulfone, and polyphenylene sulfide[44]. Elastomers, similar to thermosets, undergo the vulcanization process to attain crosslinking. Rubber is widely recognized as a prominent elastomeric material, thus leading to the common designation of elastomeric composites as rubber composites. Elastomers are distinct from thermosets and thermoplastics due to their pronounced elasticity in mechanical response [45,46].

Elastomeric composites include hoses fortified with polyester fibers, vehicle tires reinforced with aramid fibers, and heavy-duty truck tires strengthened with steel wire or mesh[47].

I.5.2. Metal matrix composite

The development of metal matrix composites was driven by improving the properties of metals, particularly their lightweight nature and the favorable mechanical attributes associated with composite structures. Various composite materials, including aluminum and its alloys, nickel, and titanium, demonstrate favorable electrical and thermal conductivity, high-temperature resistance, and commendable mechanical properties. Nevertheless, the production expenses incurred by the company are significantly elevated. These resources are typically allocated for applications that require a higher level of complexity and expertise across multiple disciplines[48].

I.5.3. Mineral matrix composite

The term "mineral matrix composites" pertains to composite materials in which the matrix consists of a mineral-based substance, serving as the continuous phase. The reinforcement, acting as the dispersed phase, can be another mineral or a distinct material such as fibers, particulates, or whiskers.

Concrete is a well-known illustration of a mineral matrix composite, in which the matrix is composed of minerals, and the aggregates, such as sand and gravel, serve as the reinforcing

elements. In certain instances, additional reinforcements such as steel rebars and various types of fibers (including steel, glass, or synthetic fibers) may be incorporated into the concrete matrix in order to augment its inherent characteristics [50,51].

The underlying concept of these composites is to amalgamate the optimal characteristics of both the matrix and the reinforcement. For example, the mineral matrix provides the structure's primary mass, volume, and overall form. On the other hand, reinforcement materials contribute to enhancing tensile strength, flexibility, and other advantageous mechanical characteristics.

Mineral matrix composites are extensively utilized in construction and civil engineering due to their inherent robustness, longevity, and cost-efficiency advantages. Ongoing progress in the field of study consistently seeks to enhance its efficacy across diverse applications, encompassing the development of sturdier infrastructure and creating environmentally sustainable building alternatives [52].

I.5.4. Carbon/carbon composites

Also referred to as C/C composites, they are highly sophisticated materials comprised predominantly of carbon fibers and a carbon matrix [53]. These composites are renowned for their outstanding mechanical and thermal characteristics. Carbon fibers, which possess exceptional tensile properties, are interlaced into multiple layers during manufacturing.

These layers are then consolidated by a carbon matrix derived from carbon-rich substances like pitch or resin, which binds the fibers together. These composite materials demonstrate exceptional properties such as high tensile strength, low weight, resilience to extreme temperatures, limited thermal expansion, thermal solid conductivity, low thermal mass, and chemical resistance. These materials' unparalleled strength, thermal resilience, and lightweight properties have led to their utilization in several industries, including aerospace, automotive, industrial, and sports equipment [54].

I.6. Utilizations of Composite Materials

The composites possess notable attributes such as high resistance to corrosion, reduced weight, improved strength and productivity, cost-effectiveness, design flexibility, and exceptional durability, which can be attributed to their fabrication technique and laminate structure. Therefore, composites find applications in various engineering disciplines, including aircraft and aerospace, the automotive industry, marine engineering, infrastructure

development, oil and energy sectors, the biomedical field, and sports and recreational activities [8]. In addition to those above, there exist alternative applications[14].

A comprehensive analysis is provided of the diverse applications of composites.

I.6.1 Aircrafts and Aerospace

Aerospace vehicles employ structures such as space antennae, optical instruments, and mirrors constructed using highly rigid and lightweight graphite composites.

This choice is primarily because graphite composites possess the desirable characteristic of exhibiting minimal hydric and thermal expansions during the fabrication process. Carbon/epoxy and graphite/titanium composites are used to construct the Boeing 787 aircraft. Approximately half of the aircraft's total weight comprises the composite material, as depicted in Figure I. 11[41].

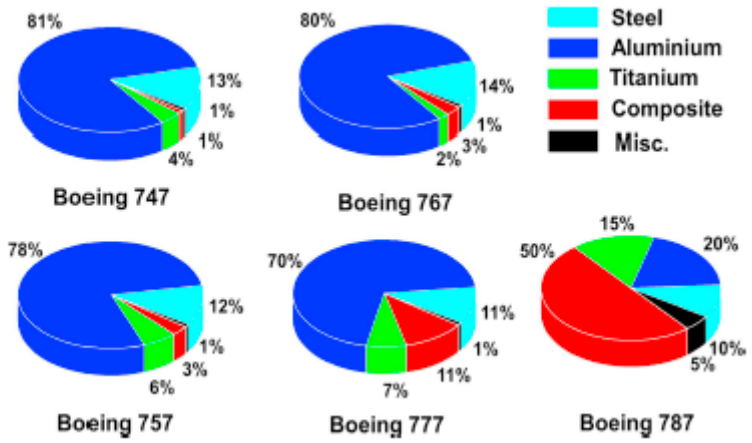

Figure I. 11. Increasing use of composite materials in Boeing commercial aircraft. [41]

I.6.2. Automotive and Transportation

Many automotive companies have extensively researched incorporating Non-Fossil Fuel Powertrains (NFPCs) into their products. European car manufacturers have specifically explored using Non-Fibrous Polymeric Composites (NFPCs) in car interiors, including seat backs, parcel shelves, boot linings, door linings, truck linings, and door-trim panels. [89].

Natural fibers are used in car interiors and exterior auto body components by incorporating them into polymers. These components, meeting stringent requirements, are often found between the headlights and above the fender of passenger buses[55].

Figure I. 12. Components of automobiles made of natural fiber composites. [55]

I.6.3. Construction and Infrastructure

Composite materials are new to infrastructure and construction. However, this application shows composites' global market potential. Composites create durable and optimal construction materials. Composites strengthen structural elements to build earthquake-resistant bridges or buildings with intricate designs that are impossible with traditional materials. Composite materials can create energy-efficient, attractive, versatile, and functional buildings with better thermal performance. [33].

Composites simplify building structures with intricate carvings, varying thickness, and traditional aesthetics like chrome, gold, copper, stone, and marble, making them affordable. Architects increasingly use composites for commercial and residential buildings. Materials like glass/polyester or Kevlar are used for water and oil pipes, roofs, wall panels, fixtures, moldings, doors, window frames, vanity sinks, shower stalls, and swimming pools. They are also used in constructing and repairing buildings

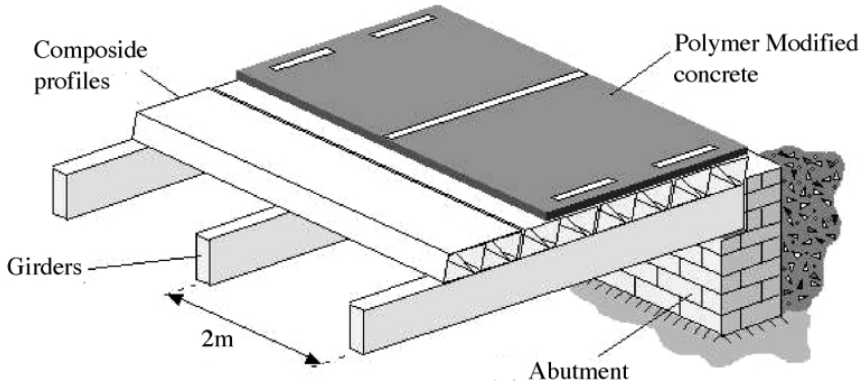

Figure I. 13. The use of composite materials in construction

I.6.4. Marine

The maritime industry strives for lightweight structures like aviation. Carbon fiber composites build ship hulls with different shapes and thick glass sections to reduce weight and increase damage resistance[51]. Sandwich structures bond thin composite face sheets to a thick, lightweight core. Such vessels include corvettes and minesweepers. Composite materials are cost-effective, have good insulation, and resist corrosion. Commercial and military ship components like decks, bulkheads, propellers, masts, and boat hulls are made from composite materials. This takes advantage of these composites' corrosion resistance. Composites make super yacht furniture and interior moldings[56].

I.6.5. Recreational/Sports Applications

Sports and recreational equipment benefit from fiber-reinforced composites. FRPs are strong, malleable, corrosion-resistant, and low-density. Sports composites include bicycle frames, fishing poles, jumping boards, hockey sticks, helmets, horizontal and parallel bars, kayaks, and tennis racquets. Carbon and glass fiber composite sports equipment is lightweight, strong, and durable[57]. This will help sports fans and athletes perform at their best without fatigue caused by sports equipment.

I.6.6. Electrical equipment and electronics

Composite materials can replace metal alloys in electrical appliances due to design and processing flexibility. Panels, power tool parts, handles, frames, and appliance trims are composite. Composites are used in dishwashers, refrigerators, ovens, dryers, and ranges. The parts include control panels, consoles, knobs, kick plates, shelf brackets, motor housings, side and vent trims, and more. Composites improved electronics. Electronics applications benefit from thermosetting polymer matrix composites' dielectric properties and arc-track resistance.[58].

I.6.7. Corrosive Environments

Chemical handling and harsh outdoor conditions are common uses for composites, which are corrosion-resistant. Oil and gas refineries, chemical processing plants, pulp and paper plants, and water treatment plants use composites. [18]. For long-term durability and corrosion resistance, these tanks, pumps, cabinets, hoods, fans, and ducts are made of composite materials. Fiber-reinforced polymer composites have solved sewer pipe, desalination, and oil and gas supply corrosion problems. [59].

I.7. The historical development of composites

Figure I.14 illustrates the extensive historical utilization of composites as an inherent component of human existence. The timeline presented encompasses significant milestones from the early development of composites to the present day.

Composite materials have advanced throughout human history. This progress is due to centuries of polymer, fiber, and ceramic discovery and development. The demand for superior materials also drove composite materials research. Lightweight materials helped the aircraft industry advance technology during World War II. In later years, the cost of these materials compared to monolithic alternatives became a factor.

In modern society, quality, reproducibility, and behavioral prognostication of materials, as well as cost and the demand for lightweight materials, drive advancements in all fields. However, advanced manufacturing methods have produced sophisticated composites. The two concepts are linked. The manufacturing process ensures quality and determines a product's final characteristics. Extensive research has produced Functional and reliable composites using cost-effective and commercially viable methods [14].

I.8. Processing techniques

The techniques employed in the manufacturing process employed in the production of composites encompass both open mold methods, such as hand lay-up and spray-up, as well as closed mold techniques like extrusion, direct long-fiber thermoplastic (D-LFT), vacuum infusion, injection molding, filament winding, resin transfer molding, compression molding, and sheet mold compounding[41]. The properties of the developed composites are influenced significantly by the processing conditions and appropriate processing methods. These parameters include dispersion, aspect ratio, orientation, and moderate temperatures. The pre-processing drying of fiber is of utmost importance due to the detrimental effect of moisture on the fiber surface, which acts as a debonding agent at the interface between the fiber and the matrix.

Moreover, water evaporation during the reaction creates empty spaces within the matrix. Both of these factors contribute to a notable reduction in the mechanical properties of composites [60].

Figure I. 14. The historical development of composites [14]

I.9. Date palm wood (phoenix dactylifera)

The date palm tree (Figure I. 15) was designated as Phoenix dactylifera by Linne in 1934. Phoenix is derived from the Greek word "Phoinix," which refers to the date palm tree. The ancient Greeks believed this tree was associated with the Phoenicians [61]. The term "Dactyliféra" is derived from the Latin word "dactylis," which originates from the Greek word "dactylus," meaning "finger" (referring to the fruit's shape). It is associated with the

Latin word "fero," meaning "carried," about the fruit. Phoenix dactylifera exhibits equal resilience to high temperatures, aridity, and low temperatures. It is commonly found in the arid Afro-Asian region that extends from North Africa to the Middle East [62]. The location is in the Orient, specifically the Oases of the Sahara. Phoenix palms exhibit dioecism, meaning they possess distinct male and female individuals. The latter generates a plethora of different types of dates. Algeria has over 800 diverse date palm cultivars within its oases [63]. Some of the most well-known types include Dokar (the male palm), DegletteNour, Elghers, and Deglabida, which are recognized by their local names.

Table I.3 displays the Area and number of palm trees planted in Algeria and their corresponding locations (MADR)[64].

Date palms possess a fibrous composition, consisting of various kinds of fiber [50]:

- Wood fibers derived from the pulverized trunk.

-The peduncles contain leaf fibers.

-The stem fibers and the date structural support (pedicels) were found in the peduncles.

- Outermost fibers encircling the trunk “fibrillium”.

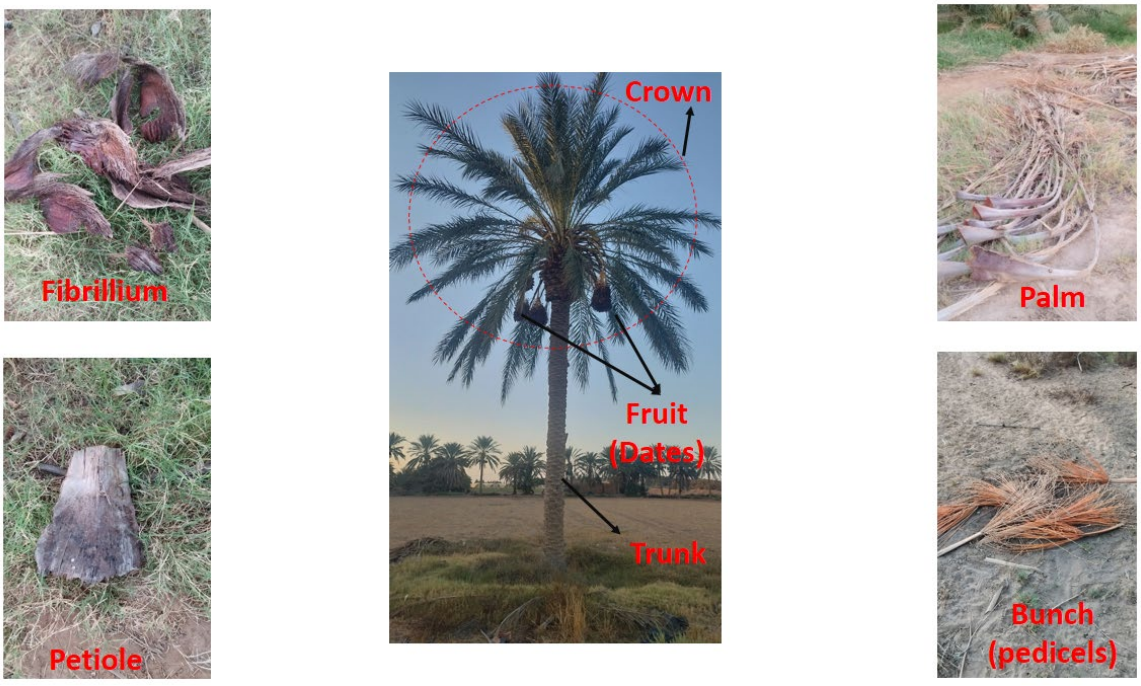

Figure I. 15. Date palm tree and its principal Components.

I.9.1. Morphology

The palm is a 20–30-m-tall grass with a cylindrical trunk (stipe) and a crown of leaves. Pinnately divided, 4–7-m leaves. Monocotyledons have one embryonic leaf in the seed. Monocotyledons have no cambium, while palm wood has a unique structure and properties.[65].

I.9.2. Components of date palm wood

Date palm wood is made up of several parts:

-Trunk

It is a stipe, generally cylindrical, elongated in its coronal part by the terminal bud or phyllophore [Figure I. 16].

-Crown

Green palms form the date palm's crown or foliage. Adult date palms have 50–200 palms. Palms last three to seven years, depending on variety and cultivation. The terminal bud or "phyllophore" emits basal crown, central crown, and heart palms. (Figure I. 15).

- Flowers

The date palm is a dioecious plant, i.e., there are male date palms (Dokar) and female date palms (Nakhla). Only female date palms bear fruit, so they are the source of the many varieties of dates. Generally speaking, two of the three carpels, uniovulate, abort, and fruits, are monosperm, which can be explained by the high density of inflorescences[66].

-Palm

The palm or "Djerid" is a pinnate leaf with leaflets regularly arranged obliquely along the rachis. The lower segments are transformed into spines, more or less numerous and more or less long Figure I. 16.

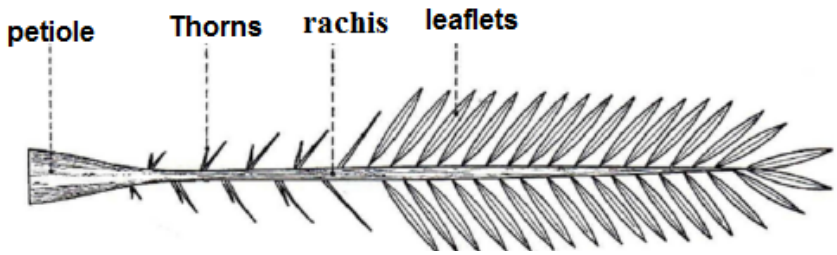

Figure I. 16. Diagram of a palm

The fruit.

Dates are drupes with one seed, the pit. A thin epicarp protects the fleshy mesocarp of date fruit. The stone's endocarp is parchment-like. Elongated and variable in size, the fruit has smooth or ridged or fins. It has ventral furrow. Top of embryo is firm and tough. Date fruit colors vary by species, from lighter or darker yellow to translucent amber, darker or lighter brown, red, or black.[67].

Table I. 3. Displays the Area and number of palm trees planted in Algeria and their corresponding locations (MADR).

City (Wilaya)	Occupied area (ha)	Deglet Nour (number of trees)	Ghers and Analogues (Soft dates) (Number of trees)	DeglaBeida (Number of trees)	Total Date Palm (Number of trees)
BISKRA	43 851	2 756 137	569 690	1 099 040	4 424 867
El- OUED	38 147	2 556 875	742 160	676 895	3 975 930
ADRAR	28 320	0	0	3 798 759	3 798 759
OUARGLA	22 512	1 435 032	1 018 559	175 223	2 628 814
BECHAR	13 919	0	1 406 138	234 626	1 640 764
GHARDAIA	11 359	563 249	239 699	494 562	1 297 510
TAMANRASSET	7 118	0	0	752 310	752 310
ILLIZI	1 254	7 758	77 585	43 760	129 103
KHENCHELA	812	51 400	70 100	11 542	133 042
TEBESSA	569	38 200	22 400	0	60 600
EL-BAYADH	477	3600	15900	28200	47700
TINDOUF	464	30	44511	1809	46350
LAGHOUAT	265	10240	12740	10260	33240
DJELFA	260	19300	5400	1300	26000

NAAMA	253	2000	39788	0	41788
BATNA	207	9338	7453	9681	26472
TOTAL	169 786	7 453 159	4 272 123	7 337 967	19 063 249

I.9.3. Distribution across regions of the date palm

I.9.3.1. On an international scale

The date palm, known as the tree of providence in arid regions, is predominantly observed between 10° and 35° parallels in the northern hemisphere. It is particularly prevalent along the Persian Gulf's shores, North Africa, and Asia. Additionally, it is noteworthy to mention California (Coatchella Valley), where it was introduced in the 18th century, and Spain, where the renowned Elche palm grove is situated at 39° North, west of Alicante. Additionally, date palms are cultivated to a lesser extent in Australia, Mexico, Argentina, and the West Indies [68].

Over 120 million date palms are estimated to exist on a global scale. The Arab world possesses over 80% of the production potential, as indicated by its spatial distribution.

I.9.3.2. In Algeria

The Ministry of Agriculture and Rural Development (MADR) reported in 2021 that date palms cover 169 786 hectares of Algeria, or 2% of the 19.06 million palm trees. Date palms grow in all areas below the Saharan Atlas, with Biskra (Tolga) in the east preceding M'Zab and Bni-Ounif in the middle and west. In the extreme south of the Sahara, the Djanet Oasis marks the southernmost Algerian palm plantation. Three-quarters of the nation's palm-growing heritage is in northeastern Sahara's Ziban, Oued-Righ, and Ouargla basins. The southern steppe wilayas (Tbessa, Khenchla, Batna, Djelfa, Laghouat, Naama, ElBayadh) have small palm plantations. Table I.3 shows MADR date palm distribution by wilaya.[64].

Algeria has 300 date palm varieties, each with a local name, according to "Bioversity International," an agricultural research institute. Date palm trees like DegletNour, El Ghers, Mechdegla, Tantboucht, Arechti, Safraya, DeglaBeida/Kountichi, Litima, Hmraya, and others are genetically identical. Most of these cultivars are from Ziben (Biskra) and Mzab. Although other palms are more productive, mature, and drought- and disease-resistant, DegletNour accounts for over 50% of cultivated palms.[30].

I.9.3.3. Within the Biskra wilaya

With over 4 million date palms, or 23.19% of the national heritage, Biskra, which covers 27.4% of the country, is the leading phoenicicultural region. Willaya palm groves are in western Zibans at Tolga, Foughala, Leghrous, Bordj Benazouz, Ourlal, OuledDjellal, and Sidi Khaled. The eastern Zibans' Djemora, Baranis, M'chounech, Loutaya, and El-Kantara have less phenoliculture. The wilaya's palm grove is known for its 60% Deglet-Nour date palms, which produce high-quality dates.[30].

I.9.4. Global and Algerian estimates of the tonnage of date palm wood.

In addition to its date production, the date palm is a source of various raw materials. Its wood is derived from the waste of date palm trees, collected annually after maintenance work. Eight forms of renewable wood can be distinguished: fibrillium, petiole, rachis, spine, leaflet, cluster, pedicel and spathe wood. They represent the raw material we are trying to enhance in the present study.

Our estimation of the tonnage of date palm waste is based on statistics from the Agricultural Research Center for Arid and Semi-Arid Regions in Biskra. These statistics pertain to the waste generated by date palm trees in a palm grove in the province of Biskra. According to this estimate, the annual waste of the palm tree consists of 27% rachis, 24% petioles, 28.7% leaflets, 6.3% fibrillium, 5% spathes, 4.9% clusters, 3.3% pedicels, and 0.8% thorns. According to the latest statistics from MADR [64], Algeria has 19 063 249 palm trees, with the Biskra willaya accounting for 4 424 867. According to reference [9], there are 120 million palm trees worldwide [69]. The annual estimation of palm date palm wood production worldwide, in Algeria and the Biskra province, will be presented in Table I.4.

Table I. 4. Annual tonnage of date palm wood.

Kind of wood	Wilaya of Biskra	Algeria	Worldwide
Fibrillium	12 945, 3	55 815, 300	360 000
Petioles	49 062, 687	211 539, 987	1 364 400
Palm (rachis/leaflets/thorns/	259790.595	1120120.04	7224600
Bunch (pedicels spathes)	27141.979	117026.079	754800
Total	348 940, 561	1 504 501, 411	9 703 800

I.9.5. Chemical composition

The chemical makeup of DPF is shown in Table I.5. Carbon (C) and oxygen (O) dominate these materials, according to the results. The amount of chlorine (Cl) in all DPF varieties except the petiole part of the Elghers variety is high but lower than the rachis ash. Due to the soil, date palms grow this way. [74].

The comparison of cellulose and lignin concentration between date palm fiber and other fibers shows its suitability as a filler for natural fiber composites (Figure I.17). The literature review showed that date palm fiber, despite having little cellulose, has the right mechanical properties and absorbs less water than hemp and sisal. It also has more cellulose than lignin, which is important in the auto industry.

Table I. 5. Date palm fiber chemical constituents.

Constituent	**Proportion (Wt.%)**
Oxygen	20.45
Calcium	0.20
Carbon	75.86
Cobalt	0.62
Magnesium	0.15
Sulphur	0.12
Nitrogen	0.07

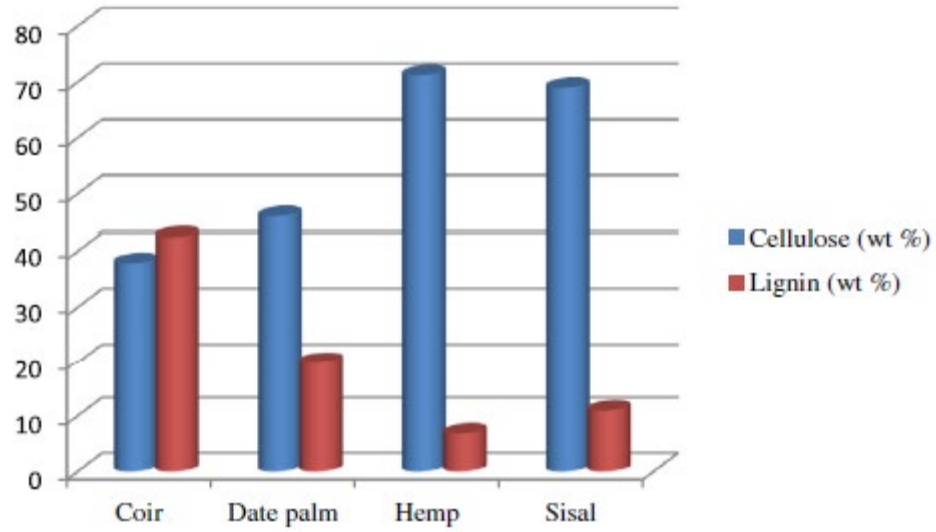

Figure I. 17. Comparative analysis of the lignin and cellulose contents of DPF and alternative natural fibers [237]

I.9.6. Density

This trait is highly coveted in natural fibers since it contributes to reduced weight and enhances the competitiveness of natural fibers against synthetic ones. This phenomenon is attributed to the inherent capacity of the mechanical qualities in the automotive industry, such as the particular tensile strength and specific modulus of elasticity. These mechanical pro perties are evaluated in relation to the density of the fibers.

Figure I.18 compares date palm fiber with coir, hemp, and sisal in terms of density properties. The comparison was conducted using the mean values documented in the literature and presented in Table 5. Evidence demonstrates that date palm fiber possesses the most minimal density value.

Consequently, date palm fiber exhibits strong competitiveness compared to other fiber types, resulting in the lightest weight composites. This makes it very ideal for the automobile industry. This outcome aids in diminishing the energy consumption required for automobiles manufactured using DPF-NFC materials, hence enhancing the sustainability of this industry.

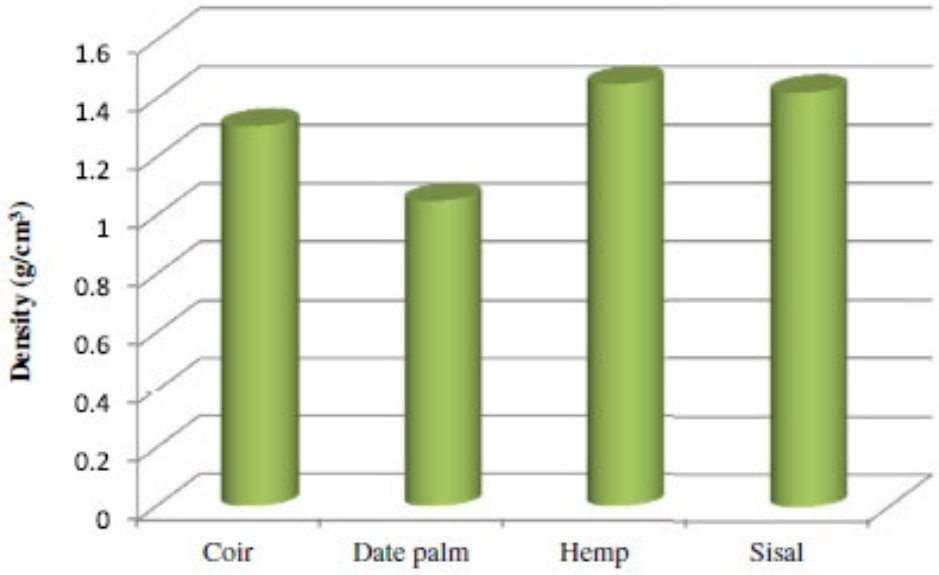

Figure I. 18. Comparing the Density of the date palm to that of alternative natural fibers Al-Oqla [237].

I.9.7. Thermal attributes

a- Thermal conductivity

Industrial applications, especially those in the automotive sector, emphasize the thermal insulation characteristics of materials utilized in the interior design of cars. First, one of the most desirable attributes of natural fibers is their hollow tube structure, which offers superior insulation against heat and noise. In automotive applications, a lower thermal conductivity is preferable. Agoudjil et al. (2011)[75] reported that the thermal conductivity values for date palm, hemp, and sisal are 0.083 (W/m K), 0.115 (W/m K), and 0.07 (W/m K), respectively.

In contrast, the thermal conductivity value for coir is 0.047 (W/m K), according to Srikanth et al.[76]. The findings demonstrate the competitive advantage of date palm fibers in automotive applications. Figure I. 19 reveals that the conductivity of date palm fibers is lower than that of hemp; however, it is still comparable to sisal. Date palm fibers possess the necessary qualities to be used as insulation materials in different sectors, such as the construction and automotive industries. DPF can serve as an advantageous addition to the automotive sector.

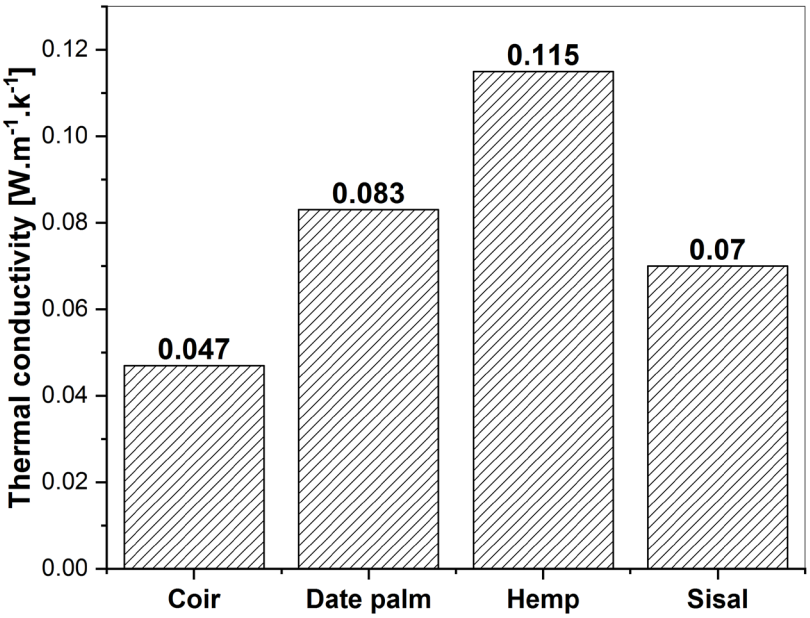

Figure I. 19. Comparing the thermal conductivity of the date palm to that of alternative natural fibers.

b-Thermal stability

The thermal stability of chemically extracted fibers was greater than that of mechanically extracted fibers. This phenomenon may be attributed to the chemical treatment's efficacy in eliminating hemicellulose and other substances that undergo degradation at lower temperatures. The thermogravimetric analysis (TGA) curves of date palm fibers exhibited similarities to those of other natural fibers, as reported by Ali and Alabdulkarem in 2017.

The degradation of fibers occurs in three stages, during which the fibers gradually lose components such as moisture infiltrates, hemicellulose and cellulose undergo degradation, resulting in a significant reduction in fiber mass (Figure I.20). Dense substances lignin is known to have a slow degradation rate, as evidenced by studies conducted by Taha et al. [77 ,78] and Ali et al. [79]

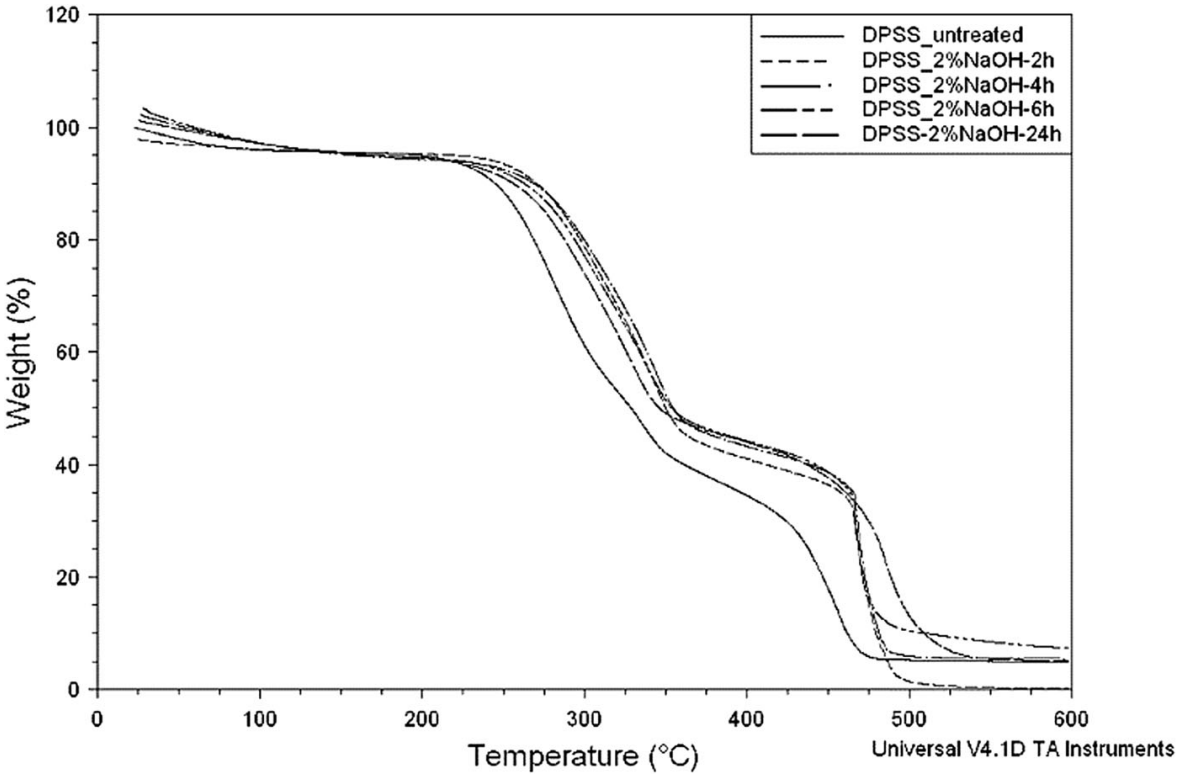

Figure I. 20. Curves of date TGA Stems of palm fibers were exposed to a 2% NaOH solution for varying amounts [67].

I.9.8. Mechanical properties

The literature compared the specific tensile strength and modulus of date palm fibers to other natural fibers, as illustrated in Figure I.21. Date palm fibers exhibit superior tensile strength compared to bamboo, coir, sisal, and banana fibers. The specific modulus of the date palm is approximately equivalent to that of flax fibers [80]. The extraction method has a substantial impact on the mechanical characteristics of fibers. The mechanical characteristics were enhanced by removing the fibers using NaOH. Nevertheless, the tensile and elastic moduli exhibit dissimilarities, with the elastic modulus demonstrating significantly higher numerical values. Other factors could contribute to this, such as the length of the treatment, the temperature, and the concentration of NaOH.

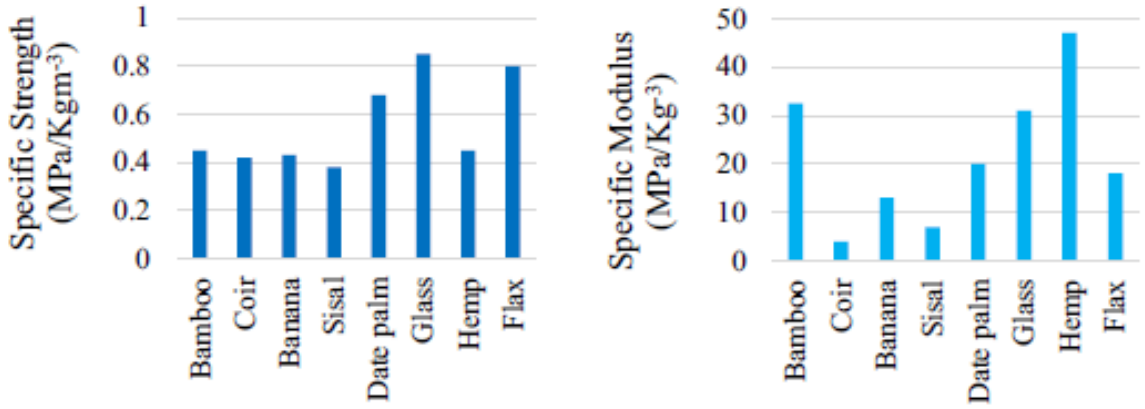

Figure I. 21.Comparing the specific tensile strength and modulus of natural fibers, date palm, and, glass . [205].

Furthermore, Figure I.23 illustrates the percentage of elongation to break date palm fibers, which was observed to be greater than that of sisal and hemp but less than that of coir. Table 8 compares the mechanical characteristics of date palm fibers obtained from various sections. Regrettably, the values documented in the literature do not fall within a specific range or exhibit proximity to one another. Furthermore, no credible source has supplied data on the tensile strength, Young's modulus, or tensile strain of date palm fibers, making it impossible to compare the findings. This may be attributed to the fact that the fibers obtained in the literature were predominantly fragmented or truncated into extremely short lengths. Nevertheless, it was noted that the fibers treated with NaOH exhibited superior mechanical qualities compared to the untreated raw fibers.

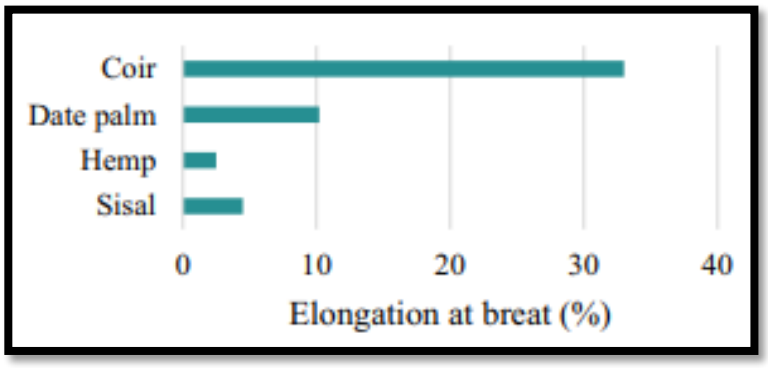

Figure I. 22. Comparison of the elongation at break percentages of several natural fibers. [205]

B. General on insulation and thermal comfort in building constructions.

I.10. Strategies for minimizing energy usage and thermal insulation methods

I.10.1. Comprehensive Approach to Minimizing Energy Consumption and Enhancing Thermal Insulation

Climate change is a paramount issue of global significance, necessitating urgent action and the formulation of measures aimed at curbing energy use and ameliorating its environmental consequences. The mitigation of greenhouse gas emissions, with a specific focus on the building industry, is paramount in addressing the challenges of climate change. Recent studies and scholarly publications have yielded significant findings regarding diverse approaches to enhancing energy efficiency across varying climatic conditions [81].

Developing energy-efficient and comfortable buildings in tropical regions necessitates primarily emphasizing heat mitigation strategies and optimizing natural ventilation. Solar protection measures, such as shading features, help mitigate heat gain. Additionally, strategic design considerations can optimize natural airflow within the building, further enhancing its thermal comfort. It is imperative to reduce the utilization of air-conditioned environments whenever feasible [82].

The implementation of heterogeneous walls is a commonly employed method in tropical regions. The walls in question comprise a primary load-bearing wall, typically constructed using concrete and reinforced by additional insulating walls. This design enables efficient insulation at elevated levels while maintaining a slim profile and cost-effectiveness. In

addition, a range of energy efficiency measures exists to enhance buildings' efficiency and diminish energy usage[83].

High-performance buildings, commonly referred to as low-energy structures, are experiencing a growing prevalence in regions characterized by cold or temperate temperatures. These structures exhibit bioclimatic architectural design principles, which consider the specific climatic conditions of the region. Effective thermal insulation, generally with a thickness ranging from 15 to 20 cm, and high-performance windows are crucial for minimizing heat dissipation to the external environment.

In order to attain a satisfactory degree of hygrothermal comfort within tropical climates, it is advisable to employ four interrelated strategies: solar protection, ventilation, thermal inertia, and insulation. These measures synergistically contribute to heat protection and the establishment of a pleasant indoor environment [84].

Recent research and studies have yielded significant findings regarding energy-efficient building strategies in tropical climes. The primary objective of these solutions is to enhance energy efficiency by maximizing the utilization of natural elements and resources, such as solar protection and natural ventilation. Substituting hollow concrete with aerated concrete for constructing walls has substantially reduced energy consumption [85].

In conclusion, recent scholarly sources and empirical studies underscore the significance of employing energy-efficient building solutions in tropical climates. The tactics above prioritize implementing measures aimed at safeguarding against heat, promoting natural airflow, enhancing thermal insulation, and utilizing suitable construction materials. Implementing these measures makes it feasible to decrease energy consumption and alleviate the influence of buildings on climate change.

Numerous researchers have researched diverse methodologies and put forth various solutions, all providing adequate thermal insulation of structures and a consequent decrease in energy usage. Several potential solutions can be identified, including sun protection, human behavior modification, interior thermal insulation, external thermal insulation, and insulation integrated into materials [86–88]. These options will be further discussed in the subsequent sections.

I.10.2. The Definition of Thermal Insulation, Its Significance, Placement of Insulators, and Selection Criteria.

The well-being and comfort of individuals within a building are essential considerations in daily life. When conducting any construction procedure, building constructors must consider this. In order to enhance comfort levels, it is imperative to develop a comprehensive grasp of the moisture and thermal characteristics shown by insulating materials employed within wall structures. Thermal insulation is crucial as an initial and rational energy efficiency measure, especially in buildings with high envelope loads in demanding climatic environments.

The notion of "thermal insulation" encompasses a range of methodologies employed to restrict the conduction-based heat transfer between a heated and a cooled environment, leveraging its substantial thermal resistance properties[89]. This technology is highly efficient in enhancing the thermal performance of the building envelope, improving internal thermal comfort, and hence leading to energy savings in buildings. Additionally, it is beneficial to mitigate the utilization of non-renewable natural resources, specifically oil and gas reserves, which are employed for energy generation to operate air conditioning and ventilation systems within buildings in tropical regions. This approach decelerates the depletion of these resources while concurrently diminishing the emission of greenhouse gases that are excessively released into our environment [90].

Thermal insulation has applications across various domains. This material is commonly utilized in several sectors, such as construction, industrial, automotive, cold storage facilities, culinary settings, and textile manufacturing [91]. The composition of the insulation can vary, ranging from a singular insulating material to a composite of multiple insulating materials. In order to optimize the performance of the building envelope in a humid tropical climate, it is imperative to consider the selection and placement of appropriate insulating materials as crucial factors in any effective thermal insulation procedure [92].

The fundamental emphasis of bioclimatic building lies in thermal insulation. The reduction of heating or air conditioning requirements yields significant environmental benefits, including the conservation of energy resources and the mitigation of greenhouse gas emissions. The concept of bioclimatic design is of paramount importance in the realm of energy saving. The objective is to mitigate the utilization of energy resources derived from fossil fuels and mitigate the levels of atmospheric pollution, all while ensuring that the

created edifice is suitably designed to accommodate the prevailing climate conditions and the unique characteristics of the land [93].

The implementation of insulation in a building serves to mitigate the transfer of heat between the interior space and the surrounding external environment. The necessity for heating or cooling can be reduced based on the prevailing climate conditions. The effectiveness of thermal insulation is influenced by several factors, including the temperature gradient between interior and outdoor environments, the geographical location, prevailing weather conditions, and the specific characteristics of the room requiring heating. In regions characterized by humid tropical climates, where structures are subjected to elevated solar radiation and temperatures, providing cooling measures is typically necessary for inside spaces. The use of thermal insulation can sustain energy efficiency in different climates. However, the effectiveness of this insulation may diminish over time as the material ages [94].

The foundation of thermal insulation is rooted in the principle of passive housing. The planning of the building should be undertaken in consideration of the climatic challenges specific to its location. In our specific scenario, characterized by a humid tropical climate, the primary focus lies in implementing measures to mitigate solar exposure. Implementing effective insulation in a building leads to a decrease in energy usage. In most instances, the reduction in energy consumption is accompanied by a corresponding decline in greenhouse gas emissions. Therefore, this is a noteworthy contribution to the ongoing efforts to mitigate climate change. The selection of appropriate insulating materials plays a crucial role in the design and renovation of buildings, as it significantly contributes to improving the energy efficiency and indoor thermal comfort of these structures. Ultimately, this leads to energy conservation. Undoubtedly, regardless of climatic conditions, it is strongly advised to employ insulation in walls and roofs to enhance a given room's comfort level and energy efficiency [95].

Thermal insulation is commonly employed to protect a building's envelope from high and low temperatures. However, in regions with tropical climates, the primary purpose of its utilization is to safeguard the walls of the structure against the detrimental effects of solar radiation. The placement of insulation is of utmost importance in determining the thermal efficiency, hygrothermal characteristics, and long-term durability of a building's walls. To effectively mitigate heat transfer, it is imperative to adopt a strategic methodology

encompassing the insulation of critical structural elements within the structure. These components encompass the roof and the walls, doors, and windows, which are particularly susceptible to heat exchange. Thermal insulation has the potential to be put on either the exterior or interior of the building envelope [96]. Both insulation arrangements possess distinct drawbacks and are commonly employed in insulating roofs, walls, ceilings, and floors.

The pursuit of comfort within the construction industry is fundamental, leading builders to employ thermal insulation in regions characterized by high humidity and tropical climates. The thermal conductivity of a material is a significant factor in determining its ability to insulate effectively. Nevertheless, additional considerations need to be considered while selecting insulation. Several factors contribute to the longevity of a material, including its specific heat, potential health risks (such as toxicity), tensile and compressive thermal resistance, cost and availability, durability and recyclability, thermal resistance, ease of implementation, resistance to direct sunlight, absorption capacity, and resistance to humidity [97].

In regions characterized by humid tropical climates, the utilization of conventional or bio-sourced insulators in conjunction with MCPs (Phase Change Materials) is effective in mitigating the transmission of heat and enhancing the thermal comfort of buildings [98]. Incorporating naturally existing plant-based bio-sourced materials has demonstrated promising results in this context. This has the potential to result in a reduction in the duration of discomfort. Nevertheless, plant fibers continue to possess a higher degree of environmental friendliness.

I.10.3. Sun protection

The implementation of solar protection measures plays a crucial role in improving the energy efficiency and natural light control of pre-existing structures and maximizing the design potential of low-energy buildings[99]. Implementing this technology has a notable influence on reducing energy consumption in buildings and enhancing the thermal and visual comfort experienced by inhabitants. The thermal transfer between buildings and their surrounding environment is influenced by the composition of the walls, regardless of whether they are opaque or transparent. According to sources [35], the solar input received through the roof constitutes approximately 60% of the total, while the walls contribute between 20% and 30%. Additionally, windows are responsible for approximately 15% to 30% of the solar

input. Hence, solar protection systems enable the modification of window and façade characteristics in response to environmental conditions and the requirements of occupants[100]. During the summer season, the implementation of solar protection measures on glazed openings and exterior surfaces is of considerable importance in managing solar radiation and its impact on thermal comfort conditions and energy consumption within buildings[101].

Sun protectors are employed in regions with humid tropical climates, such as Guadeloupe and Haiti, to mitigate the impact of sun radiation throughout the year. Solar protections for building envelopes in the intertropical zone play a crucial role in mitigating the impact of high sunlight and insolation temperatures, particularly during the peak hot time when the sun reaches its zenith. These protective measures serve a dual purpose by not only minimizing solar input but also effectively reducing the cooling requirements of buildings [102,103].

Including the requirement of plant protection surrounding the building and the implementation of solar protection measures on the roof, walls, and openings [104] (Figure I. 24). The presence of vegetation in the vicinity of a building has a beneficial effect on the comfort of its occupants. This is primarily due to the provision of shade, the effectiveness of which is contingent upon the density of the foliage. According to a study conducted by researchers [30], it has been found that this particular material can effectively obstruct a significant portion of solar light, ranging from 60% to 90%. As per the Thermal Acoustic and Ventilation Regulations (RTAA-DOM 2016), the strategy for solar radiation mitigation involves the use of sun protection measures [105].

-The creation of shadow can be achieved through a sunshade, which exhibits a distinct masking coefficient denoted as Cm.

-One can minimize radiation absorption by selecting lighter hues.

-If deemed essential, it is imperative to minimize thermal transmission by employing effective thermal insulation techniques. Thierry et al.[106] suggest that the sun protection method encompasses meticulous plan design, judicious building orientation selection, and appropriate utilization of vegetation. It is imperative to incorporate solar protection measures for every constituent element of the building envelope.

-Implementing solar protection measures for roofs includes using high albedo surfaces, incorporating double-vented roofing systems, and applying insulating materials, particularly in buildings that rely on artificial air conditioning.

-Sunscreens, such as shutters or canopies, are commonly employed in architectural design to provide shade and protection for openings, windows, and doors. Additionally, it is desirable for these sunscreens to possess airtight qualities, particularly in the context of air-conditioned buildings.

-The implementation of a high albedo coating on walls that are subject to significant solar radiation, along with thermal insulation in buildings that rely on artificial air conditioning, is a recommended approach.

In addition, it has been observed that in the context of daytime building usage, solar protection measures should prioritize the walls oriented towards the East, in conjunction with the roof. In order to ensure continuous usage, it is imperative to safeguard both the Eastern and Western barriers. The walls oriented towards the East and West experience the highest levels of sun radiation. Multiple strategies exist for mitigating the effects of solar radiation on a wall [107].

Figure I. 23. An Example of an EcoHousse is in Milan- Italy.

-Utilizing horizontal shielding mechanisms, particularly for the North and South facades exposed to near-vertical solar radiation, such as canopies, visors, and roof overhangs, is recommended.

-The utilization of vertical solar protections, such as vented siding or double ventilated walls, plants, lattices, and similar methods, is being explored in this context.

-The selection of lighter tints, while a potentially beneficial strategy, needs to be improved in addressing the issue, particularly in the Eastern and Western regions.

- Insulation is not advised if the North and South walls are light-colored. The East and West walls are primarily recommended for this purpose [107].

Bioclimatic or air-conditioned structures can protect the roof from direct sunlight. Adding flora or bright colors always works. The author suggests that thermal insulation could reduce the solar factor and protect against solar radiation. In air-conditioned buildings, roof thermal insulation may hinder nighttime cooling. To reduce solar heat gain in bioclimatic buildings, window and opening orientation and placement should be chosen. A comprehensive solar protection strategy, including plant and architectural protections, is needed. Type and placement of these protections depend on structure orientations and purposes. These protections may be fixed, mobile, external, or internal. [108].

The author also noted that bioclimatic and air-conditioned buildings share sun protection concepts. Unless the building operates as a hybrid, alternating between air conditioning and natural ventilation based on seasonal conditions, natural ventilation is less important.

I.10.4. The Study of Human Behavior

Effective energy management in buildings encompasses more than only the thermal insulation of opaque walls (including walls and roofs) and solar protection for windows.

The building features opaque walls, including the walls, roof, and solar protection windows. Additionally, it is important to emphasize the utilization of electrical equipment by the tenants. Implementing thermal insulation on roofs and walls enhances the comfort of naturally ventilated buildings in various climatic conditions. It reduces energy consumption by air-conditioning units during periods when air-conditioning is necessary (Kumar, Ashok)[109]. The latter approach has little impact on using electric bulbs, irons, and other human household equipment. It is essential to acknowledge that the sole method of mitigating the ingress of natural light is through the insulation of windows. If not controlled, this ingress

may result in a heightened reliance on artificial lighting [49]. The behavior of individuals has a significant influence on the energy performance of buildings.

The factors mentioned by Lee, Chun Kwong, et al. [110] should be considered. The presence of humans in buildings can result in substantial energy loss due to their negligent behavior, such as leaving lights on in unoccupied rooms, keeping appliances plugged in unnecessarily, or setting air conditioners to too-low temperatures. The study conducted by K.F. Fong et al.[110] demonstrated the impact of human behavior on building consumption in Hong Kong.

Various solutions were created to reduce energy usage in buildings. The study showed that by raising the air-conditioning setpoint from 24°C to 25.5°C, a reduction in air-conditioning energy consumption of 19.6% was achieved. An additional decrease of 17.9% was attained through deactivating the bedroom lighting while the bedrooms were not in use. The implementation of a strategy to turn off bedroom lights when they are not being used resulted in a significant reduction of 27.4% in energy consumption related to lighting.

During periods of non-occupancy. Deactivating all extraneous appliances while they are not being utilized results in a reduction in energy consumption by 5.5%. The researchers have indicated that the measures implemented, which are exclusively associated with human behavior, contribute to a 15.1% reduction in energy consumption for the building under investigation. Based on the above information, it can be inferred that human behavior significantly influences energy management within the construction sector. The energy consumption within the building sector holds significant importance, as its contribution cannot be disregarded. Implementing thermal insulation techniques in conjunction with modifications in human behavior within a tropical climate would yield substantial energy conservation in buildings.

I.10.5. Thermal insulation on the inside

The Interior Thermal Insulation (ITI) process entails affixing an insulating material to the interior of a building in direct contact with the structural components. This is achieved by applying an insulating layer to the inner surface of the building's walls [111]. One advantage of this system is its convenient application within the building. However, a negative of this system is the potential construction of thermal bridges at the points where floors and partition walls are located. The technological accessibility and cost-effectiveness of implementing ITI surpass those of external thermal insulation.

Figure I. 24. Diagram of internal isolation of a wall.

However, it is essential to note that ITI does present certain drawbacks, including the reduction of interior space within the room and the impact on thermal inertia [112].

The most straightforward and prevalent approach is maintaining the building's exterior aesthetics without any alterations. When determining the extra thickness of interior walls, it is essential to consider several factors, such as window apertures, outlets, and pipelines.

In a humid tropical climate, the significance of ITI (inside thermal insulation) is acknowledged. However, ITI may not be the most optimal or suitable approach in addressing the primary objective of shielding the building from solar radiation. In a given climatic context, it is plausible for wall performance to diminish during rainy periods due to the potential accumulation of moisture [113].

I.10.6. Thermal isolation of the exterior

Exterior Thermal Insulation (ETI) involves installing an insulation layer and various cladding material layers (mineral or organic coating, timber, etc.) on a building's exterior walls. It is commonly found in homes and offices. Technically, this is the optimal course of action, as it ensures complete insulation. Eliminating thermal bridges responsible for heat loss and maintaining good thermal inertia within the building yields a thermal envelope with superior thermal performance. The thermal performance of a building is affected by its envelope; one of the most common ways to enhance the envelope is to insulate the exterior [114].

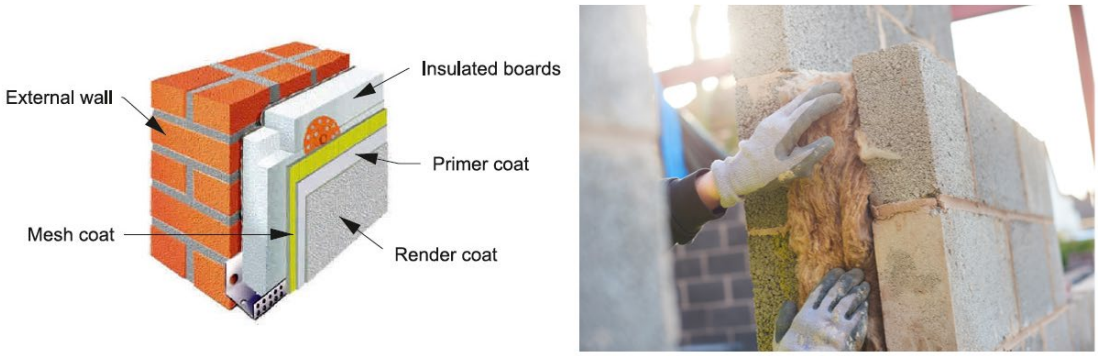

Figure I. 25. Diagram of exterior insulation of a wall.

According to Chengcheng Xu et al. (2019) [115], several studies have been conducted on the characteristics of exterior thermal insulation (ETI) and interior thermal insulation (ITI) walls in various buildings and regions.

These studies demonstrated that the ITI wall configuration reduces energy consumption in air-conditioned buildings more effectively. However, ETI walls are generally 2 to 11% more efficient than ITI walls. We have yet to find any research on ETI in tropical climates, but according to the sustainable construction guide, walls can be insulated from the outside in tropical climates. The mortar of granules (expanded polystyrene, perlite) and an adhesive (e.g., cement) should be applied to the exterior using a bonding layer. In a humid tropical climate, roof insulation can be performed inside or outside. This involves minimizing heat transfer from the roof, so exterior insulation is preferable. In a humid tropical climate, ETI could shield the building envelope's components from humidity, reduce temperature fluctuations, and extend the envelope's lifespan. In fact, Mendes et al. [116] demonstrated in their research that ignoring the influence of wall humidity can result in a 59% underestimation of the annual integrated thermal flux.

Despite its significance, ETI has the disadvantage of being susceptible to weather and accidental damage. It cannot be used on historic structures due to the need to preserve their unique and primordial appearance. According to Boudenne et al. [117] research, there are three ETI techniques:

-ETI under plaster consists of rigid insulation (typically polystyrene or mineral wool) affixed to the wall with glue and/or mechanically with dowels or profiles, over which a weatherproof coating is applied.

-ETI under cladding is a mechanical fastening system that permits the insulation and battens that support the cladding to be fastened. The air cavity created between the cladding and insulation mitigates external forces.

-ETI under veneer/cladding is a hybrid solution: insulated sandwich panels are mechanically attached to the wall and coated directly with cladding without an air gap.

The author was able to conduct ETI experiments in a bioclimatic chamber insulated with polystyrene and bio-based materials such as glass wool and wood wool. The installation of ETI systems was observed to reduce thermal flows to less than 3 Wm-2.

I.10.7. Integrated insulation in construction materials

Thermal insulation of a building's walls is predominantly carried out on the exterior or inside. Nevertheless, it is worth noting that insulation can also be incorporated into construction materials, specifically in mortars such as hemp concrete and aerated concrete.

Incorporating insulation into cement can potentially improve the thermal insulation properties of construction materials [118]. The proposal for creating composites by combining cement with plant fibers such as banana, coconut, sisal, and sugarcane bagasse has been suggested to acquire affordable insulating materials for building [119].

Extensive research has been conducted on the macroscopic properties of cement, mortar, or concrete when reinforced with glass fibers. The existing body of research on composite materials demonstrates their notable efficiency, resulting in significant energy conservation and waste reduction. The research conducted by Bilba et al.[120] involved the analysis of banana samples, including leaves and trunks, as well as the husk and tissue of coconuts. These samples were investigated to assess their suitability for integration into cement matrices, aiming to develop insulating materials for use in building construction. The recently acquired reinforced composite materials' thermal performance and mechanical qualities have been improved.

I.10.8. Highlighted criteria for selecting an insulating material

Thermal insulation holds significant relevance in tropical climates. Undoubtedly, in light of the present circumstances characterized by a rising average surface temperature of the Earth, the pursuit of thermal comfort for individuals inhabiting a structure is of utmost importance. The level of comfort experienced within a structure is contingent upon using bio-based

insulating materials throughout the building envelope. When selecting insulating materials for efficient thermal insulation of buildings, it is crucial to consider numerous criteria.

The factors to consider when evaluating an insulating material include its thermal resistance, durability, recyclability, cost, availability, ease of transport, toxicity in terms of health risks, mechanical resistance to compression and tension (traction), absorption and resistance to humidity, ease of application or installation, thermal conductivity, specific heat storage capacity, and resistance to direct sunlight[89].

I.11. Thermal comfort definition and approach

Thermal comfort refers to the subjective experience of feeling physically and psychologically at ease within an interior environment, particularly within the confines of a structure. This methodology facilitates the examination of the thermal responses of the human body in order to adapt to its surroundings [121].

Simultaneously, it evaluates the requisite and permissible technological circumstances for implementation, contingent upon five parameters [35], namely:

-The metabolic rate of an individual.

-The attire of the person

-The thermal conditions within the residential environment, including the dry, radiant, and ambient temperatures.

-The velocity of air flow surrounding an individual

-The atmospheric humidity.

The human body generates thermal energy, which is subject to variation in magnitude based on levels of physical exertion. In order to sustain a consistent body temperature of approximately 37°C, the human body must engage in thermal regulation mechanisms, which involve the adjustment of blood circulation and sweat levels. According to the American Society of Heating, Refrigerating, and Air Conditioning Engineers (ASHRAE) [122], comfort is defined as the psychological state in which individuals express happiness with the thermal environment. Individuals may experience different thermal sensations in the same setting, influencing their unique degrees of comfort and resulting in varying impressions. The assessment of satisfaction with the thermal environment is a multifaceted subjective reaction influenced by various interrelated factors and possesses a less concrete

nature [123]. Thermal comfort is influenced by various behavioral and action-oriented factors, including but not limited to altering clothing, modifying activities, changing positions, adjusting the thermostat or air conditioner, opening windows, expressing dissatisfaction, or vacating a particular location.

I.12. Thermophysical and hygrothermal parameters of bio-based materials for thermal insulation.

I.12.1.Definition of bio-sourced materials

Biosourced materials are characterized as materials in which at least one of their constituents originates from biomass. Biomass encompasses a wide range of plant-derived substances, including but not limited to wood, hemp, straw, bamboo, coconut, banana, bagasse, and flax [124]. Additionally, biomass includes animal-derived materials such as skin and fat, with the exception of those sourced from geological or fossil origins [125]. Biomass is widely recognized as a sustainable and optimal energy resource capable of substituting fossil fuels.

Using bio-sourced materials in constructing building envelopes has economic, social, and environmental advantages owing to their renewable, environmentally benign, and recyclable characteristics. Indeed, utilizing these methods can contribute to mitigating the depletion of fossil energy resources and reducing greenhouse gas emissions, specifically, the atmospheric carbon dioxide that plants absorb during photosynthesis. In recent decades, it has been widely acknowledged that climate change on a global scale has mostly been driven by anthropogenic greenhouse gas emissions. This process is notably characterized by the increase in mean air and ocean surface temperatures, the depletion of the ozone layer, extensive melting of snow and polar ice, escalating sea levels, and instances of drought. Using biosourced materials in the building envelope within tropical regions might contribute to establishing a conducive indoor environment, particularly by enhancing indoor air quality and promoting thermal comfort.

Biosourced materials can be utilized in many applications within the present construction industry. Natural fibers can be effective thermal insulation materials, including coconut, banana, bagasse, wood wool, straw bales, cellulose wadding, and hemp. In addition, various elements such as wood, hemp concrete, and flax concrete can be employed as structural or filling components to enhance the overall stability of the building. Ultimately, these materials have the potential to serve as effective coatings, exemplified by the utilization of hemp-lime and earth-straw mixes.

I.12.2. The Concept of Thermal Conductivity

The thermal conductivity of a substance is a fundamental property that describes its capacity to transport heat through mediums without any noticeable movement of matter at a macroscopic level. The term "thermal conductivity" refers to the quotient of the rate of heat transfer (expressed in Watts) and the temperature gradient across a given surface area [126]. Thermal conductivity is a highly desirable thermo-physical property in construction materials. It quantifies the capacity of heat to efficiently propagate through a solid object in a condition of equilibrium. The thermal conductivity is influenced by the inherent characteristics of the material as well as its temperature [127]. Thermal conductivity can be regarded as the primary thermal attribute of any insulating material, as the material's thermal resistance determines it. Insulating materials are distinguished by their low thermal conductivity and high thermal resistance. At the nanoscale, heat transfer in materials can occur through several particles or quasi-particles.

The combined effects of each particle determine a material's thermal conductivity. Atomic and molecular structure, porosity (air pockets), and anisotropy affect thermal conductivity in insulators at the microscopic level [127]. Biomaterials like plant fibers are porous. In humid tropical climates, hourly temperature and humidity changes can affect thermo-physical properties like thermal conductivity. Thus, humidity, density, temperature rise, and applied pressure affect thermal conductivity [128]. Temperature and humidity can increase thermal conductivity and compromise an insulating material's hygrothermal performance. The energy conservation efficiency of a structure decreases as thermal conductivity increases.In arid environments, the determination of thermal conductivity follows the principles outlined in Fourier's law, which provides a mathematical expression for its calculation during a state of equilibrium [129].

$$\lambda_0 = \frac{\emptyset_e}{S(T_1 - T_2)}$$

When materials experience substantial fluctuations in humidity levels (H), it is possible to establish a correlation that enables the estimation of the thermal conductivities of both the dry and wet materials without direct measurements. This correlation involves using the exponential function, denoted as "exp."

The equation (1) is an exponential decay model, where λ represents the decay rate, λ_0 represents the initial decay rate, and H represents the decay time [35]. The equation may be written as:

$$\lambda = \lambda_0 e^{0.08H} \qquad (1)$$

I.12.3. The Concept of Thermal Resistance

Thermal resistance, symbolized as Rth measures the resistance to the passage of heat between two isotherms where heat transfer occurs by conduction, convection, or radiation. Isotherms can manifest as flat and parallel surfaces, such as the walls or roofs of buildings. This text elucidates thermal insulation's capacity to withstand high and low temperatures. It is observed that insulation becomes more efficient as its thermal resistance increases.

When a uniform layer of plant fiber with a thickness denoted as 'e' is subjected to a unidirectional heat flow in a one-dimensional manner perpendicular to its cross-section, the thermal resistance of the layer may be determined using the relationship provided in references [1].

$$R_{th} = \frac{e}{\lambda_0 S}$$

I.12.4. Thermal Effusivity and Thermal Diffusivity

Thermal effusivity pertains to the capacity of materials to absorb or dissipate thermal energy rapidly. The concept of effusivity pertains to the perception of thermal experience, precisely the degree of warmth or coldness conveyed by a specific material. A substance with a high effusivity (E) efficiently absorbs a substantial amount of energy while experiencing minimal surface temperature increase. Such materials include metal, stone, and pottery [130].

Insulating materials like wood have a low effusivity number because they rapidly increase in temperature and absorb little heat. Thermal effusivity is inversely proportional to heating rate, so lower values heat faster. Conversely, higher thermal effusivity values increase heat absorption without increasing temperature.

After one second, a material surface of one square meter transfers thermal energy, measured in kilojoules (KJ), to another surface one square meter hotter and one degree Celsius higher.Similar to the diffusivity (α), the thermal effusivity (E) is determined by the thermal capacity and thermal conductivity (λ) of the material. The thermal effusivity is stated in $W.S^{1/2}m^2K^{-1}$, while the thermal conductivity (λ) is expressed in $Wm^{-1}K^{-1}$. Additionally, the

material's specific heat (Cp) is measured in $JKg^{-1}K^{-1}$, and the density of the material (ρ) is measured in Kgm^{-3}.

$$E = \sqrt{\rho \lambda C_P}$$

A substance conducts heat at thermal diffusivity, measured in square meters per second. Heat conduction is mostly affected by wall insulators like plant fibers. Low thermal diffusivity slows material heat transfer [130].

$$\alpha = \frac{\lambda}{\rho C_P}$$

Thermal effusivity is a parameter that can be used to describe the capacity of a material to undergo temperature variations in response to thermal energy absorption. Two phenomena co-occur concurrently [35].

-The absorption of energy occurs in a localized manner, contingent upon the thermal capacity of the material.

-The transfer of energy occurs between adjacent regions, and the extent of this transfer is contingent upon the material's thermal conductivity.

The concepts of effusivity and diffusivity are utilized to assess a material's thermal inertia, which refers to its capacity to retain and disperse thermal energy over time.

Conclusion

In summary, Chapter 1 introduces composite materials and thermal insulation. Composite materials, made by combining different materials, offer enhanced properties. Natural and synthetic fibres are used for reinforcement, with adhesion optimization methods improving performance. Thermal insulation materials are crucial for human comfort in buildings, and various options are available. The chapter also discusses using natural fibres from date palm trees for sustainable materials. Understanding these materials is vital for designing efficient solutions.

Chapter II. BIBLIOGRAPHIC REMINDER

Introduction

Chapter 2 provides a comprehensive review of relevant research in the field of composite materials and thermal insulation. The chapter is structured into three parts, each highlighting different aspects of previous studies. The first part discusses the utilization of polystyrene in composite materials, while the second part focuses on the use of gypsum as a matrix. The third part summarizes studies involving date palm fiber as reinforcement. This review aims to provide a solid foundation for understanding the current state of research in the field, setting the stage for the research presented in this thesis.

II .1.Works on polystyrene composite

Hittini et al.[7]: In this investigation, Authors explored the mechanical behavior of composites comprising date pit and polystyrene (DPP-PS). These composites were designed as thermally insulating materials for the construction industry, featuring varied proportions of date pit content (0%, 10%, 20%, 30%, 40%, and 50%). Generally, they found that an increase in filler content resulted in a weakening of mechanical properties. The decrease in the compressive strength of the composite was negligible when the filler content was below 30%. The DPP-PS composites exhibited higher tensile strength (ranging from 1.12 to 0.34 MPa), compressive strength (ranging from 11.58 to 2.31 MPa), and flexural strength (ranging from 21.10 to 2.37 MPa). The deterioration in mechanical properties when incorporating DPP into PS was explained by the agglomeration of natural fillers, creating stress concentration points, and the poor compatibility between fillers and the polymer matrix. Agglomeration of filler particles, facilitated by hydrogen bonds, and the weaker strength of filler particles compared to the polymer matrix hindered stress transfer and led to stress concentration.

Notably, an alkaline treatment of DPP using NaOH solution effectively enhanced the tensile and flexural strength of all prepared composites. This treatment improved compatibility between the matrix and natural fillers. SEM image analysis revealed alterations in the surface roughness of DPP, indicating enhanced interaction between fillers and the PS matrix. TGA analysis and FTIR spectra of the treated filler confirm that improved adhesion resulted from removing hydrophilic components from DPP.

In the other side Basim Abu-Jdayil et al.[131] investigate the thermophysical proprieties of the previous composite material elaborated by Hittini et al.[7], The results obtained in this study demonstrate that date pit powder can serve as a filler in a polystyrene matrix, resulting in the formation of insulating composites with both low thermal conductivity and low density. The authors found that as the date pit content increased, there were slight increases in both the thermal conductivity and density. The composite, containing 40 wt.% date pit powder, exhibits the following properties: a thermal conductivity of 0.0558 W/m K, a water retention of 26.0%, and a bulk density of 565 kg/m^3.

In contrast, composites with 10-DPP, 20-DPP, and 30-DPP exhibited lower water retention at room temperature and hot water immersion. The substitution of one-third of the traditional building wall material with DPP-polystyrene composite demonstrates the potential for use in construction, functioning as a thermal insulator and resulting in an 85% decrease in overall thermal conductivity.

Masri et al. [2] present an experimental study on the characterization of innovative wood-plastic composites based on waste materials (date palm fibers, expanded polystyrene). Date palm leaflets are used as reinforcing particles, and expanded polystyrene EPS waste dissolved in gasoline is used as a matrix. The results were obtained after mechanical, thermal, and morphological tests on composite materials prepared in different particle sizes and mass fractions. The results obtained from mechanical, thermal, and morphological tests on composite materials prepared in different particle sizes and mass fractions show the excellent adhesion of the wood/matrix interface. According to the authors, Mechanical properties are acceptable, with a flexural modulus and maximum stress of up to 0.78GPa and 2.84MPa, respectively, and densities ranging from 542 to824 kg/m3, comparable to conventional materials such as hardwood, softwood, and MDF. The average thermal conductivity was between 0.11 and 0.16 W/m.K. Using date palm waste as reinforcement in composites is considered an excellent natural reinforcement.

Adewale George Adeniyi et al. [11] fabricated and analyzed polystyrene composites reinforced with wood dust from the isoberlinia doka tree. The composites were made using the hand lay-up method under moderate pressure. The effects of different factors, including filler concentration (15%, 30%, and 45%), filler size (149 μm, 250 μm, and 841 μm), and NaOH concentration (2%, 4%, and 6%), on the mechanical properties of the composite were

investigated. Additionally, the impact of filler content on the thermal characteristics of the composite was examined. The composites were analyzed to assess their mechanical, thermal, and microstructural properties. The study found that the mechanical characteristics were significantly enhanced when the filler concentration was 30%, the filler size was 841 μm, and the NaOH concentration was 4% during the process. Furthermore, the composite notably enhanced its thermal properties when the filler content reached 30%. Additionally, the microstructural analysis suggested a positive indication of effective interaction between the filler and the polymer matrix.

Poletto et al.[8] their study examined the mechanical and dynamic mechanical properties of cellulose fibers-reinforced polystyrene composites as a function of cellulose fiber content and coupling agent effect (styrene-maleic anhydride (SMA). The composites were fabricated via a corotating twin-screw extruder and subjected to injection molding. The experiment involved three different degrees of filler loading (10, 20, and 30 wt%) and a constant dose of coupling agent (2 wt%). The findings indicated an increase in cellulose fiber content over 20 wt% reduced mechanical characteristics (Flexural Strength and Impact strength). On the other hand, including a coupling agent significantly enhances the mechanical and dynamic mechanical properties. Incorporating a coupling agent enhanced the storage modulus and decreased the damping peak values of the composites as a result of the enhanced interfacial adhesion. The height of the damping peak was determined to be contingent upon the cellulose fiber concentration and the interfacial adhesion between the fiber and matrix. The adhesion factor values validate that the utilization of a coupling agent leads to superior adherence.

Singha et al. [132] prepared and characterized composites using both untreated and chemically modified Agave fibers to investigate the impact of reinforcement on the mechanical properties of the polystyrene matrix. The Agave fiber underwent surface modification using the process of graft copolymerization, where methyl methacrylate (MMA) was grafted onto it using ceric ammonium nitrate (CAN) as the initiator. These composites were prepared using various fiber contents of both raw and grafted fibers, ranging from 10% to 30% by weight. Research has determined that a fiber concentration of 20% yields the most favorable mechanical qualities (tensile, compressive, and flexural strength). An investigation has also been conducted on how the mechanical properties of

composites are affected by varying fiber diameters, including particle, short, and long fibers. Particle reinforcement has been discovered to yield superior mechanical qualities compared to both short and long-fiber reinforcement. Scanning electron microscopy (SEM) study of composite samples that underwent tensile fracture revealed a more uniform dispersion of particles and short fibers in the polystyrene (PS) matrix, in contrast to the presence of long fibers. The thermogravimetric analysis/differential thermal analysis (TGA/DTA) techniques result in the surface-modified fiber-reinforced composites exhibiting greater thermal stability than the raw fiber-reinforced composites.

Zafar et al. [133] produce Polystyrene composites using an in-situ polymerization process, utilizing wheat, rice, and mustard husk as fillers. The study utilized three distinct loading levels (5%, 10%, and 15%) of filler material, as well as three different sizes (250–355 μ, 355–500 μ, 500–710 μ) of the filler particles. The objective was to investigate the impact of these compositions on various mechanical properties of the synthesized composites. It may be inferred that the tensile strength, flexural strength, and hardness generally rise as the amount of filler material increases and decreases as the size of the filler particles grows. The results indicate that using filler size between 250-355 μ with a loading of 5% yields the highest mechanical values across all three types of fillers regarding water absorptivity; a minor

Raza et al.[134] have developed thermoplastic insulating composites witch formed by melting expandable polystyrene (PS) and date palm surface fibers (DSF) at varying weight percentages (10-40%) in order to enhance biodegradability and encourage sustainability. The developed insulating composites had outstanding thermal characteristics, characterized by a low thermal conductivity of 0.053 W/(m.K) and a low thermal diffusivity of 0.045 mm^2/sec. The thermogravimetric investigation revealed exceptional thermal stability, with a T_{onset} above 300 ◦C and a negligible mass loss of roughly 6%. The differential scanning calorimetry revealed a glass transition temperature (Tg) of approximately 100 ◦C. The investigation of the lifespan of the PS-DSF composites revealed that they retained about 100% of their mass over 10 years when subjected to temperatures between 30 and 120 ◦C. This indicates that they are well-suited for insulating applications that need long-term durability. The incorporation of DSF also demonstrated favorable synergistic impacts on

thermal stability. The insulating composites exhibited enhanced compressive strength (19.33 to 22.66 MPa) compared to pure PS.

A novel technique for producing a composite material using polystyrene and hazelnut shell powder has been performed by Natalia Igorevna et al.[135] In their work. Results show that The ideal mixture of the composite consists of 60-80 weight percent of polystyrene and 20-40 weight percent of modified hazelnut shell powder. At a filler concentration of 30 wt.%, the composite exhibits the following properties: a density of 1154 kg/m3, a Vickers hardness of 20.19 at a load of 200 g, a water absorption rate of 2.1%, and a flexural strength of 20.41 MPa.

Abdu Mohammed et al.[136] examined the mechanical properties of flax fibers reinforced with extended polystyrene composites (FFEPS) with varying fiber content, including tensile strength, flexural strength, impact strength, and water absorption qualities. Results show that tensile strength significantly rose from 18.57 MPa to 25.28 MPa, representing a 36% improvement at a maximum of 30% fiber loading. However, it decreased to 12.08 MPa when the fiber loading reached 40%. Likewise, the tensile modulus increased from 2.64 GPa to 3.11 GPa, representing a significant 17.6% peak rise at a fiber loading of 30%, but then decreased to 2.56 GPa with a fiber loading of 40%. The impact strength and flexure strength of composites made from flax fiber and extended polystyrene increased as the fiber content increased to 30%, then decreased at fiber loading of 40%. The authors explained the decrease in tensile strength, tensile modulus, impact, and flexural strength values seen at a fiber content of 40% due to insufficient wetting and weak bonding between the fibers and the matrix. Simultaneously, the water absorption properties significantly increased from 1.49% at 20% fiber level to 3.48% at 40% fiber content due to the hydrophilic characteristics of flax fiber.

Ayse Bicer et al.[137] Examined The employment potential of Expanded Polystyrene waste Foam (EPS) as a filler material in plaster(Containing varying proportions of gypsum, namely 20%, 40%, 60%, and 80%.), which is enhanced with the addition of tragacanth resin (0.5%, 1%, and 1.5%) of the weight of the mixture To generate fake pores on gypsum block. The study reveals that the thermal conductivity, compression, and tensile strength exhibit a reduction when the proportion of EPS and tragacanth in the combination increases. The thermal conductivity of the material with 80% EPS and 1.5% resin content was measured to

be 0.047 W/mK, the lowest value obtained. On the other hand, while the EPS ratio increased, the water absorption rate decreased. They found that samples exhibited a water absorption ratio of over 30%. Consequently, the samples are unsuitable for use as outside plaster, according to this study.

The objective of the study conducted by Gehad et al. [138] was to create banana leaves-polystyrene composites (BL-PS) that can serve as an affordable and environmentally friendly thermal insulator. The BL powder was combined with PS in various weight ratios, specifically 90:10, 80:20, 70:30, and 60:40. Thermal conductivity, electrical conductivity, scanning electron microscopy (SEM), X-ray diffraction (XRD), Fourier-transform infrared spectroscopy (FTIR), thermogravimetric analysis (TGA), and differential scanning calorimetry (DSC) were performed on BL and BL-PS composites containing 10 wt.% (BL-PS1) and 30 wt.% (BL-PS3) of polystyrene (PS) powder. The produced composites have a low thermal conductivity, ranging from 0.0183 to 0.03168 W/m.K. The BL-PS1 had the lowest thermal conductivity of 0.0183 W/m.K, which can be attributed to its high crystallinity and thermal stability, which was found at 61.09%.

II .2.Works on gypsum composite

Achille D´esir´e et al. [139] studied the effect of adding fiber bundles taken from Rhecktophyllum camerunense (RC) and Ananas comosus (AC) to gypsum plaster composites.

The mean values for Young's modulus, tensile strength, and elongation at break of AC (respectively RC) fiber bundles were 12.2 GPa, 487 MPa, and 3.2% (respectively 5.2 GPa, 268 MPa, and 21.6%). For composite, results show that the dispersion correlated with the geometric characteristics of the fiber bundle's cross-sections, the gauge length, and the type of plant. Gypsum plaster composites were fabricated by casting/evaporation, utilizing a water/plaster mixing ratio of 0.8 and a fiber bundle volume content of 1%. The composites were evaluated utilizing bending and indentation tests. The investigation demonstrated that the examined fiber bundles resulted in a significant enhancement of the flexural stiffness, stress at fracture, and toughness of gypsum composites. However, these improvements needed to be improved to those achieved by an equivalent volume of glass fiber bundles.

The paper of Amara et al.[140] described a study that combines experiments and theory to investigate the thermal physical properties of composites made from plaster reinforced with

fibers from date palm trees. The "DICO" method was employed to ascertain the thermal conductivity and diffusivity of composites in this study (2%, 5%, 8% and 10%). The palm tree fibers are directly integrated into a plaster mixture without prior treatment. In addition, the interface of palm tree fibers is examined using Scanning Electron Microscopy (SEM). The experimental results demonstrate that The thermal conductivity of composites decreases from 0.431 W/m K for the sample lacking fibers to 0.232 W/m K for the most highly insulating material(reinforced with 10% of fibers). In addition, It has been shown that an increase in the ratio of fiber mass results in a reduction in the effective thermal diffusivity of the composite (from 4.225 to 3.417)10^{-7} m^2/s.

The objective of this study, realized by Djoudi et al. [141], was to investigate the impact of length and fiber content on the thermal and physical characteristics of date palm fibers mesh reinforced plaster concrete. The analysis of the results revealed that the thermal conductivity was strongly dependent on the fiber content. Therefore, the thermal conductivity decreased as the amount of fiber material rose. The specimen with the highest insulation properties was seen when 2% of the ratio consisted of date palm fibers measuring 20 mm in length. The statistics on lightweight aggregate concrete reported in the literature ranged from 0.3 to 0.6 W/mK, which aligns with the estimate provided. The experimental results demonstrated an inverse relationship between the heat-insulating effectiveness of a material and its dry unit weight. The authors explained that the decline in the thermal diffusivity and effusivity of this composite material as the fiber content in the matrix increases by the presence of fiber, regardless of concentration, does not facilitate the conduction of heat energy within the material.

Naiiri et al. [13] assessed the viability of employing doum palm fibers reinforced gypsum plaster as a thermal insulator in construction materials. For mechanical and thermo-physical characterization, several composite configurations containing three diameters and five weight ratios (ranging from 0.5% to 2.5%) of doum palm fiber were elaborated. Doum palm fibers were treated with a 1% concentration of NaOH solution to strengthen their resistance. Furthermore, the specimens underwent mechanical property testing after seven (07) days, twenty-eight (28) days, and one year of normal curing. The obtained results demonstrate that composites reinforced with treated fibers perform better mechanically. In actuality, gypsum mortar reinforced with treated reinforcement sieve at 1% of fibers produced better outcomes.

The study examined the long-term durability of gypsum mortar reinforced with doum fiber under natural aging conditions. After one year of natural aging, it was noted that the composite's performance had increased, with an average increase in flexural strength from 1.53MPa to 3.25MPa. In addition, the findings suggested a correlation between the thermal conductivity and the amount of fibers present. Consequently, the thermal conductivity diminished as the amount of fibers increased.

Gallala et al.[142] examined the impact of using date palm fiber waste (DPFW) (7, 10, 15, 17, and 20 %) as a reinforcing material on the mechanical characteristics of the plaster-based composite. An investigation has also been conducted on the effects of an alkaline treatment (1 %, 2 %, and 4 %) for 24 hours and the temperature used for drying. Results show that including DPFW enhances mechanical robustness as the proportion and length of the fibers increase compared to a control plaster. Additionally, The use of NaOH improved the rheological characteristics (flexion and compression) of the biocomposite. It decreased the delay in its performance by eliminating contaminants and certain soluble substances. In addition, the epoxy coating significantly aided in decreasing water absorption. The physical characteristics exhibited greater porosity and hydrophilicity, resulting in a high absorption capacity. The flexural and compressive strength gradually rose over time, which can be attributed to the process of plaster hardening and the enhanced adhesion between the matrix and fiber. An experimental demonstration showed that including 17% DPFW resulted in a composite material with a thermal conductivity of 0.52 $Wm^{-1}K^{-1}$ and a density of 1415 kg m^{-3}.

The primary aim of the study conducted by Ouakarrouch et al.[143] was to enhance the thermal characteristics of gypsum plaster by including chicken feather waste (CFW) and to utilize it in constructing wall and ceiling mortars. The thermal conductivity, thermal diffusivity, and thermal effusivity of the samples under investigation were determined using the steady hot plate, flash, and transient hot plate methods, respectively. The results demonstrate that increasing the mass percentage of chicken feathers (2%, 3%, 4%, and 5%) led to a notable enhancement characterized by a decrease in the thermal characteristics of the material.

The reduction in thermal conductivity was as high as 36% (0.481 W/m.K, for pure plaster to 0.309 W/m.K, which corresponds to the CFW composite of P + 5%., while the reduction in

thermal diffusivity was 13%, in thermal effusivity was 23% (It decreases from 946.67 $J/m^2.K.s^{1/2}$ for the purified plaster sample to 731 J/m2K.$s^{1/2}$ for the P+5% CFW composite.), and in volumetric thermal capacity was 16% (ranging from 1550 kJ/m3.K for the pure plaster sample to 1310 $kJ/m^3.K$ for the composite P + 5% CFW.). Using the Design Builder software, The obtained data were used to conduct dynamic thermal simulations on a standard residential structure. The study found that using a composite material of 5% chicken feather waste in the external walls and roof of the building resulted in a 24.8% reduction in cooling consumption during summer and a 29.4% decrease in heating requirements during winter. Additionally, this approach significantly reduced CO_2 emissions by approximately 408 kg per unit area.

The paper of Braiek et al.[144] presents the findings of an experimental study on the thermophysical characteristics of a composite material made from DPF and gypsum. The thermophysical characteristics were measured using both the periodic and flash methods. The study's objective was to assess the feasibility of utilizing the novel composite PDF/gypsum as an insulating material to decrease energy consumption in buildings. A substantial enhancement in the thermal characteristics of the DPF/gypsum composite is seen in comparison to gypsum alone. In addition, the thermal conductivity and density decreased as the concentration of DPF in the gypsum matrix increased (from 0 to 20%). Subsequently, the acquired behaviors indicate that the inclusion of 20% DPF resulted in a composite material with a thermal conductivity of 0.17 W $m^{-1}K^{-1}$ and a density of 736 kg m−3. These obtained values are lower than or equal to numerous insulating materials' thermal conductivity and density. The authors noted that adding 20% DPF to gypsum results in a composite material with favorable thermophysical properties. This composite can be effectively utilized in the construction industry as a new material for improving building energy efficiency.

The study by Mutuk et al. [145] aimed to utilize hemp fiber and banana fiber as natural fiber additives in the gypsum composite to create an environmentally friendly bio-composite. The natural fibers undergo chemical modification using a 5% NaOH solution to facilitate a strong connection between the fiber and matrix interface. The composite hardness test yielded a score of 50.4 for the sample containing 5 wt% fiber. A marginal drop is observed compared to the control plaster sample test result 53.6. Nevertheless, it has been noted that

the fibers effectively maintained the structural integrity and prevented the spread of cracks. The addition of fibers to the composite increased its porous structure, which in turn led to a reduction in its heat conductivity. The thermal conductivity of a 5 wt% fiber-reinforced gypsum composite (0.131 W/mK) was compared to that of pure gypsum (0.237 W/mK). The comparison yielded a good result, indicating that the composite has potential as an insulating material.

The study of Nafis et al. [146] aimed to assess the influence of jute fiber on the mechanical characteristics of gypsum plasterboard. To create this board, a mixture of Plaster of Paris and water was meticulously blended to form a suspension initially. Gypsum composites were prepared with varying fiber loadings of 2, 4, 6, and 8%. The addition of 6% fiber resulted in the highest tensile properties, approximately (1.04 Mpa), whereas the inclusion of 8% fiber led to lower tensile and flexural values.

The impact test findings demonstrated a progressive enhancement in performance with the addition of fibers (reaching 42.25 j/m for 8% fiber-reinforced composite). However, the hardness values exhibited a decline in hardness as the fiber loading increased, which reached 6.9% fiber-reinforced composite). The FTIR data and SEM results indicated no substantial chemical bonding in the composites. Instead, the composite primarily relied on mechanical bonding between the resin crystals and the fiber and gypsum matrix.

Chikhi [147] et al. present an experimental study examined the utilization of DPF as reinforcement in a gypsum matrix. This study investigates the impact of date palm fibers (DPF) derived from the Phoenix dactyliferaL plant in Biskra Oasis, Algeria, on gypsum-based composites' thermal conductivity, water absorption, and mechanical properties. The objective was to assess the feasibility of utilizing date palm fibers (DPF) derived from the Phoenix dactyliferaL plant in Biskra Oasis, Algeria, as reinforcement for gypsum-based composites. The compressive and flexural strength of the biocomposite samples, made using a gypsum matrix, decreases as the amount of fibers in the samples increases. The gypsum materials based on DPF (3mm in length) exhibit superior compressive strength and flexural strength compared to those packed with bigger particles (DPF6). The HG/DPF composites achieve greater compressive strength by incorporating 5% of DPF3 and 1.2% of DPF6. On the other hand, greater flexural strength is achieved when using 3% DPF for both types of fibers. Furthermore, the study of thermophysical behavior revealed that the higher the

concentration of DPF in the gypsum matrix, the lower the thermal conductivity and density of the composites. The authors found that the impact of DPF size on thermal characteristics is less apparent compared to DPF concentration. Subsequently, an experimental demonstration revealed that including 10% DPF resulted in a composite material with a thermal conductivity (k) of 0.15 W $m^{-1}K^{-1}$ and a density (ρ) of 753 kg m^{-3}. Results show that the lowest values of both thermal conductivity and density of HG/DPF are achieved with a 10% loading of DPF.

Charai et al. [148] examined how coal fly ash (CFA) and shoot plant fibers (AF) affect gypsum plaster's thermophysical, mechanical, and moisture properties. CFA replaced gypsum at 0–80% weight. Short AF were used as bio-aggregates at 0–6% weight. The composites have bulk density of 934–1340 kg/m^3, compressive strength of 1.38–6.98 MPa, thermal conductivity of 0.26–0.57 W/mK, and moisture buffering of 0.41–1.71 g/m2%RH. The experiments showed that CFA optimized hygrothermal conditions. In contrast, AF was a hygroscopic agent and reinforcement to counteract the compressive strength loss from pores. A lightweight gypsum composite with improved hygrothermal properties and compressive strength greater than 2 MPa was made by incorporating 50% CFA and 6% short AF.

The study of Kharrati et al. [149] aimed to enhance the mechanical properties of the plaster matrix by investigating its microstructure and conducting compression and bending tests. This is particularly important as plaster is known to have low mechanical strength. Results proved that the alkaline treatment demonstrated significant advantages in enhancing the adhesion between the matrix and the reinforcement, thereby reducing the brittleness of plaster and enhancing its compressive strength. The mechanical property reaches a maximum value of 10.4 MPa, while the flexural strength achieves its highest value of 1.5 MPa at a reinforcement level of 1%. Regarding thermal qualities, specifically conductivity, and diffusivity, the test findings confirmed that plaster is an effective insulator. Furthermore, its thermal properties are improved by its reinforcement. The composite performs best when adding 7% of Luffa fibers, resulting in a conductivity of 0.162 $W.m^{-1}.K^{-1}$ and a diffusivity of 1.96.10-7 $m^2.s^{-1}$.

II .3.Works on date palm fiber reinforcement

Basim Abu-Jdayil et Al.[1] examined the viability of using date palm seeds (DS), which are the main byproduct of the date industry, as a filler in unsaturated polyester (UPR) matrix for the purpose of creating thermal insulation material. Homogeneous and stable DS-UPR composites containing a maximum volume of 70% natural filler were produced at ambient temperature using a thermoset curing method. The created composites underwent various physical, thermal, and mechanical tests.

In addition, the composites that were created underwent characterization utilizing various techniques, including scanning electron microscopy (SEM), differential scanning calorimetry (DSC), thermogravimetric analysis (TGA), and Fourier-transform infrared spectroscopy (FTIR). Various theoretical models were employed to validate density and water retention observations. FTIR study indicates the presence of hydrogen bonding between DS fibers and UPR, particularly at higher filler loadings. By substituting up to 50 volume percent of unsaturated polyester resin (UPR) with DS, The composite samples exhibit promising thermal insulation and construction properties, characterized by relatively low thermal conductivity (0.126 - 0.138 W/(m·K)), low thermal diffusivity (0.109 - 0.096 mm2/s), low water retention (0.47 - 3.44%), and high compressive (38.4 - 88.0 MPa) and tensile strengths (9.4 - 35.1 MPa). In addition, incorporating date seeds into the unsaturated polyester matrix resulted in a modest rise in its glass transition temperature and enhanced its thermal stability. The DS-UPR-created composite can be a viable substitute for insulation materials due to its exceptional characteristics surpassing those of conventional thermal insulators.

R. Belakroum et al.[10] They presented an empirical study of a novel environmentally-friendly material derived from date palm fiber (DPF) and lime. The experiments conducted on the elaborated material aim to study its mechanical, thermal, and acoustic properties and its moisture buffering ability. A systematic study was conducted to investigate the impact of the fiber/lime ratio on the behavior of the lightweight aggregate. The compressive strength testing findings showed that the inclusion of PDF decreased the resistance threshold. The samples with a 50% DPF exhibited an average compressive strength of 0.2 MPa and a Young's modulus of 20.74 MPa. Nevertheless, the measured average values remain within acceptable limits. Furthermore, it was noted that the thermal conductivity is very responsive

to changes in the fiber-to-lime content ratio. The thermal conductivity was tested to have a minimum value of 0.091 W/m.K for samples containing 50% fiber. The new material demonstrates excellent sound absorption capabilities, as evidenced by the measured sound absorption coefficient. Specifically, for 50% of fiber, the material exhibits absorption coefficients of 0.65 and 0.55 for medium and high frequencies, respectively. On the other hand, owing to its porous structure, the suggested material can absorb water vapor in a high relative humidity setting and release it in a dry environment. Thus, it has the potential to function as a moisture regulator. The moisture buffer value measurements indicate that the material is rated as good or excellent, depending on the percentage of fiber present.

Novel insulating materials are suggested by Abdullah Alabdulkarem [150], employing various binders, including cornstarch, wood adhesive, and white cement. Five hybrid samples were created by combining surface fibers from date palm trees (PTSF) and fibers from the Apple of Sodom plant (AOSF) in various mass ratios and densities. A single hybrid sample was created by combining AOSF, agave fiber (AF), and glue (wood adhesive) as a binding agent. Thermal conductivity measurements were performed on all samples within a temperature range of 10 C to 50 C, yielding average values of 0.04234–0.05291 W/m K. AF's Fourier-transformed infrared (FT-IR) spectra exhibited distinct wavenumber ranges corresponding to different functional groups. Thermogravimetric analysis (TGA and DTGA) was conducted on AF, revealing that the fibers undergo degradation and decomposition at around 221 C, resulting in a 5% reduction in their initial mass. The AF sample was subjected to Differential Scanning Calorimetry (DSC) examination, which revealed a wide range of endothermic transition spanning from 292 to 357 C, with a peak observed at 353 C. The hybrid samples were tested for sound absorption coefficients, which demonstrate their potential for use in sound absorption. The recent tests demonstrate the viability of utilizing hybrid samples as insulating materials for thermal and acoustic purposes.

Salah Amroune [151] This study focuses on characterizing the fibers obtained from the branches of date palm fruits, which are abundant in Algeria. The findings of the tensile tests unequivocally demonstrate that the chemical treatment with NaOH employed in this study leads to a substantial enhancement in the mechanical characteristics, precisely the strength and Young's modulus, while having minimal impact on the strain at failure. In addition,

optimal mechanical properties are achieved by subjecting the fibers to treatment with a 3% NaOH solution for 2 hours. This treatment results in a significant increase of 178% and 268% in the strength and Young's modulus of the fibers, respectively, compared to untreated fibers. The average experimental results for the strength of the untreated (Raw) and treated fibers (3% NaOH-2h) are 112 MPa and 170 MPa, respectively. The values obtained using Weibull are 122 MPa and 187 MPa, respectively. In the other study, TGA-XRD measurements demonstrate that chemical treatment can alter the chemical composition of fibers derived from date palm fruit branches. The processed fibers exhibit enhanced thermal stability and a greater crystallinity index than the untreated fibers.

The study of Bezazi et al. [152] examined the mechanical properties of date palm fibers, namely their tensile behavior and cyclic fatigue. According to the authors, this is the first time such testing has been conducted on these fibers. The findings suggest that these fibers could be utilized to reinforce green composites. The stress and strain values at failure and Young's modulus of 18 samples tested under quasistatic tensile loading are being compared to the findings reported in the literature for other fibers. Cyclic fatigue tests were conducted at 2 Hz using sinusoidal stimulation. The tests were carried out at various loading levels, ranging from 0.6 to 0.95. These loading levels corresponded to maximum recorded forces of 15.36 N and 39.82 N, respectively. The variation of the force was recorded as a function of the number of cycles. This enables us to track the decline in stiffness. The load-displacement hysteresis curves demonstrate how the number of cycles and the loading level affect the size and shape of the hysteresis loops. This allows for the computation of the energy dissipated per cycle for the technical fibers.

The study of Semlali Aouragh Hassani et al. [153]aimed to create coated Dpf trays by utilizing novel, non-toxic, and environmentally acceptable materials, specifically date palm fibers coated with a bio-composite of modified clay (Mt-Tbz). Thiabendazolium was inserted into the interlayer space of montmorillonite to augment the biological characteristics of the resulting materials. This material was fabricated as a bilayer structure, with the first layer consisting of treated palm fibers and the second layer composed of bio-composite films using a coating process. The detailed coated Dpf trays were analyzed using various techniques. The morphological analysis of the Dpf trays and coated Dpf trays (Dpf@Cs/Mt-Tbz) reveals a more even distribution of the chitosan/montmorillonite-modified

thiabendazole salt-based coating bio-composite on the surface of the fibers. These findings suggest that the mechanical properties of the newly coated Dpf trays, specifically Young's modulus (increased from 330 MPa to 1035 MPa) and tensile strength (increased from 0.5 MPa to 4 MPa), may be enhanced.

Furthermore, their ability to inhibit the growth of Escherichia coli, Staphylococcus aureus, and Pseudomonas aeruginosa has been examined. In addition, the coating layer also enhances the surface hydrophobicity in comparison to the uncoated surface. The current study indicates that sophisticated coated Dpf trays can be a bilayer material in the smart packaging market.

An experimental analysis was conducted by H. Khakpour et al. [154] to examine the impact of bio fibers derived from various components of date palm trees on the tensile strength of different types of structural adhesives. The variables considered were fiber type, length, density, and the method used for treating the fiber surface. It was noted that the incorporation of date palm fiber led to a substantial enhancement in the tensile strength of structural adhesives. The strength witnessed a surge of over 60% in many instances. Based on the acquired results, it is essential to conduct tests on various components of date palm tree fibers to optimize the strength of each specific type of structural adhesive used with these fibers.

Furthermore, it has been shown that detrimental consequences such as stress concentration become increasingly significant when weight ratios exceed a specific threshold. This leads to a decrease in the reinforcing impact of fiber on the adhesive's tensile strength. The significant fluctuations in the strength of the composite specimens, resulting from alterations in the fiber density, clearly demonstrate the necessity of determining an appropriate range for the fiber-to-adhesive weight ratio. The experimental results indicate a positive correlation between the fiber length and the increase in the tensile strength of the glue. For instance, when considering composite samples of one of the adhesives analyzed, altering the fiber length from around 0.5 mm to 20 mm enhanced adhesive strength, with the improvement ranging from 21% to 65%. This is likely due to reduced fiber extraction from the matrix or increased friction during the fiber extraction process.

The study of Mohammad Asim et al.[73] focused on investigating the effects of different weight percentages (0%, 40%, 50%, and 60%) of date palm fibers (DPF) as a reinforcing

element in phenolic composites. DPF-reinforced phenolic composites were fabricated using the hand lay-up approach. The composites were then subjected to mechanical (tensile, flexural, and impact) testing, as well as morphological and dynamic mechanical property analysis. The goal was to determine the optimal fiber loading for the composites. Including 50% DPF loading enhanced the tensile modulus and impact characteristics while decreasing the tensile strength, flexural strength, and modulus. The interfacial connection between the fiber and matrix in composites was examined using a scanning electron microscope. The storage modulus of DPF composites was enhanced, with the most outstanding storage modulus observed at a 50% DPF loading. The loss modulus exhibited an increase upon reinforcement with DPF. The composite with a 40% fiber loading showed the highest glass transition temperature (Tg) for the loss modulus. However, the composite with a 50% fiber loading had a Tg similar to the one with a 40% fiber loading. The tan delta of DPF composites exhibits a low value. However, when the fiber loading increases, the glass transition temperature (Tg) of the damping factor also increases. The results indicate that composites with a 50% DPF content exhibit superior mechanical and thermal properties and improved interfacial bonding between the fibers and matrix. This material can be used as insulation in structures and for artificial ceilings and walls.

Bellatrache et al. [155] examined how incorporating plant fibers derived from date palm waste modifies bitumen characteristics. The chemical composition, structure, mass loss by heating, and tensile strength of palm fibers were analyzed. The properties of the bitumen-fiber mixtures were assessed before and after aging using consistency tests (penetration, Ring, and Ball softening point), rheological tests, and thermal tests. The investigations involved conducting binder drainage tests on asphalt mixes to evaluate the capacity of palm fibers to retain bitumen. The results indicated that including up to 6 wt% fibers in pure bitumen resulted in a somewhat higher consistency, a 50% increase in viscosity, and a 40% rise in complex modulus norm at temperatures experienced over the service life, both before and after aging. These recent trends enable predicting the asphalt mixtures' response to permanent deformations. Thermal investigation of the various mixes revealed that including fibers resulted in an augmentation of bitumen crystallinity. A partially crystalline fiber network within the bitumen matrix enhances the physico-mechanical properties of bitumen. The binder drainage tests conducted on asphalt mixes revealed the absorption of bitumen by

the fibers, which can be linked to their microstructure and roughness. The findings of this study are promising for the future utilization of date palm fibers in asphalt mixtures.

The paper of Almi et al.[156] presents the findings of an experimental investigation into the physical, chemical, and mechanical characteristics, as well as the thermal properties, of eight different types of date palm residues originating from the same region (biskra-Algeria). The objective is to assess each type of this organic substance for potential usage, independently or in combination, in producing composite materials. The results indicate that the Rachis variety demonstrates comparatively elevated levels of tensile strength and Young's modulus, reaching 213 MPa and 8.5 GPa, respectively. On the other hand, the Petiole variety demonstrates comparatively elevated levels of particular mechanical qualities. This is because of its low bulk density, which is at 0.160 g/cm3. In addition, the Petiole variety is distinguished by its relatively high porosity and a high water absorption rate, measuring 81.52 and 140%, respectively. On the other hand, the thermal analysis results indicate that the leaflets variety has the greatest resistance to heat degradation, with its primary degradation occurring at a temperature of 360°C.

Boussehel et al.[157] described the process of compounding and pressing test samples using date palm fibers reinforced PVC composites. The samples were prepared with and without treatments, and the loading rate was 10 or 30 wt%. A comparative analysis was conducted to assess and evaluate composites' mechanical, thermal properties, and water absorption characteristics in relation to pure PVC. The results indicate a modification in the structure of the fibers following the treatments, as evidenced by a decrease in the intensity of the hydroxyl group band of cellulose. Alkaline treatment results in the partial removal of hemicellulose and lignin. Acetylated fibers enhance the mechanical properties of PVC composites by establishing a chemical link between the surface of the fibers and the polymeric matrix. The assessment of the thermal characteristics of the composites reveals that the breakdown temperature of the composites rises from 229 °C (for untreated composites) to 231.3 °C and 228.1 °C (for acetylated and alkali composites, respectively) when the fiber loading is 30 wt%. The water uptake test demonstrates a correlation between the fiber content and immersion time with increased absorption. The composites that have been acetylated exhibit the most minimal water absorption rate.

The work conducted by Abdalla Abdal-hay [158] examined the characteristics of date palm fibers (DPFs) with three distinct size ranges of diameters (800-600, 600-400, and 400-200 μm). It investigated the impact of alkali treatment on these fibers. Observations of morphology using scanning electron microscopy (SEM), quantitative elemental analysis using energy-dispersive X-ray spectroscopy (EDS) density mapping, X-ray diffraction (X-RD), and Fourier-transform infrared (FTIR) spectroscopy were conducted on both treated and untreated fibers. The study also examined the tensile characteristics of individual fibers and composites made up of fibers/epoxy, both with and without chemical treatment, where the fibers were randomly aligned and discontinuous.

The findings demonstrated that DPFs can be easily altered through chemical alteration, especially when dealing with fine fibers. After undergoing alkali treatment, the single fiber exhibited a 57% improvement in ultimate tensile strength and a 24.7% increase in percentage elongation. Applying alkali treatment to the DPFs enhanced adhesion inside the matrix, improving the composite's tensile strength, elastic modulus, and fiber-matrix interaction.

Marwa Lahouioui et al. [159] examined the effects of palm fiber treatment on the thermal, physical, and acoustic properties of newly developed composites made of cement, sand, and untreated and chemically treated date palm fibers. Various mass ratios (2.5%, 10%, and 20%) of untreated and chemically treated palm fibers were combined with cement, water, and sand to create innovative composites. The composites were assessed by quantifying their water absorption, thermal conductivity, compressive strength, and sonic transmission. The results indicate that the inclusion of both untreated and chemically treated date palm fibers decreases the thermal conductivity and enhances the mechanical strength of the new composites. Thermal studies have demonstrated that the inclusion of fibers in composites results in a reduction of thermal conductivity. Specifically, the thermal conductivity drops from 1.38 W m−1 K−1 for the reference material to 0.31 W m^{-1} K^{-1} for composites containing 5% of treated and untreated fibers. The untreated palm fiber-reinforced composites (DPF) had the most excellent acoustical insulation ability when the fiber percentage was 20%. On the other hand, the treated palm fiber-reinforced composites (TPF) demonstrated the maximum sound insulation coefficient for fiber content below 10%. The link between compressive strength, thermal conductivity, and density indicates that only

fiber-reinforced composites (TPF) that have undergone chemical treatment are suitable options for thermal and acoustic building insulations.

In their study, AL-Oqla et al. [160] examined the mechanical characteristics, thermal stability, and morphological examination of date palms and polypropylene composites. The relationship between the microstructure and the performance of the composite was investigated using different reinforcement conditions, chemical treatments, surface topology, thermogravimetric analysis, and its derivative. The ideal samples of date palm leaflets (DPLs) were determined by subjecting them to different settings of sodium hydroxide treatment. Additionally, a morphological analysis was conducted. The results indicate that this treatment enhances the tensile strength and modulus of the composites.

Furthermore, DPL fibers benefit both the tensile and flexural modulus. The fibers achieved the highest values when they included 30 wt% of DPL fibers. The thermal gravimetric analysis (TGA) and differential thermal gravimetry (DTG) indicate that DPL fibers have high thermal stability, withstanding temperatures as high as 227 °C. Furthermore, TG-DTG thermograms demonstrate that using DPL fibers has significantly improved the thermal stability of polypropylene composites.

Epoxy-date palm fiber (DPF) composites have been successfully created and analyzed using varied ratios of DPF reinforcement (i.e., 5, 10, 15, and 20 wt%) in the work of Ali, Malek et al. [161]. Increasing the DPF ratio in the Epoxy matrix led to improvements in mechanical test results such as impact, creep, and tensile strength. The hardness of the material rises as the content of DPF (Dried Pulp Fiber) is increased up to 15 wt% due to the high concentration of lignin (20–28 wt%) in the fiber structure, efficient fiber dispersion and strong interfacial bonding between the Epoxy and DPF. The hardness of the Epoxy-DPF composites with 20 wt% DPF decreased due to agglomeration, porosity, weak interfacial bonding, poor wettability, and the absence of the Epoxy matrix between fibers. As a consequence, the mechanical test results were unsatisfactory. The impact strength of Epoxy-DPF composites, with fiber ratios of 5, 10, 15, and 20 wt%, was measured to be 0.1, 0.11, 0.12, and 0.13 J/mm2, respectively. The optimal impact strength is achieved by utilizing an appropriate length of DPF and including 20 wt% of resilient DPF.

Furthermore, the maximal impact strength is achieved through excellent stress transmission, resulting from the robust interfacial adhesion between Epoxy and DPF and the favorable random distribution of DPF, which enhances resistance to crack propagation. Compared to composites with a low weight percentage of DPF, an epoxy-DPF composite with a 20% creep strain can withstand more strain before failing and is significantly more malleable. The tensile strength of samples with 5, 10, 15, and 20 weight percent DPF content is measured to be 18.5, 19.7, 21.3, and 23.4 Newtons per square millimeter, respectively. Including a limited quantity of reinforced DPF hinders the efficient and straightforward passage of applied stress inside the composite material, specifically between the fibers and the matrix. As a result, epoxy-DPF composites with a DPF concentration of 5 wt% exhibit poor tensile strength values. However, the tensile strength of Epoxy-DPF composites with 20 wt% and a defined length of DPF is rather high due to an adequate DPF. This allows for the efficient and seamless transfer of longitudinal stress between the DPF and the matrix.

Conclusion

Based on the comprehensive review of relevant literature presented in this chapter, it is evident that there is significant potential in using various materials, such as polystyrene, gypsum, and date palm fibre, in composite materials and thermal insulation. Previous studies have demonstrated these materials' effectiveness in enhancing composites' mechanical properties and thermal performance. However, this area still has room for further research and development. Our research aims to build upon these findings and contribute to the existing knowledge by exploring novel approaches and applications in composite materials and thermal insulation. By leveraging the insights gained from the literature review, we seek to address key challenges and advance the field towards more sustainable and efficient solutions.

CHAPTER III. MATERIALS AND METHODS

Introduction

Chapter 03 describes the materials used and the methodology employed in developing and characterizing the two biocomposite materials for thermal insulation. The chapter outlines the sources and preparation methods of the waste plant compounds, as well as the experimental procedures for fabricating and testing the composites. The materials' physical, mechanical, thermal, and morphological properties were analyzed using various techniques described in this chapter.

III.1. Materials

III.1.1. Polystyrene

The matrix employed in this study is expandable polystyrene (EPS). It is a thermoplastic material composed of 98% air and 2% polystyrene. The thermal conductivity of Expanded Polystyrene (EPS) has a range of values between 0.035 and 0.04 W/mK, with variations seen based on its density [139] .

For the first composite material, which is date palm fiber reinforced polystyrene composite, The Sunchem D-105 fasted cycling polystyrene grade was used (Figure III.1). The product supply was provided by SARL POLYMOST, a company based in Setif, Algeria. The primary focus of this organization is the production of polystyrene plates. The utilization of the D series is prevalent in packaging materials, primarily safeguarding items from potential damage and offering thermal insulation properties [162]. The provider provides detailed technical parameters for the polymer in Table III.1.

Figure III. 1. The EPS used for PS-DPF composite material.

Table III. 1 Technical parameter of EPS.

EPS specification	values
Beads size (mm)	0.70-1.00
sieving	95%
Blowing agent	Pentane
Residual monomer	≤0.3%
Moisture content	≤0.5%
CFC content	nil

It is important to note that this type of EPS was used to manufacture the PS-DPF composite material due to its ease of use in the melt-extruder.

For the second composite material wich, we used gypsum as a binder. EPS waste was retrieved from proprietors of electrical appliance retailers; the remnants were manually segregated into diminutive pellets utilizing an abrasion technique (Figure III.2). Following that, the shots were subjected to a process of sifting to attain consistent size, whereby pellets that fell within the 0 to 3mm range were selected to generate hybrid composite material samples.

Figure III. 2. Photograph of (a) expanded polystyrene wastes and (b) expanded polystyrene pearls used.

III.1.2. Date palm Fibers

For the first composite material, a date palm fiber reinforced polystyrene composite, using fibers obtained from date palm leaflets as reinforcement, was conducted in Figure III.3-d. On the other side, we used the petiole part Figure III.3-c for the gypsum hybrid composite. The decision to employ the petiole component can be ascribed to its favorable attributes, specifically its low Bulk density of 590 kg/m3 and thermal conductivity of 0.0895 W/m.K [4,163,164]. The fibers were derived from the Deglet Noor species of date palm (Figure III.3- a) and served as a means of reinforcing. The selection of this specific cultivar is predicated upon its notable prevalence within Algeria.

The waste (Figure III.3-b) materials were gathered from a palm oasis in the Horaya district of Biskra, in the southeastern part of Algeria. Before the grinding process, the waste of the date palm was thoroughly washed and left to air-dry for four days. Subsequently, the materials underwent crushing via a ball mill apparatus and subsequent sieving. The composites were manufactured using exclusively date palm fibers (DPF), with diameters ranging from 90 to 120 microns. The unprocessed fiber, commonly referred to as raw fiber, is denoted as UDPF (Figure III.4-a).

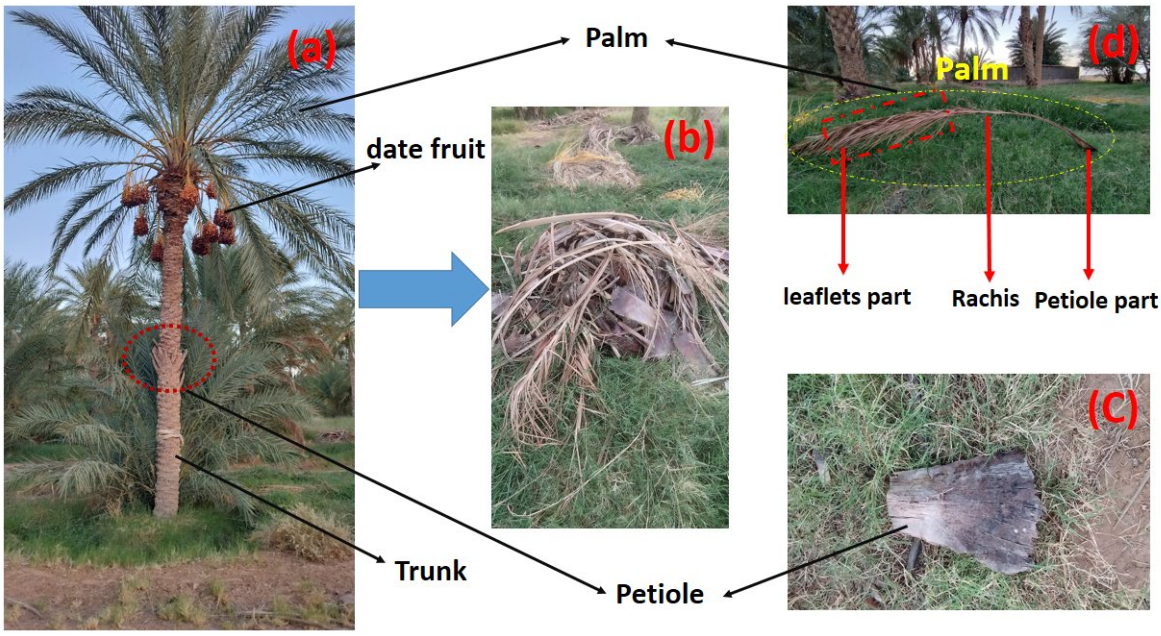

Figure III. 3. Distinct sections of a palm tree: (a) date palm tree, (b) the palm.

III.1.3. Chemical treatments applied to leaflets of date palm fiber

III.1.3.1. Alkaline Processing

This stage involves submerging the fibers in a 10% sodium hydroxide (NaOH) solution provided by the company "BIOCHEM Chermopharma." The experiment was conducted under ambient conditions for 12 hours. After that, the fibers are subjected to multiple rinses using distilled water supplemented with a concentration of 10 to 1 mol/l of acetic acid to counterbalance the soda surplus. Ultimately, the substance undergoes a rinsing process with distilled water to achieve pH neutrality. Subsequently, the specimen was subjected to a thermal treatment by being placed into an oven set at a temperature of 80°C for 24 hours [165]. The alkali fibers are denoted as ADPF (Figure III.4-b).

III.1.3.2. Benzoylation Processing

A portion of the ADPF sample was subjected to additional treatment involving the addition of 50 ml of benzoyl chloride, which was thoroughly mixed with a 10% NaOH solution for 15 minutes [166,167]. Following the designated time intervals, the DPF that underwent treatment was subjected to a water wash and subsequently immersed in ethanol for one hour. Subsequently, the final cleansing procedure was carried out employing tap water. The fibers that had been washed were subjected to a drying process in an oven for 24 hours at a temperature of 80˚C, as reported in references 19 and 20. The fiber that has been subjected to benzoylation is denoted as BDPF (Figure III.4-c)

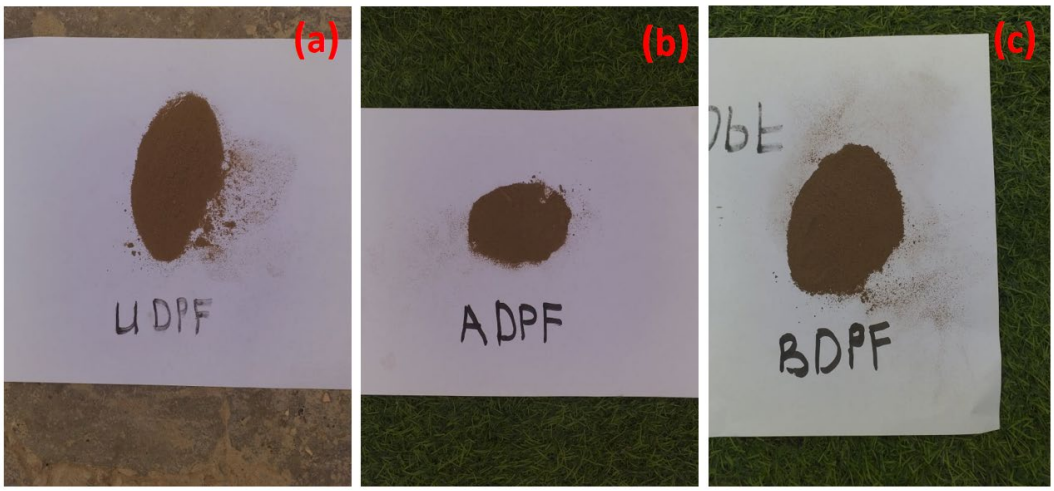

Figure III. 4. The used fibers for PS-DPF manufacturing (a) UDPF (b) ADPF (c) BDPF.

III.1.4. Gypsum plaster

The gypsum plaster used in this investigation was obtained from commercial vendors specializing in construction materials (Figure III.5).

The gypsum sample in question was sourced from the Oueled Djalal brand, produced by the Alpha Cristo Company for Industry located in the Ouled Djellal region of Algeria. The gypsum plaster is obtained through extraction and subsequent exposure of gypsum to elevated temperatures of 150 °C, as described by the equation (2).

$$2CaSO_4 \cdot 4H_2O + Heat \rightarrow 2CaSO_4 \cdot H_2O + 3H_2O \quad (2)$$

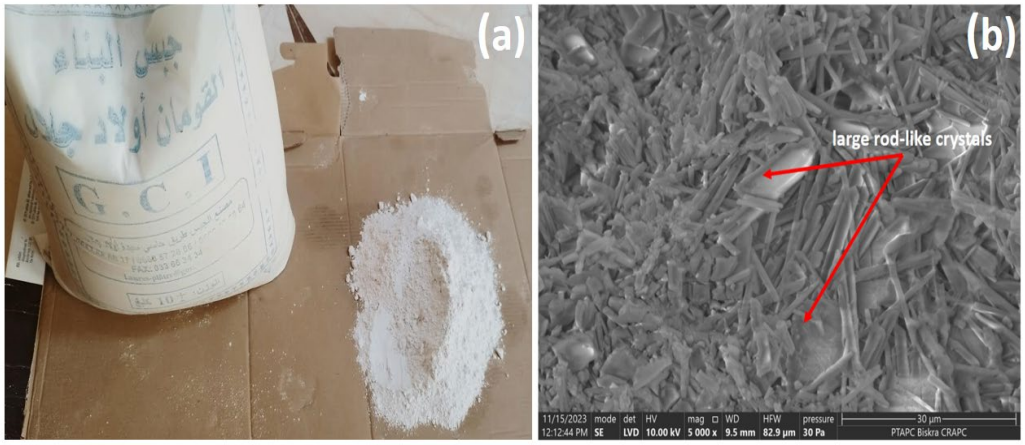

Figure III. 5. Photograph of gypsum powder (a) and its SEM micrograph (b)

III.2. Preparation of composites

III.2.1. Date palm leaflets fiber reinforced polystyrene (PS-DPF)

The composites were fabricated using a HAAKE PolyLab OC melt extruder manufactured by Thermo Scientific (Figure III.6-a). The extrusion process involved a mixing speed of 30 revolutions per minute, an extruding temperature ranging from 170 to 190 degrees Celsius, and a torque of 4.5 N. m. It is important to note that the extrusion conditions remained consistent for all samples.

The extruded strips are placed within the mold, positioned between two aluminum sheets, and subjected to compression for 10 minutes at a temperature of 180 °C and a pressure of 300 bar. This compression process utilizes a hydraulic press known as the Schwabenthan polystat 300S (Figure III.6-b). In order to mitigate the occurrence of air bubbles, the mixture is subjected to preheating until it attains its initial melting point. Before

applying the final pressure, a degassing process is performed. Once the sheets measuring 130×130×2.4 mm^3 are acquired (Figure III.7), they are adjusted to the necessary dimensions for the diverse characterization tests. Figure III.8 illustrates the many stages of the experimental procedure.

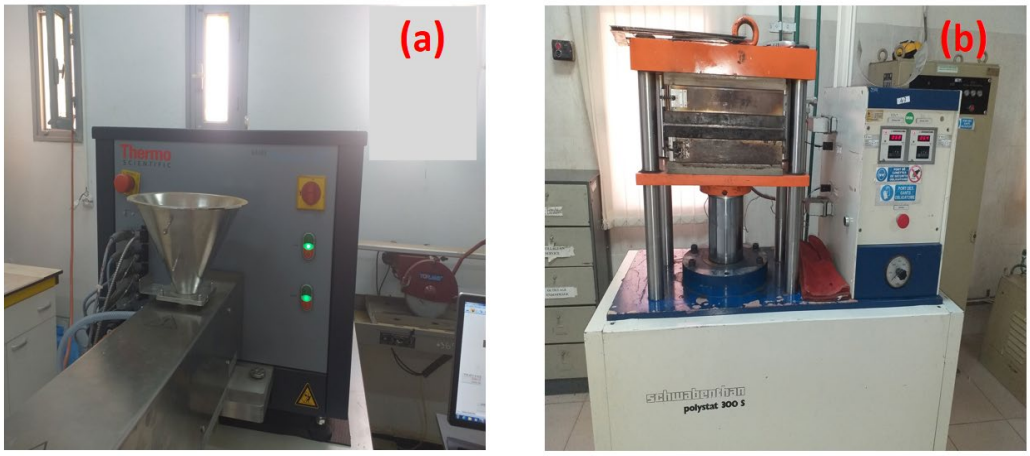

Figure III. 6. Photograph of (a) melt extruder and (b) hydraulic press.

To streamline the terminology used for PS-DPF composite formulations, the numerical value is employed to denote the fiber loading, while the alphabetical character following the numerical value signifies the specific type of chemical treatment applied (U: untreated; A: alkaline treatment; B: benzoylation treatment). PS-10% BDPF denotes polystyrene strengthened with 10% benzoylated date palm fibers. On the other hand, VPS represents virgin polystyrene.

Figure III. 7. PS-DPF sheets

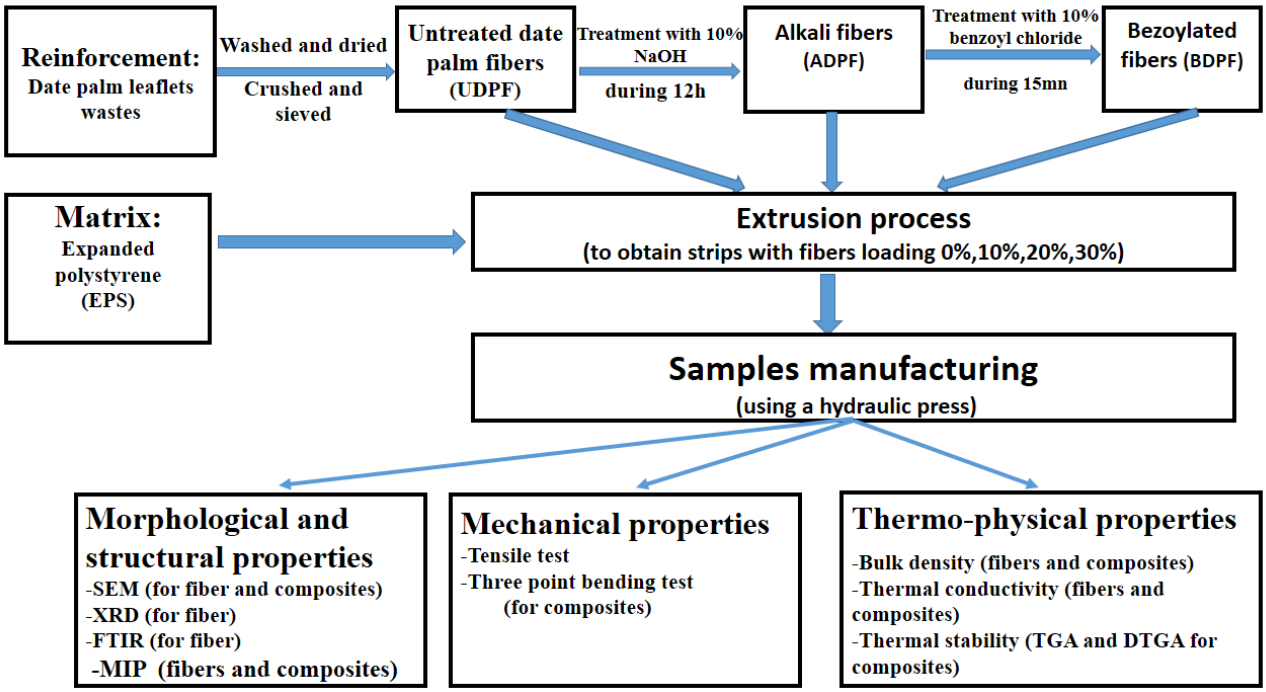

Figure III. 8. The experimental procedure's phases.

III.2.2. Gypsum-Expanded polystyrene-date palm petiole fibers hybrid biocomposite (G-EPS-DPP)

The process for preparing the test specimens was as follows:

Initially, gypsum plaster powder and date palm petiole fibers (DPP) were prepared with different mass fractions of fibers (0%, 5%, 10%, and 15%). The mass of DPP was determined using equation (3).

$$W_{DPP}(\%)=\frac{m_{DPP}}{m_{DPP}+m_G}$$

$$m_{DPP} = W_{DPP}(m_{DPP} + m_G)$$

$$m_{DPP}(1 - W_{DPF}) = W_{DPP}m_G$$

$$m_{DPP} = \frac{W_{DPP}m_G}{1-W_{DPP}} \qquad (3)$$

The weight ratios of DPF, gypsum plaster mass, and DPP are denoted as W_{DPF}, mG, and m_{DPP}, respectively.

After thoroughly blending the combination of Gypsum and DPP, we slowly introduced it into the water. The mixing process follows the manufacturer's recommendation of (M_{water}/m_G=0.82). The mixture is gently mixed thoroughly for a duration of 6 minutes.

When EPS is included in the composition of the samples, the granules of EPS are incrementally introduced into the mixture using a constant mass ratio of 0.3%. The Expanded Polystyrene (EPS) mass is calculated by equation (4).

$$m_{EPS} = \frac{W_{EPS} m_G}{1 - W_{EPS}}$$

Given that the percentage of EPS has been set at 0.3%, it can be observed that:

$$m_{EPS} = \frac{0.003\ m_G}{0.997} \quad (4)$$

EPS's mass and weight ratio are denoted as m_{EPS} and W_{EPS}, respectively.

It is essential to acknowledge that the mass content of DPP and EPS is determined based solely on the mass of the plaster, excluding the mixture. Subsequently, the amalgamation was carefully transferred into manually crafted molds Figure III.9-a, wherein the inner surface was coated with oil to expedite the samples' extraction. In addition, the molds are subjected to multiple shaking motions in order to prevent the occurrence of air bubbles within the samples.

The samples were meticulously removed from the molds (Figure III.9-b) after being left to dry initially, with the duration varying depending on whether the samples contained or did not contain fibers. Subsequently, the specimens were allowed to dry for 28 days while exposed to typical environmental circumstances. The composite formulations are denoted according to the nomenclature provided in the table. III.2.

Table III. 2. Samples codification

Samples code	**DPP (wt%)**	**EPS (wt%)**	**Samples code**	**DPP (wt %)**	**EPS (wt %)**
NG	0	0	**G-EPS-15F**	15	0.3
G-EPS	0	0.3	**G-5F**	5	0
G-EPS-5F	5	0.3	**G-10F**	10	0
G-EPS-10F	10	0.3	**G-15F**	15	0

The various stages of the experimental procedure are depicted in Figure III.9.

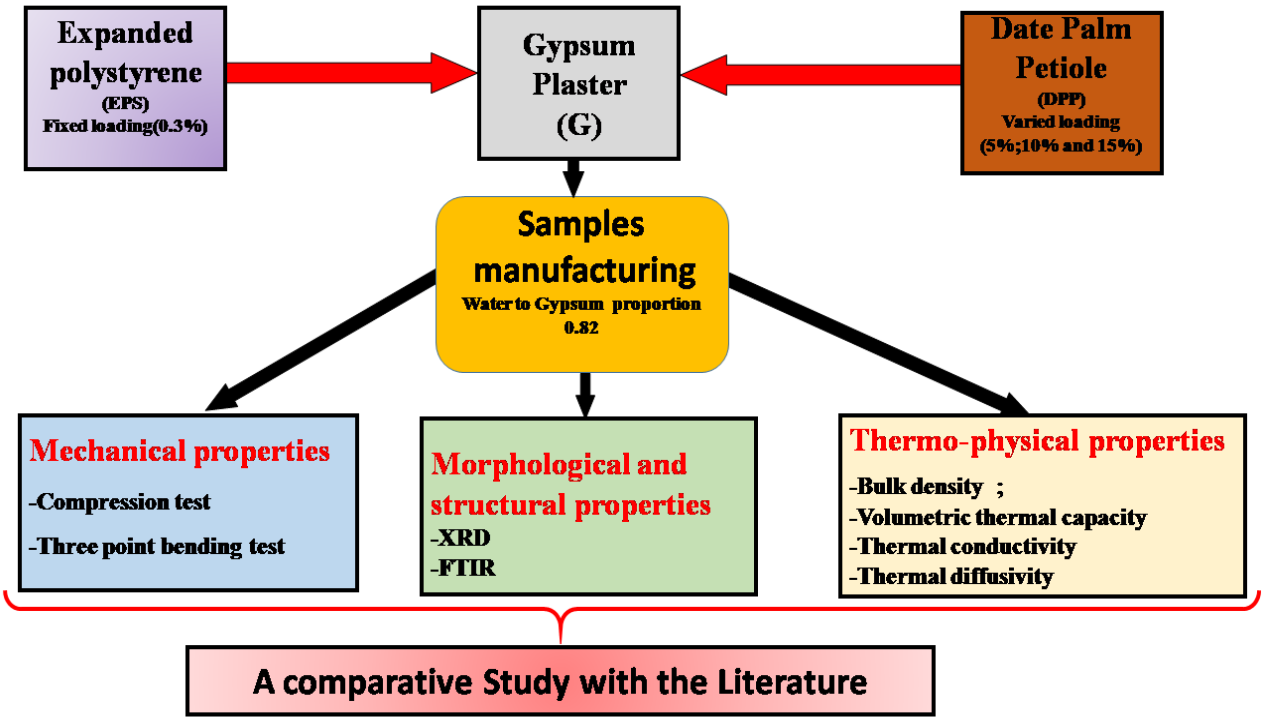

Figure III. 9. Diagram of the experimental procedure.

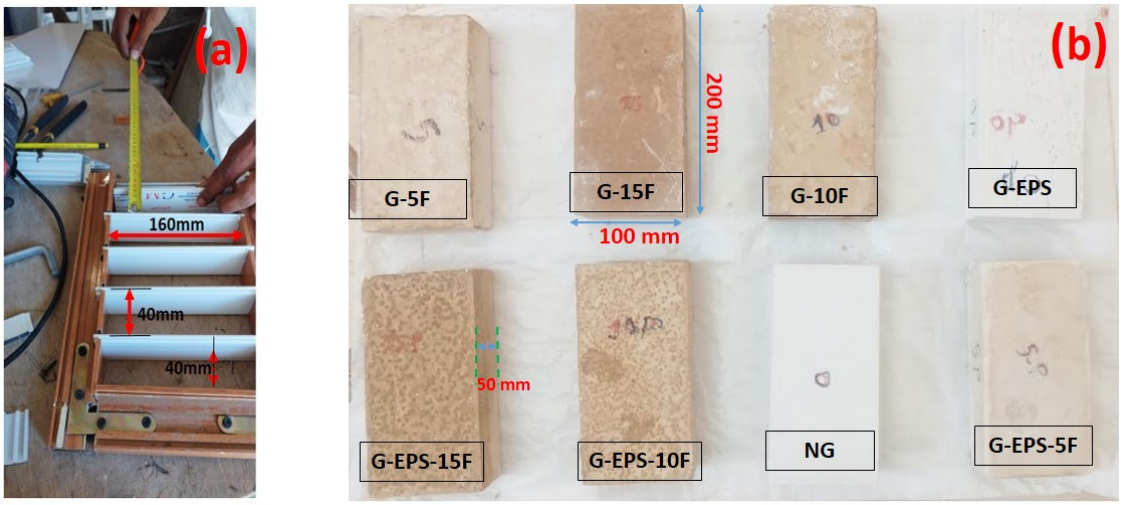

Figure III. 10. Photograph of (a) handcrafted molds and (b) prepared specimens.

III.3. Mechanical characterization

III.3.1. Tensile test

The tensile properties (including tensile strength, tensile modulus, and strain at failure) of the PS-DPF fabricated composites were evaluated using an INSTRON 5969 traction machine (Figure III.11-b) with a maximum capacity of 50KN, following the guidelines

outlined in the ASTM D 3039M standard[168]. The specimens were appropriately processed and afterward sectioned into rectangular shapes with dimensions of 120×10.7×2.4 mm^3(Figure III.11-a).

The experiment was performed using a standard head movement rate of 2 mm/min in normal environmental conditions. Five samples were used for the tensile test in each instance.

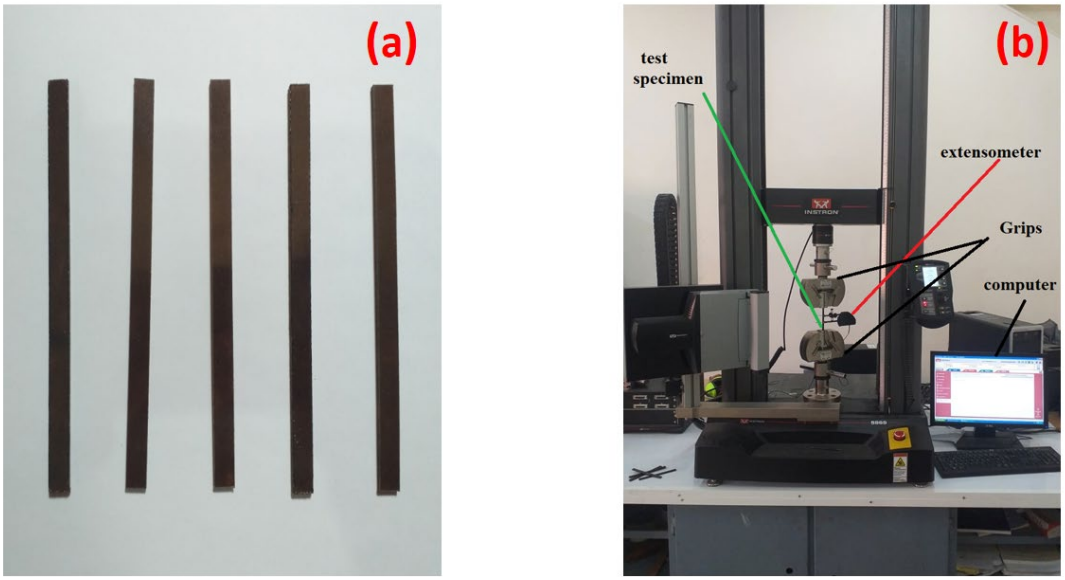

Figure III. 11. Photograph of (a) Traction PS-DPF specimens

(b) INSTRON 5969 traction machine.

III.3.2. Three-point bending test

The flexural properties of the composites produced were assessed by a three-point bending test, following the guidelines outlined in ASTM D790-03 [169]. The support span was established as 60 mm. A total of five samples are gathered, and their respective measurements are subsequently averaged in order to ascertain the ultimate outcomes.

-For the PS-DPF, the dimensions and apparatus employed in the tensile test were replicated for this purpose. The strain rate was designated as 0.01 mm/min. The measurements were conducted at ambient temperature until the sample experienced fracture, at which juncture they were concluded.

-For gypsum reinforced with DPP, EPS, or both, The specimens have rectangular cross-sections of 160×160×40 mm^3 (Figure III.12). The support span was predetermined to have a set length of 60 mm, while the strain rate was measured and found to be 2 mm/min. The measurements were conducted under ambient temperature conditions of 30˚C until the sample reached the fracture point when the experiments were terminated.

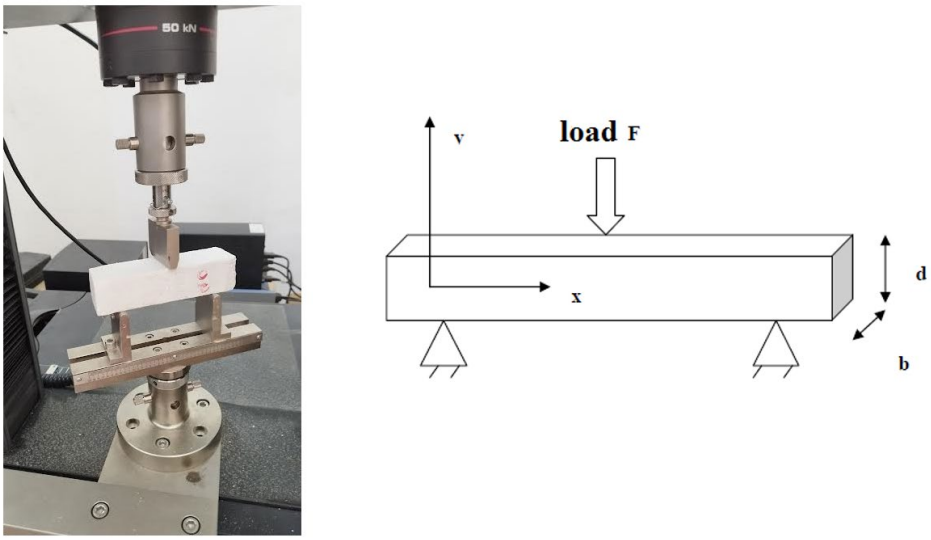

Figure III. 12. Three bending tests for reinforced gypsum.

III.3.3. Compression Test

The compressive testing technique (Figure III.13 was utilized to test the compressive strength, using a cross-head speed of 1 mm/min. The evaluation of compressive strength involved the application of force to cube-shaped samples measuring 40×40×40 mm3. These samples were derived from the broken sections of the original specimen used for the flexural strength test.

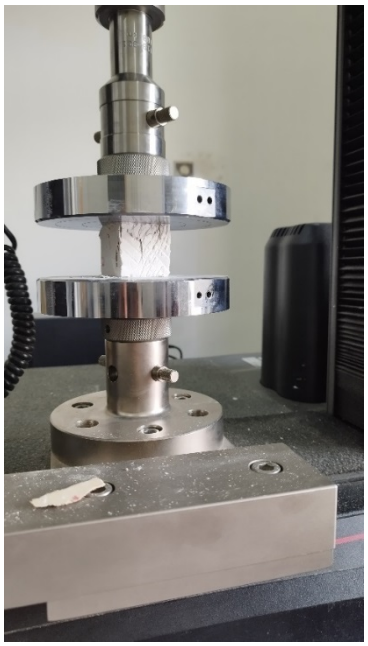

Figure III. 13. Compression test.

III.4. Morphological and microstructural characterization

III.4.1. Fourier transform infrared (FTIR) spectroscopy

The chemical bonds present in raw (UDPF, DPP), processed date palm fibers (ADPF and BDPF), NG, and EPS were evaluated using an Agilent Cary 630 FTIR Spectrometer (Figure III.14) equipped with an attenuated total reflection (ATR) sampling approach. This analysis involved the examination of FTIR spectra. The infrared spectra were acquired at a scanning rate of 140 scans per minute in transmission mode, covering the 4000–450 cm-1 range with a precision of 4 cm^{-1}.

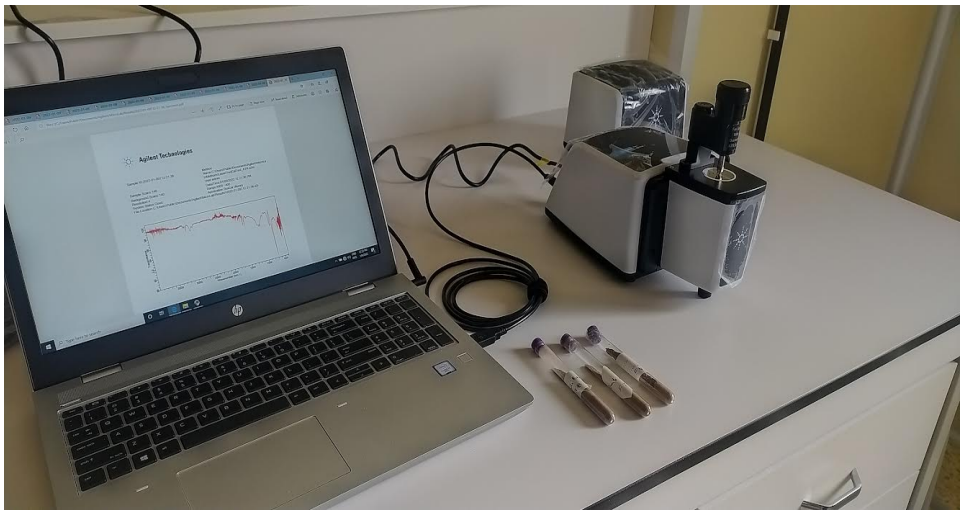

Figure III. 14. Agilent Cary 630 FTIR Spectrometer.

III.4.2. X-ray diffraction (XRD) analysis

X-ray diffraction (XRD) is a non-invasive analytical method used to analyze crystalline materials, facilitating the identification and analysis of the structural properties of distinct crystalline phases within a mixture, whether in the form of powders or slides.

The X-ray diffraction (XRD) analysis of untreated date palm leaflets fibers (UDPF), alkaline date palm leaflets fibers (ADPF), benzolayted date palm leaflets fibers (BDPF), gypsum plasters, date palm petiole fibers, and polystyrene was performed using a Bruker D8 X-ray diffractometer (Figure III.15). The analysis employed copper Kα radiation with a wavelength of λ = 0.154 nm, produced using an electrical potential of 40 kilovolts and a current of 40 milliamperes. The investigation scope ranged from 0 to 80 degrees (2θ).

The calculation of the degree of crystallinity (X_{Cryst}) for each sample involved dividing the area under the crystalline peaks (A_{Cryst}) by the total area under the complete diffraction curve ($A_{Cryst} + A_{Amorph}$), as outlined by [170] in equation (5).

$$X_{cryst} = \frac{A_{cryst}}{A_{cryst}+A_{amorph}} \times 100 \quad (5)$$

The crystallinity index (Ic) for both untreated and treated DPFs was determined using equations.

$$I_c = (I002\text{-}Iam)/I002 \quad (6)$$

The counter reading at peak intensity at 22° corresponds to crystalline material, denoted as I(002), while the counter reading near 18° represents amorphous material in cellulosic fibers, designated as I(am) [138,171].

Figure III. 15. Bruker D8 X-ray diffractometer.

III.4.3. Scanning Electron Microscope (SEM) analysis

To examine the microstructure and morphological characteristics of date palm fibers and composite samples, a Thermo Scientific Prisma E Scanning Electron Microscope (SEM) (Figure III.16) was utilized, operating at an accelerating voltage of 10 kV.

Figure III. 16. Thermo Scientific Prisma E Scanning Electron Microscope (SEM).

The fundamental advantage of this scanning electron microscope (SEM) is its capability to do imaging and analysis of nonconductive and/or hydrated specimens without charging. The gadget has an energy-dispersive X-ray spectroscopy (EDS) microanalysis system. The examination samples were affixed onto aluminum stubs and afterward subjected to scanning at different levels of magnification.

III.4.4. Porosity parameters measurement

The technique used, known as Mercury Intrusion Porosimetry (MIP), is utilized to measure pore size, volume, and distribution of PS-DPF composite and fibers (UDPF, ADPF, BDPF), employing the penetration of a non-wetting liquid. The technique above holds great importance in the characterization of porous materials (Figure III.17), as it allows for determining pore sizes within a range of about 3 nm (subject to the specific contact angle between mercury and the solid surface) to approximately 1000 µm. The mercury intrusion technique enables the determination of pore sizes that exceed 500 nm, surpassing the range achievable using gas physisorption.

The operational principle of mercury intrusion porosimetry (MIP) involves the introduction of mercury into a sample under high pressure, causing the mercury to infiltrate the pores of the sample. Specifically, the pressure was increased from 6.89×10^{-9} Pa in the low-pressure port to 4.13×10^{-3} Pa in the high-pressure chamber. Further technical details regarding this procedure can be found in the study conducted by Guise et al. (2017)[172].

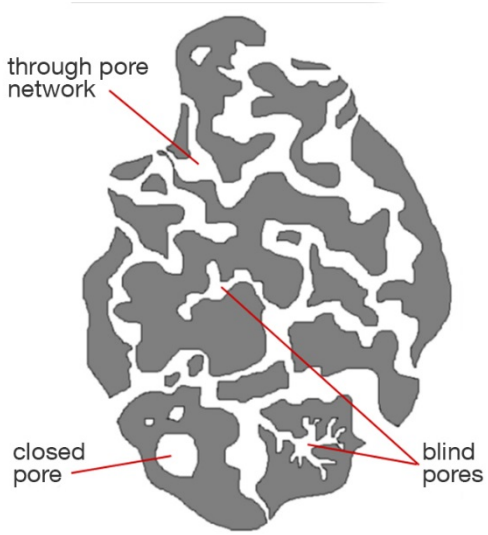

Figure III. 17. A schematic depiction of a porous solid.

The MIP measurements were performed using a Micromeritics AutoPore IV 9500 Series porosimeter (Figure III.18) and in compliance with the standards published in ASTM D4404 [173]. The data is acquired in the format of a pressure-volume graph. The provided data is utilized to compute pore size by applying the Washburn equation (7), assuming that all pores possess a cylindrical morphology [174].

$$d = -4\gamma\cos\theta/P \qquad (7)$$

Where

d = diameter of the intruding pore,

γ= mercury's surface tension,

θ = contact angle between mercury and the pore wall

And P = pressure exerted.

The measurement of coating porosity by MIP involves three distinct phases.

Initial phase

Before the actual analysis of the sample is conducted, a baseline analysis must be performed. Blank is performed to eliminate mercury volume decrease values not due to sample pore intrusion. This includes the mercury entering the pores of the glass dilatometer as well as the effect of mercury's compressibility under high pressure, which would otherwise be interpreted as volume entering pores. Blank executes every phase of the actual sample analysis. The only difference between blank and sample is that blank contains no example. Once the blank measurement has been obtained, it is routinely subtracted from the sample reading.

Second phase

Second, analyze the alumina tile. Alumina's blank reading is gone. Appendix 8(a) shows instrument-extracted alumina results. Subtracting the alumina result from the sample results is laborious.

Phase 3

Both blank and alumina are only run once. In stage 3, all samples are analyzed. The sample result is presented in the results and discussions section.

Figure III. 18. (a) The Micromeritics AutoPore IV 9500 series; (b) penetrometer closure

III.5. Thermo-physical characterizations

III.5.1. Bulk Density Test

The bulk density of the fibers and composite (UDPF, ADPF, BDPF, and PS-DPF) was determined using the mercury intrusion Pore Measurement method (MIP) as will describe in section (3.4.4).

For gypsum plaster composites, The determination of Bulk density was performed by measuring the mass (m_c) and volume (v_c) of the hybrid composite samples generated, as outlined by Ouakarrouch et al. [143] in equation (8).

$$\rho=\frac{m_c}{v_c} \qquad (8)$$

The sample weight was determined using the Kern analytical balance ALS-A / ALJ-A, which can measure up to four significant digits (Figure III.19).

Figure III. 19. The Kern analytical balance ALS-A / ALJ-A

Furthermore, the sample volume was determined using a caliper with a precision of two significant figures. The experiment was conducted on two samples, and the mean results were calculated.

III.5.2. Volumetric thermal capacity and thermal conductivity

The thermal conductivity (λ) and volumetric thermal capacity (ρ_c) of Fibers and composite samples were assessed using a CT meter, as depicted in Figure III.20 . The measurement methodology utilized in this investigation is based on the hot wire method. The estimation presented in this study is based on the examination of temperature changes that were obtained through the use of a thermocouple positioned close to a resistive wire.

The fibers are put in two parallelepiped boxes 120x80x10mm3 Figure III.20-(c), and the ring probe is set in the middle. For the composite, the probe is placed in the interstitial space between two parallelepiped samples, with dimensions of 200×100×5 mm^3 for gypsum plaster composite and 130×65×2.4 mm^3 for polystyrene composite samples, as depicted in Figure III.20-(a) and (d) respectively.

The ambient temperature was 18- 24˚C, while the relative humidity was around 65.2%. The measurements are duplicated in two separate instances on opposing sides of the specimen to evaluate the likelihood of measurement inaccuracies.

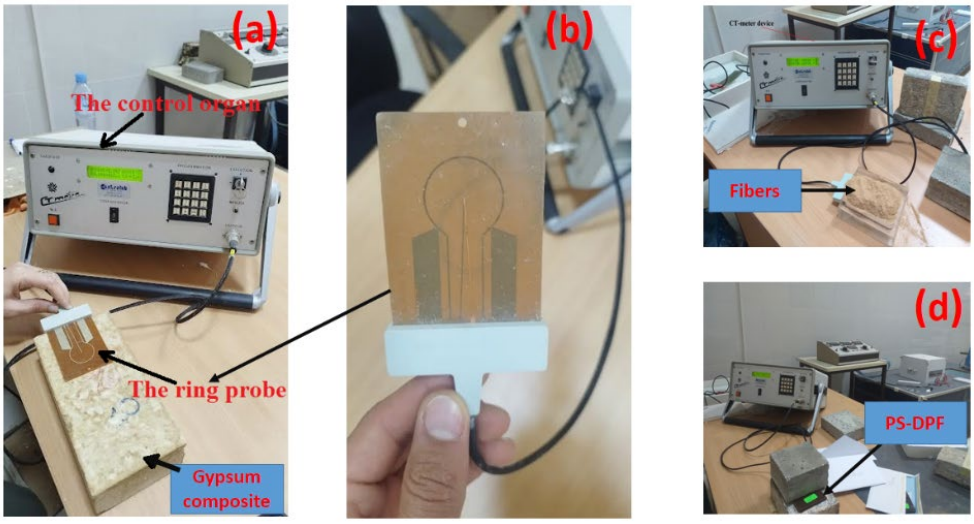

Figure III. 20. Photograph of conductivity test for (a) Gypsum composite, (b) ring probe, (c) Fibers, and (d) Polystyrene composite .

III.5.3. Thermal diffusivity

Thermal diffusivity is a fundamental property that warrants examination as it provides a quantitative measure of the rate at which heat is transferred inside a material, namely from regions of greater temperature to areas of lower temperature. The determination of thermal diffusivity (α) can be achieved by employing equation (9), as indicated by Abu-Jdayil et al. (2021) [1].

$$\alpha = \frac{\lambda}{\rho_c} \qquad (9)$$

The thermal diffusivity (α) is in (m^2/s), while the thermal conductivity (λ) is in [W/m.k].The volumetric thermal capacity, in J/m3.k

With: (α) thermal diffusivity measuring in [m^2/s]; (ρ_c) volumetric thermal capacity in [$J/m^3.k$].(λ) is the thermal conductivity [W/m.k]

III.6. CT METRE description

III.6.1. Purpose and measurement method

The CT METRE (Figure III.20 -a) is a portable device that has been designed to facilitate the accurate assessment of thermal properties in various materials, including:

- Brick, rocks, and earth.
- Cellular concrete.
- Bitumen.
- Powdered substances.
- Liquids.
- Resins or complex products.

The operational principle involves integrating a heating element and a temperature sensor within a single probe. This configuration allows for the measurement of the temperature increase experienced by the sensor during a user-selected heating period. The duration of the heating period is determined based on the specific material being tested and the type of probe employed.

III.6.2. Constitution

The CT METRE is comprised of two distinct components:

-The control unit generates the heating power and interprets the temperature rise curve induced by the tested material.

-The sensor is responsible for transmitting the heating power and gathering the resulting temperature.

III.6.3. Presentation

III.6.3.1. The control module

Included in the portable case are the following:

The front panel consists of data input and result readout elements (keypad, display screen, encoder for configuration preselection) and probe connection connector.

-The rear panel contains the wall outlet, the power supply, and the RS232C serial connector.

- Inside, a microprocessor-based electronic system manages the internal control orders.

The control unit's mechanical and electrical traits are presented in Table III.3

Table III. 3. Control unit's specification.

control unit's specification	Value
Weight	8kg
dimension	400 x 145 x 260
power supply	230V/50-60Hz
Intrastat number	90278017

III.6.3.2 The probe

Currently, two types of probes are available:

- A ring-shaped probe

A flexible printed circuit board (thickness 0.2 mm - dimensions 60x90 mm) is intended to be inserted between two previously ground flat pieces of the sample to be measured (Figure III.21). Type 30. R: diameter of heating element = 30 mm

Type 15. R: diameter of heating element = 15 mm.

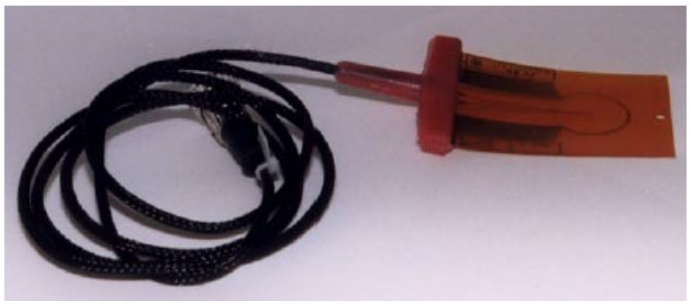

Figure III. 21. A ring-shaped probe.

- The single-rod probe or wire probe

Flexible printed circuit board (0.2 mm thick) made to fit between two flat pieces of the sample to be measured, whose surfaces ha ve already been ground. Standard type: 160 x 45 mm. The size for type FIL 50/A is 95 x 40 mm.

III.6.4. Running principle

By turning a key, the user can choose between two functioning modes.

III.6.4.1 Configuration programming

The process involves selecting a configuration number from a set of 10 options.

Figure III. 22. The single-rod probe or wire probe.

Subsequently, a specific number of parameters are assigned to this number chosen using an encoder situated on the front panel of the CT METRE.

- Thermal power,
- Radius or length of the heating element,
- Duration of heating,
- Duration of measurement, etc.

The system will consider these factors when executing this configuration. The parameters are inputted through a 16-key keypad, accompanied by a screen control that consists of two lines, each capable of displaying up to 20 characters. After a configuration is programmed, it can be permanently saved or rewritten.

III.6.4.2. Execution of a configuration

The operator initiates the measurement by pushing the MEASURE button after appropriately positioning the probe. Subsequently, the cycle operates autonomously, and upon completion of the predetermined measurement duration, the display exhibits the anticipated outcomes, presented in Table III.4.

Table III. 4. The displayed expected results.

The ring probe	**Wire (or single-rod) probe**
Thermal conductivity is measured in W/m.K	Conductivity W/m.K
Specific heat is measured in kJ/m3 K.	Correlation coefficient
Starting temperature °C.	/
The maximum change in temperature °C.	/
Adjustment coefficient (%).	/

III.6.4.3 Measurement options in detail

✓ Control parameter features

- **Power output**

For ring probes (average resistance 2.5Ω), from 0 to 2.5W (0 to 1A in 32.25mA steps).

For wire probes, (10Ω average resistance) from 0 to 1W (0 to 1A in 32.25mA steps).

- Temperature measurement from -20 to +80°C with 0.025°C resolution.
- Measurement and warm-up time, 1 to 500 seconds in multiples of a second (wire (or single-rod) probes have the same time).

✓ **Features of measurement results**

Table III.5 presents the features of measurement results

- The adjustment coefficient (for ring probes) is used to check the validity of the test. It can vary from 2% to zero, with the optimum value of zero.
- Correlation coefficient (for wire probes) Used to check the validity of the test; it can vary from 0.98 to 1, the optimum value being 1.

Table III. 5. Features of the measured parameters.

Features	Thermal conductivity	Specific heat kj/m3K
Range	0.02 to 5W/m.K	/
Accuracy	+ 5%	+ 5%
Reproducibility	+ 2%	+ 2%

III.6.5. Functioning

III.6.5.1. Access to programming mode

To access programming, write, or read mode, simply by turning the key to PROGRAMMING:

- I.e., before the unit is switched on,
- Or, at any time during the run, we can press the "C" (Clear) key.

The device will then display a menu prompting you to:

- To the configuration reading ⇨ button “A”
- To write configuration ⇨ button “B”

In read mode, the ENTR key scrolls through the parameters. In write mode, it validates the parameter entered.

At the end of reading or writing, we can either return to programming mode (A or B) or switch to execution mode. Select the desired configuration first, turn the key to the EXECUTION position, and press ENTER.

NOTE:

In programming mode, we can only exit at the end of the cycle, unlike execution mode, which can be interrupted at any time by pressing the "C" key.

III.6.5.2. Sensor programming parameters

Parameters are validated by pressing ENTER.

a) Ring probe

Sensor type 1

Radius

The heating element radius value will be entered in meters (up to 4 digits after the decimal point). The diameter is engraved on the probe (in mm).

- Type 15.R: diameter 15mm means radius 7.5mm = 0.0075 m.

- Type 30.R: width 30mm means radius 15mm = 0.015 m.

Electrical Resistance

The user is required to input the value of the resistance of the heating element in Ohms, with a maximum of three decimal places.

The probes are supplied with a precise indication of their resistance in Ohms.

Power

Enter the power to be injected into the heating element in Watts (up to 2 digits after the decimal point).

The power value to be set depends on the resistance value of the probe's heating element (in Ohms) and on the value towards which the thermal conductivity measurement will tend.

The following table can be used (Table III.6).

Table III. 6. Power values depend on the ring probe's measured thermal conductivity range.

Heating element resistance	thermal conductivity of the material to be	Power settings
2,5Ω	0.05 to 0.2 W/m.K	0.1 to 0.2 W
2,5Ω	0.2 to 0.5 W/m.K	0.2 to 0.4 W
2,5Ω	0.5 to 1 W/m.K	0.4 to 0.8 W

Power settings can be validated as follows:

When measuring with the CT-METRE, the maximum temperature variation displayed during the test must be between 1 and 2°C.

✓ If temperature variation is < 1°C: increase heating power.

✓ If temperature variation is > 2°C: reduce heating power.

Caution: measurement causes heating of the material to be measured. The material must cool down between 2 measurements.

Heating time

The user is required to input an integer value representing a duration in seconds, with a maximum limit of 500 seconds.

When there is little availability of exact data regarding the material to be evaluated, it is common practice to establish a heating time range of 20 to 40 seconds, effectively encompassing 95% of typical applications.

Time Measurement

The user is required to input an integer value in seconds, with a maximum limit of 500 seconds.

In the absence of very accurate data regarding the material under measurement, the designated measurement period is established as 180 seconds.

However, the measurement time can be refined when the material is characterized. When the CT-METRE performs a measurement, it displays the temperature variation during the measurement. The minimum measurement time to be set is to reach the maximum temperature plus 20 seconds.

The scanning step

-Integer value to be entered in seconds (max. 500s).

-The scanning phase is set to 1 second in case of the absence of exact data on the material to be measured.

Max. Permissible temperature variation

Enter integer value in °C (max. 80°C).

Given the lack of accurate information regarding the material under consideration, it is deemed appropriate to establish a maximum allowable temperature deviation of 5°C.

The purpose of this value is to protect the probes against destructive heating. If the temperature rise during the test exceeds the setpoint, heating and measurement stop.

b) Wire probe

Sensor type 2

Length

The heating element length value will be entered in meters (up to 4 digits after the decimal point).

Length of type Sdt: 0.05m

Length of type FIL 50/A: 0.05m

Resistance

The heating element resistance value is to be entered in Ohms (up to 3 digits after the decimal point).

The probes are supplied with a precise indication of their resistance in Ohms.

Power

Enter the power to be injected into the heating element in Watts (up to 2 digits after the decimal point).

The power value to be set depends on the length of the heating element (in meters), the resistance value of the probe's heating element (in Ohms), and the value towards which the thermal conductivity measurement will tend.

As a general rule, the following table can be used (Table III.7) Power settings can be validated as follows:

Table III. 7. Power values depend on the wire probe's measured thermal conductivity range.

Element length heating	Average element resistance heating	thermal conductivity of the material to be measured	Power settings
0,05m	10Ω	0.05 to 0.2 W/m.K	0.1 to 0.2 W
0,05m	10Ω	0.2 to 0.5 W/m.K	0.2 to 0.4 W
0,05m	10Ω	0.5 to 1 W/m.K	0.4 to 0.8 W

When measuring with the CT-METRE, the maximum temperature variation displayed during the test should be between 10 and 15°C.

✓ If temperature variation is < 10°C: increase heating power.

✓ If temperature variation is > 15°C: reduce heating power.

Caution: measurement causes heating of the material to be measured. The material must cool down between 2 measurements.

Measurement/heating time

Integer value to be entered in seconds (max. 500s).

In the absence of exact data on the material to be measured, the measurement/heating time is set between 120 and 240 seconds (covers 95% of applications).

The scanning step

Integer value to be entered in seconds (max. 500s).

Given the lack of highly accurate information about the substance under consideration, the scanning interval has been established at 1 second.

Max. Permissible temperature variation

Enter integer value in °C (max. 80°C).

Given the lack of specific information regarding the material under consideration, it is deemed appropriate to establish a maximum allowable temperature fluctuation of 25°C.

The purpose of this value is to protect the probes against destructive heating. If the temperature rise during the test exceeds the setpoint, heating and measurement stop.

III.6.5.3 Access to "run" mode

a)- To access execution mode, position the key on EXECUTION

- I.e., before the unit is switched on,
- Or, at the end of the programming cycle, before pressing ENTER.

The display shows the configuration number selected on the encoder if the selected configuration is valid.

Otherwise:

If no program has been saved in the selected position, the device beeps and displays "Invalid configuration."

If the saved configuration contains out-of-limit parameters, the device emits a burst of "beeps."

Pressing the "C" key after changing a configuration or switching the key to programming enables you to execute another configuration or to read or write a configuration.

b)- Once the selected configuration has been validated, the device displays the type of probe to be connected via the connector on the front panel and the power to be sent to the probe's heating resistor.

NB: This power may differ slightly from that written in the configuration due to the resolution of the power unit (1 step = 32.25mA).

The user is then offered three options:

✓ Permanent temperature display ⇨ press "A".

To return to the menu, press "C".

✓ Start measurement without waiting for the temperature to stabilize at sample level

⇨ press "D"

Then press the MEASURE button.

✓ Start an automatic measurement process, including a temperature stability verification sequence,

⇨ press the MEASURE button. The unit then starts test sequences, measuring the temperature every 6 seconds for 60 seconds. If there is no change in temperature during these 60 seconds (approx.), the heating cycle starts (the heating indicator lights up).

Otherwise, a "beep" sounds when two temperature values differ, and a new cycle of 10 beeps starts again.

Two faulty cycles generate a burst of "beeps" and a message on the display, after which a new cycle of waiting for stability starts automatically.

III.6.6. CT-METRE Parameters used for our work

For the two elaborated composite materials, and after many times to validate the thermal test, we identify the CT- METRE's parameters as presented in Table III.8

Table III. 8. CT-METRE Parameters used for our work.

Parameters selection	Polystyrene composites	Gypsum composite
Probe	Wire probe	Ring probe (Type 30.R)
Resistance	10 Ω	2.5 Ω
Power	0.18 W	0.2 W
Heating time	240 S	120 S
Measurement/heating time	240 s	180 S
scanning step	1 S	1 S
Max. Permissible temperature variation	2 °C	15°C

Conclusion

This chapter details the materials and methods used in our study. We employed expandable polystyrene (EPS) as the matrix, date palm fibres for reinforcement, and gypsum plaster as a binder. The composites were prepared using specific procedures, including melt extrusion and compression moulding. Mechanical characterization was performed through tensile, bending, and compression tests, while morphological and microstructural analyses were conducted using FTIR spectroscopy, XRD analysis, SEM imaging, and porosity measurements. Thermo-physical properties such as bulk density, thermal conductivity, and thermal diffusivity were also determined. These methodologies lay the foundation for our subsequent discussions on the properties and performance of the developed composites.

CHAPTER IV: RESULTS AND DISCUSSION

Introduction

This chapter presents and discusses the key findings of this research, integrating the results with existing literature to highlight their significance. The objectives are to present the quantitative and qualitative data, analyze the results in the context of the research questions, and discuss their implications. The chapter is structured into two parts: the first deals with the PS-DPF composite materials, and the second deals with G-EPS and /or DPP. This is followed by a comparative discussion linking the findings to the broader literature.

IV.1. FIRST WORK PS-DPF MATERIAL COMPOSITE

IV.1.1. FTIR Results

Figure IV. 1 displays the Fourier Transform Infrared (FTIR) spectra of the untreated fibers, alkaline-treated fibers, and fibers subjected to benzoylation. No substantial alterations were observed in any samples, whether untreated or treated. The presence of peaks at approximately 3310 cm^{-1} suggests the occurrence of intense and wide-ranging O-H stretching, as reported in reference [175]. It is observed that the untreated fibers exhibit a little higher peak intensity compared to the treated fibers. The cited source provides evidence supporting the assertion that applying chemical treatment reduces the number of OH bonds. The presence of stretched solid peaks in the vicinity of 2915 and 2841 cm^{-1} suggests the potential involvement of the alkane (C-H) functional group [157]. The presence of a peak at around 1739 cm^{-1} in the spectra of the unprocessed fiber can be ascribed to the presence of the carbonyl functional group (C=O). The band exhibits complete disappearance when subjected to alkaline and benzoylated fibers. The observed disappearance can be attributed to the elimination of hemicelluloses using various treatment methods[155] and [176]. The band observed at 1640 cm^{-1} can be attributed to water absorption by the untreated palm fiber, which can be attributed to its notable hydrophilic nature [176].

The beak exhibited a significant reduction in size following the application of benzoylation therapy. The observed peak at 1082 cm^{-1} is ascribed to the presence of the C-O bond originating from lignin, cellulose, and hemicelluloses, as reported by reference [155]. An anomaly arises in the form of a discernible peak observed at a wavenumber of 712 cm^{-1} for the BDPF, suggesting aromatic moieties exist. The findings of previous investigations on DPF, as indicated by references [177] and [138], are consistent with the data presented in this study.

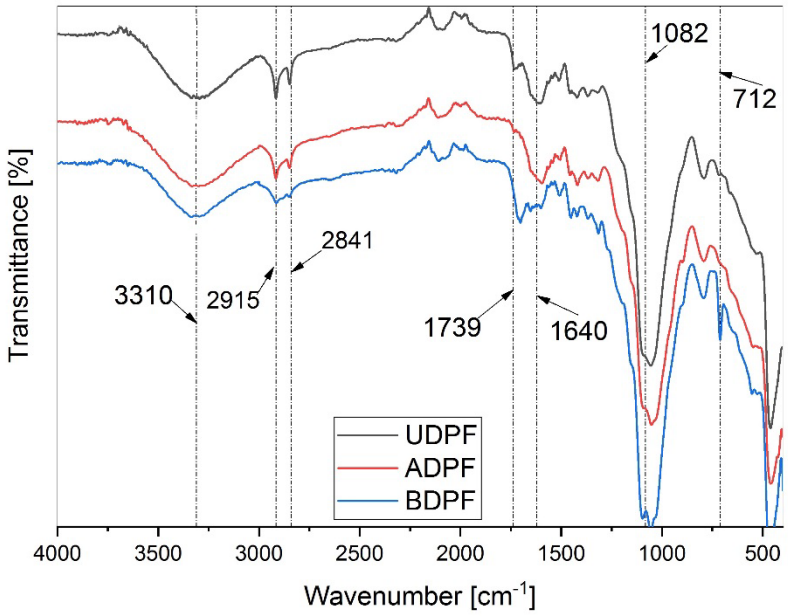

Figure IV. 1. The treated (ADPF/BDPF) and untreated (UDPF) fibers' FTIR spectra

IV.1.2. X-ray diffraction (XRD) results

Figure IV.2 displays the X-ray diffraction patterns of both untreated and treated fiber. The reflection at a high angle (about 2θ = 22˚) had a distinct and strong peak, whereas the reflection at a low angle (approximately 2θ = 18˚) displayed a broader and less dramatic profile. These two peaks are commonly observed in most vegetable fibers. All three samples exhibited an additional signal at approximately 2θ = 34˚, thereby verifying the presence of native cellulose I within the fibers [141]. Table IV.1 presents the peaks, crystallinity index (Ic), and crystallinity percentage (Cr %) associated with the given data. As per the equation 5, the Cr% values for UDPF, ADPF, and BDPF are determined to be 68.42%, 70.06%, and 67.98% correspondingly. In comparison to raw and benzoylation fibers, mercerization has been found to enhance crystallinity, as indicated by comparable findings in previous studies.

Applying an alkaline treatment effectively eliminates the amorphous component on the surfaces of the fibers, thereby liberating the cellulose and facilitating the enhancement of crystallinity. The process of benzoylation involves introducing a benzoyl group into the cellulose substrate. This process leads to a decrease in unbound cellulose and a reduction in crystallinity. The values for the crystallinity index (Ic) and crystallinity percentage (Cr %) are comparable to those reported in previous studies by Hachaich et al. [178], M. Kethiri et al. [179], and T. Djoudi et al. [141]. The authors provide an account of the variability in values based on factors such as geographical location, palm tree species, and specific parts of the palm trees.

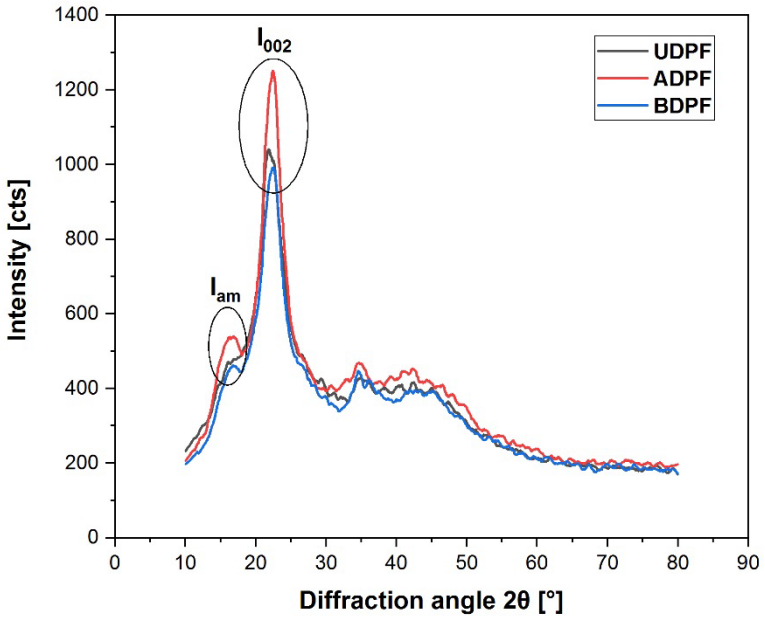

Figure IV. 2. X-ray diffractogram of untreated (UDPF) and treated (ADPF/BDPF) fibers.

Table IV. 1. Values of corresponding samples and the measured crystallinity parameters.

Fiber	I_{am} (cts)	I_{002} (cts)	Cr (%)	I_C
UDPF	465,93	1009,65	68,42	0,54
ADPF	539,81	1261,88	70,06	0,57
BDPF	461,32	979,43	67,98	0,53

IV.1.3. SEM results

IV.1.3.1 DPF Morphology

In order to assess the microstructure of the sample, an analysis was conducted using scanning electron microscopy on leaflets derived from date palm fibers of the Deglet Noor variety. The findings indicate that the UDPF, ADPF, and BDPF exhibit a lack of consistent shape and non-uniform dimensions (Figure IV.3). The SEM micrographs demonstrate that the surface of untreated fibers exhibits a notable presence of waxes, oils, and other impurities (Figure IV. 3-a). These impurities are predominantly attributed to the Saharan origin of this particular variety of palm. The findings above were documented by researchers Oushabi et al. [21] and Khakpour et al.[154]. In contrast, scanning electron microscopy (SEM) micrographs reveal a discernible enhancement in the surface's topographical characteristics

after the soda treatment application. The indicated augmentation can be observed in Figure IV. 3-b solubilization of various impurities from the fiber's surface, as evidenced by the SEM micrographs. Furthermore, it is widely recognized that sodium hydroxide (NaOH) undergoes a chemical reaction with the hydroxyl groups present in the cementing components of hemicellulose and lignin during mercerization. This reaction disrupts the cellular structure and subsequent separation of the fibers into individual filaments. The occurrence described is commonly referred to as fibrillation (Figure IV.4 -d). The morphological changes resulting from the alkali treatment on the fiber surface are consistent with the findings reported in the literature [180–182].

In contrast to the untreated and alkaline-treated DPF, the benzoylation-treated DPF exhibits a surface characterized by roughness and pockmarks [183], as depicted in Figure IV. 3-c. Additionally, the benzoylation treatment is observed to reduce the size of the DPF, as one would anticipate. The exclusion of alkali-soluble components, such as the waxy layer and lignin, is performed [184]. Introducing the benzoyl group onto the fibers enhances their reactivity through benzoylation. Additionally, it forms chemical connections with active areas on the polystyrene matrix characterized by benzene rings.

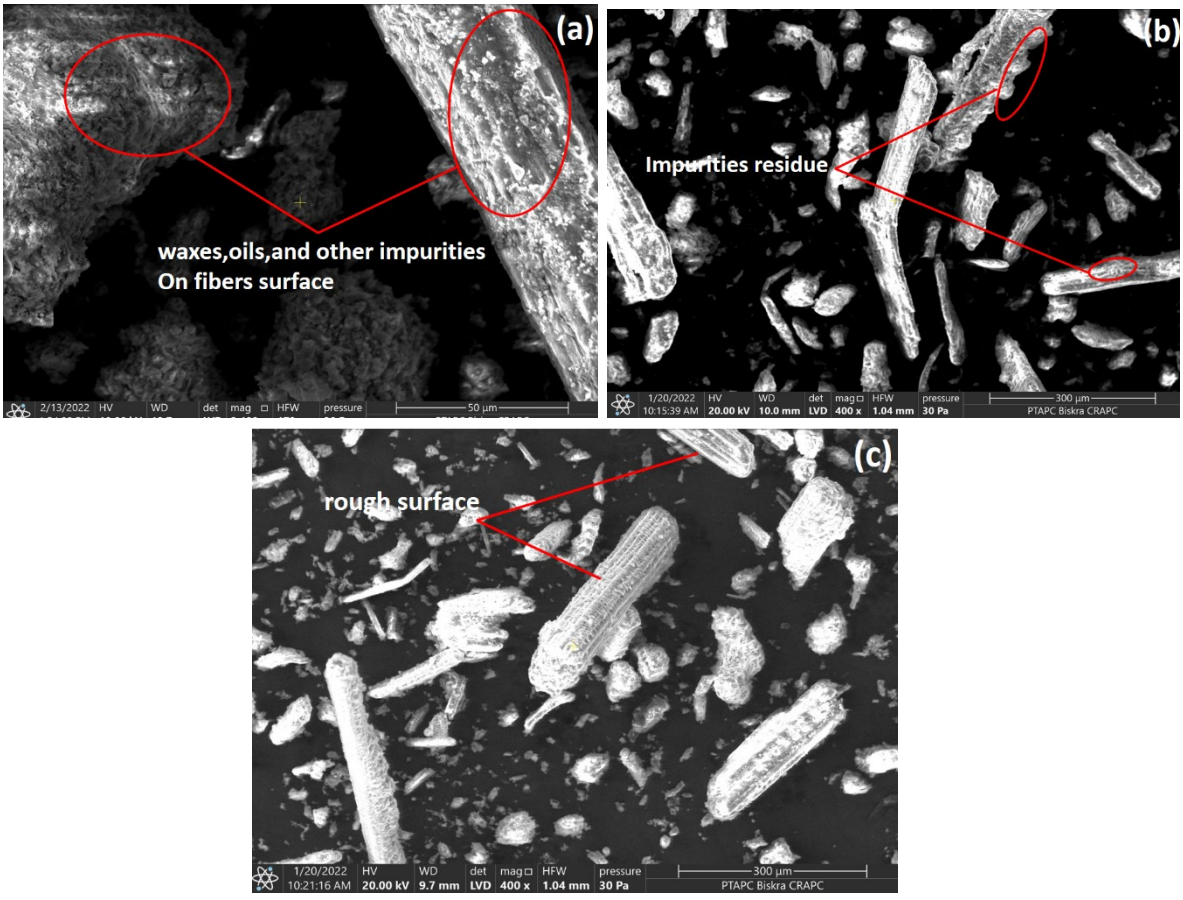

Figure IV. 3. UDPF, ADPF, and BDPF fiber SEM micrographs.

IV.1.3.2. Composite Morphology

Figure IV.4 illustrates the morphological characteristics of PS-DPP composites with varying filler loadings (0%, 10%, and 30%) of untreated and treated date palm fibers. Onifade et al. (2020) [185] reported that an examination of virgin polystyrene VPS (Figure IV. 4-a) demonstrated a surface that seemed smooth, with the presence of undissolved polystyrene beads. This observation suggests that insufficient melting may have occurred during the process. Including these microparticles within the polystyrene matrix does not induce any chemical changes in the polystyrene matrix and, consequently, does not significantly impact the resulting composite derived from the specimen.

Following the integration of fibers into the polymer, the data illustrates a stochastic arrangement of fibers inside the matrix across all specimens. The PS-UDPF composite exhibits a noticeable level of separation between the filler particle and the polymer, creating small voids or gaps within the polystyrene-DPP matrix (Figure IV.4-b). This detachment is attributed to the hydroxyl groups (−OH) found in natural fillers, which absorb moisture and weaken the interfacial bonding between the hydrophilic fibers and the hydrophobic polymer. Furthermore, the occurrence of hydrogen bonds among the particles of natural fillers results in the agglomeration of particles (Figure IV.4-c). The increased filler loading substantiates this phenomenon from 10% to 30%. According to a previous study [19], it was observed that the pure polystyrene beads included some gases, resulting in the formation of gas voids within the fabricated samples. This process facilitates the aggregation of fibers within these intriguing spaces, resulting in their subsequent filling. The elements above collectively contribute to the initiation of cracks originating from the introduced particles, hence substantiating the role of these particles as stress concentration sites. Several researchers have made the observations above: Hittini et al., 2021 [7]; Poletto & Zattera [8]; Masri et al., 2018 [2]; and Singha & Rana [132].

In contrast, Figure IV.4-e shows that ADPF improves polystyrene matrix adherence relative to untreated fibers. The treatment eliminated contaminants from the DPP surface, improving PS-ADPF adhesion, according to Adeniyi et al. [185]. The mechanical characteristics analysis shows a preference for composite material in mechanical strength. Figure IV.4 -d shows PS-10%BDPF fractured surfaces by scanning electron microscopy.

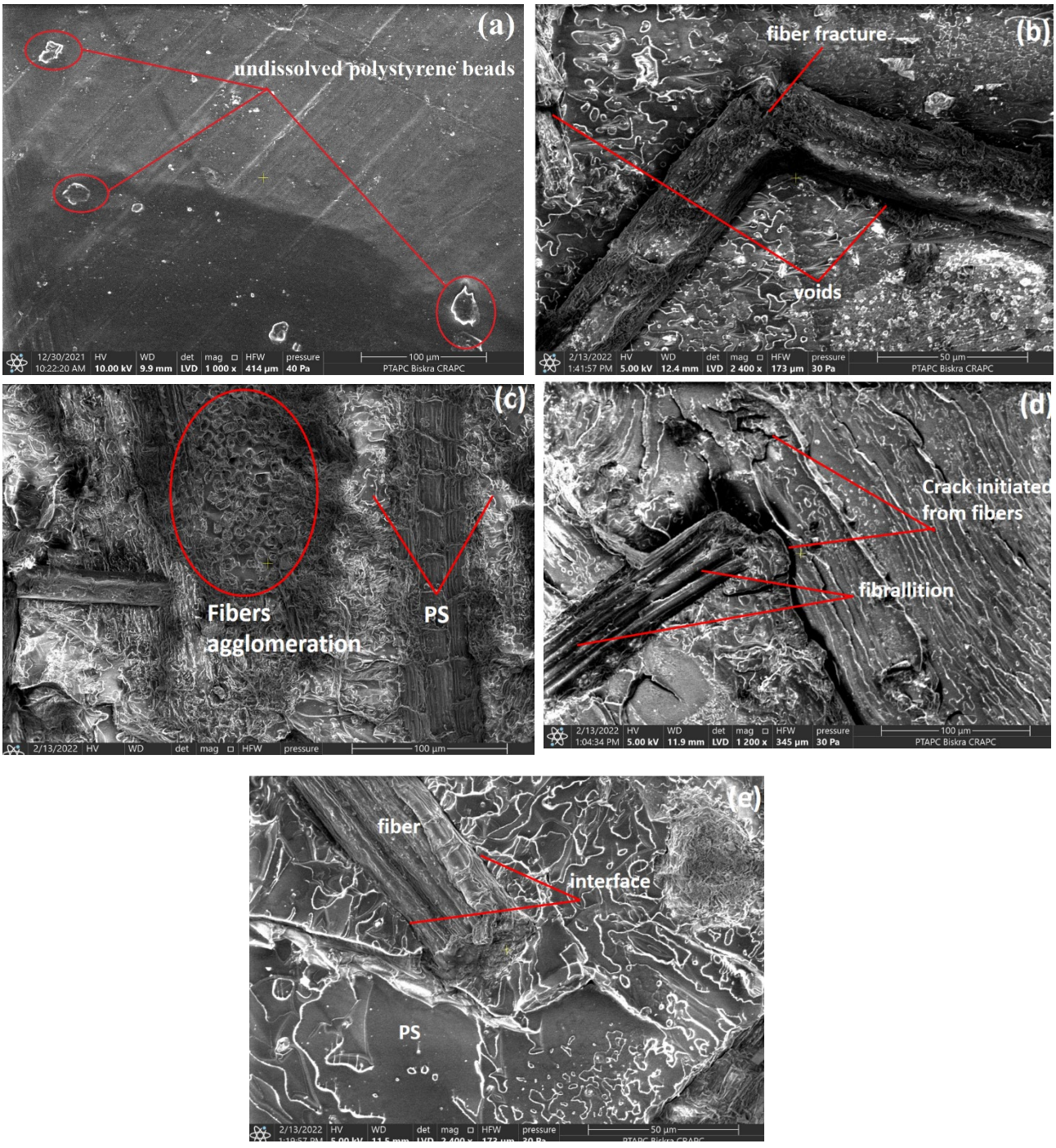

Figure IV. 4. Composite sample SEM micrographs: (a) VPS (b) PS-10%UDPF (c) PS-30%UDPF (d) PS-10%BDPF (e) PS-10%ADPF.

The observations above apply to the samples of benzoylated fiber reinforced with polystyrene and the composite materials manufactured using ADPF. Following the process of benzoylation, there is an observed enhancement in the adhesion properties between the benzoyl diphenyl phosphine oxide (BDPF) and polystyrene (PS) [184].

IV.1.4. Tensile proprieties

IV.1.4.1. Tensile strengths

Figure IV.5 illustrates the relationship between the matrix's proportion of untreated and treated fibers and the resulting variance in tensile strength. The tensile strength of virgin polystyrene is measured to be 16,466 MPa. Except for PS-20%UDPF and PS-30%UDPF, the incorporation of fibers leads to an enhancement in the tensile strength compared to VPS. The observed enhancement in tensile strength due to the inclusion of fillers can be attributed to the higher tensile strength exhibited by fibers compared to polystyrene, as reported in previous studies Zafar et al. [133].

Regarding the influence of the weight fraction of fibers on tensile strength, it has been observed that as the weight % of both untreated and treated fibers increases across all specimens, there is a corresponding decrease in the tensile strength. This phenomenon may be attributed to the formation of filler aggregates resulting from robust hydrogen bonds among them. This phenomenon may give rise to incomplete coverage of the filler by the polystyrene, producing empty spaces inside the composite material. Consequently, these voids can cause stress concentration and contribute to the brittleness of the composite material. The results presented in this study align with previous research conducted by other scholars, as evidenced by the works cited Abu-Jdayil, Hittini, & Mourad [131], Nachtigall et al. [186], Demir, et al. [187], Hammiche et al. [188] and Sapuan & Bachtiar[189].

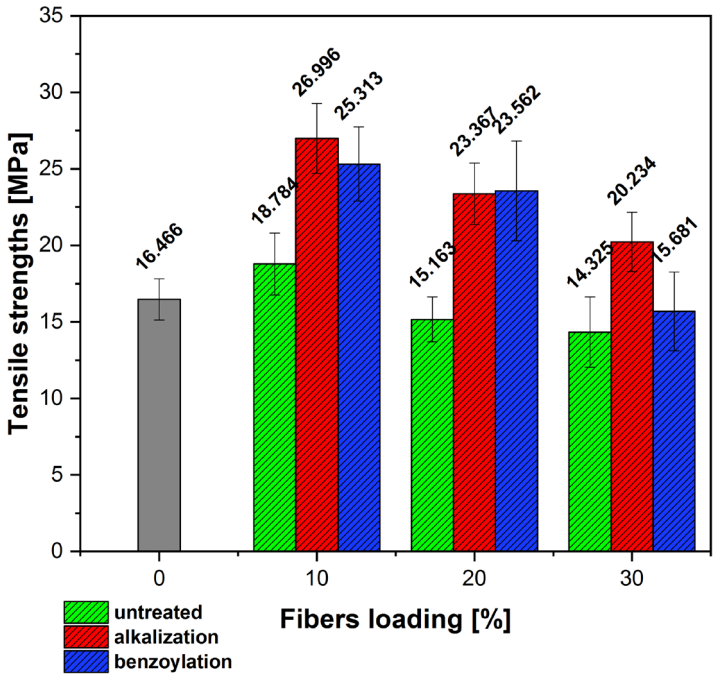

Figure IV. 5. The composite's tensile strengths.

The tensile strength of composite materials containing 10%, 20%, and 30% ADPF was found to be significantly higher than that of PS-UDPF composite materials, with increases of 43.71%, 54.10%, and 41.25% seen in comparison to PS-10% UDPF, PS-20% UDPF, and PS-30% UDPF, respectively. The observed enhancement is attributed to soda treatment, which increases the compatibility between hydrophilic fibers and hydrophobic polystyrene. This is achieved by eliminating wholly or partially hydrogen groups and lowering the fibers' interaction. Consequently, the bonding between the fibers and polymers is improved[158], [151]. The results of this study are consistent with previous research conducted by authors Boussehel et al. [157], Oushabi et al.[21], Khakpour et al. [154] and Krishnan et al.[190]

Using benzoyl chloride (C6H5COCL) leads to a marginal reduction in tensile strength compared to composites fabricated using fibers treated with soda. The therapeutic application of benzoyl chloride mainly relies on its treatment with sodium hydroxide [183]. The authors suggest that the formation of phenyl groups on the fiber surface resulted in the re-establishment of inter-fiber connections, which proved to be more influential than the interactions between the fibers and the phenyl groups contained in the polystyrene, leading to the formation of aggregates inside the matrix. Nevertheless, it remains more advantageous compared to products made from untreated fibers, exhibiting enhancements of 34.76%, 55.40%, and 9.47% for PS-10% BDPF, PS-20% BDPF, and PS-30% BDPF samples, respectively, in contrast to PS-10% UDPF, PS-20% UDPF, and PS-30% UDPF samples.

IV.1.4.2. Tensile modulus

Figure IV.6. illustrates the progression of the tensile modulus for several composite material formulations. It is observed that the VPS formulation exhibits an estimated tensile modulus of 3,581 GPa. On the other hand, the tensile modulus demonstrates an increase when incorporating either treated or untreated fibers. Compared to the VPS, the PS-10%UDPF, PS-20%UDPF, and PS-30%UDPF demonstrate enhancements of 7.12%, 24.89%, and 62.67% correspondingly. Additionally, it was noted that the tensile modulus exhibits a rise with an increase in the proportion of fibers. The PS-20% ADPF sample exhibits a 7.70% improvement, whereas the PS-30%ADPF sample shows a 27.62% improvement compared to the PS-10% ADPF sample. The observed enhancement in performance could be attributed to the increased rigidity of the fibers in comparison to the polymer, as shown by previous studies [191,192]. Chaari et al. [6] reported comparable findings.

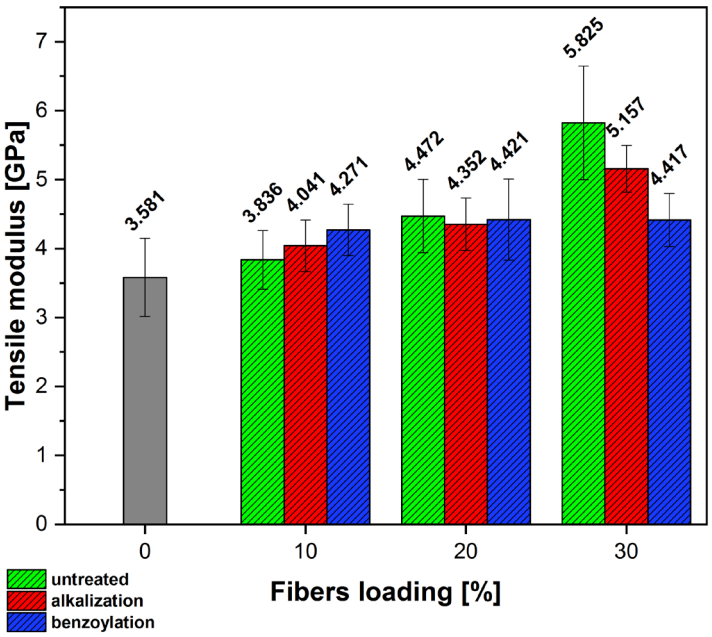

Figure IV. 6. The composite's tensile modulus.

The tensile modulus of PS-10% ADPF is higher than that of PS-10% UDPF. Additionally, the tensile modulus of PS-20% ADPF and PS-30% ADPF is lower than that of PS-20% UDPF and PS-30% UDPF, respectively. The potential cause of this phenomenon may be attributed to an increased concentration of the solution or an excessive amount of delignification, as shown by references [151,193]. The removal of impure materials is contingent upon the chemical concentration and duration of soaking, factors that have been found to impact the tensile modulus [194]. Siakeng et al. (2018) [193] discovered similar adverse impacts on the tensile modulus of coir fibers reinforced with polylactic acid following NaOH treatments, as described in their study.

The tensile modulus of PS-10% BDPF and PS-20% BDPF exhibits a somewhat higher significance level than that of PS-10% ADPF and PS-20% ADPF, respectively. The observed phenomenon can be ascribed to the heightened adhesion between the BDPF and PS matrix, which augments fiber-matrix interactions. An identical observation was made by Manikandan Nair et al.[195].

IV.1.4.3. Strain at break

Figure IV.7 illustrates the relationship between the strain at composites' failure and the date palm fiber rate.

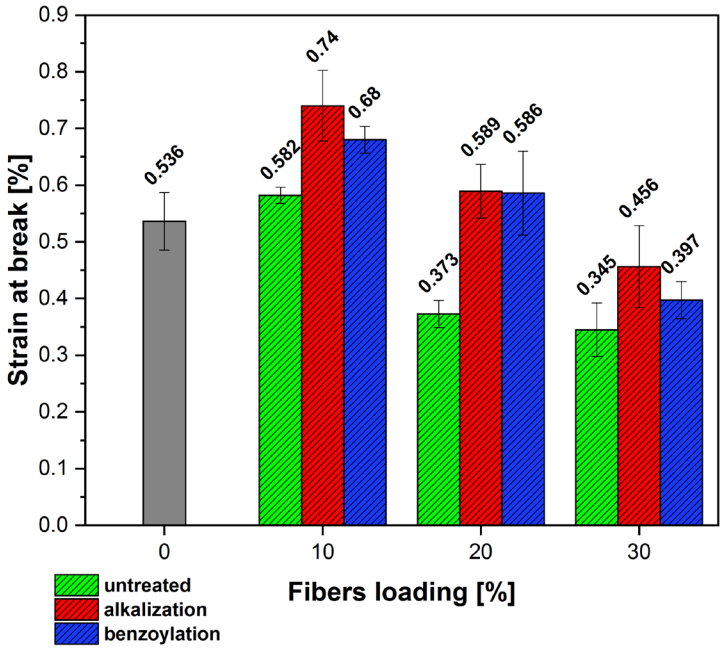

Figure IV. 7. The composite's strain at break.

Initially, it is observed that the strain at the point of fracture exhibits a slight increase across all composite formulations upon the addition of 10% DPF, as compared to the use of VPS. When the percentage of filler content is increased from 20% to 30%, there is a decrease in the elongation at break. The decrease in strength can be attributed in part to the hydrophilic properties of the fibers, which result in increased moisture absorption and subsequent swelling of the PS matrix, leading to material weakening [157]. Additionally, fibers hinder the mobility and slippage of polymer molecules [196].

The strain at break results of the PS-ADPF and PS-BDPF composites show a slight variation compared to the PS-UDPF composites, with an estimated increase of 27.14%, 57.99%, and 32.17% for PS-10% ADPF, PS-20% ADPF, and PS-30% ADPF, respectively, in comparison to PS-10% UDPF, PS-20% UDPF, and PS-30% UDPF. The improved performance might be attributed to the uniform distribution of fibers, which provides the material with a certain degree of flexibility [197].

IV.1.5. Three bending proprieties

IV.1.5.1. Flexural strengths

Figure IV.8 illustrates the variation in flexural strengths of the manufactured composites in relation to the ratio of treated to untreated fibers. Except for formulas PS-10%ADPF and PS-10%BDPF, it has been observed that the flexural strength of the composite material decreases compared to VPS which has a flexural strength of 42,529 MPa after incorporating

both raw and treated DPF. Compared to VPS, the PS-10 %ADPF, PS-20 %ADPF, and PS-30 %ADPF demonstrated reductions of 20.48 %, 9.61 %, and 22.29 %, respectively. The loss in performance can be attributed to the filler's lack of compatibility with the matrix material and the brittleness observed in both PS and DPF [7].

Moreover, it is widely acknowledged that the augmentation of cellulose fiber content in composites reduces their flexural strength. When comparing the PS-20%ADPF and PS-30%ADPF to the PS-10%ADPF, a decrease of 10.15% and 15.64% is seen, respectively.

The decrease seen can be attributed to insufficient dispersion of fibers inside the matrix, as stated by Poletto and al. [8]. Cellulose fibers tend to form agglomerates due to inter-fiber solid hydrogen bonding. Furthermore, the individual fibers' dispersion was limited when the filler concentration increased. Another factor that contributed to the diminished flexural strength was the insufficient bonding between the hydrophilic filler and hydrophobic matrix.

Regarding the impact of DPF treatment on flexural strengths, it is apparent that PS composites reinforced with ADPF exhibit higher flexural strengths than those reinforced with UDPF. Specifically, there are observed improvements of 29.44%, 2.06%, and 11.7% for PS-10% ADPF, PS-20% ADPF, and PS-30% ADPF, respectively, when compared to PS-10%UDPF, PS-20%UDPF, and PS-30%UDPF. Based on the researchers' findings, it has been observed that the alkalinization of fillers leads to an enhancement in the interlocking mechanism between the fiber and the matrix. This improvement is attributed to the enhanced wettability of the materials involved. Furthermore, applying NaOH treatment has been found to effectively eliminate impurities and lignocellulosic substances from the surface of the DPF. Consequently, this treatment facilitates stronger adhesion between the PS and the DPF, thereby positively influencing the mechanical strength of the composite material. The SEM micrograph analysis has supported these observations.

Furthermore, it is worth noting that PS-BDPF composites exhibit comparable results to PS-ADPF composites, albeit with a slight decrease in flexural strength. Nevertheless, PS-BDPF composites remain superior to PS-UDPF composites due to the prior treatment of BDPF with NaOH. The dual approach to treatment has the potential to cause excessive removal of lignin from natural fibers, leading to a fiber that is either weakened or impaired [198].

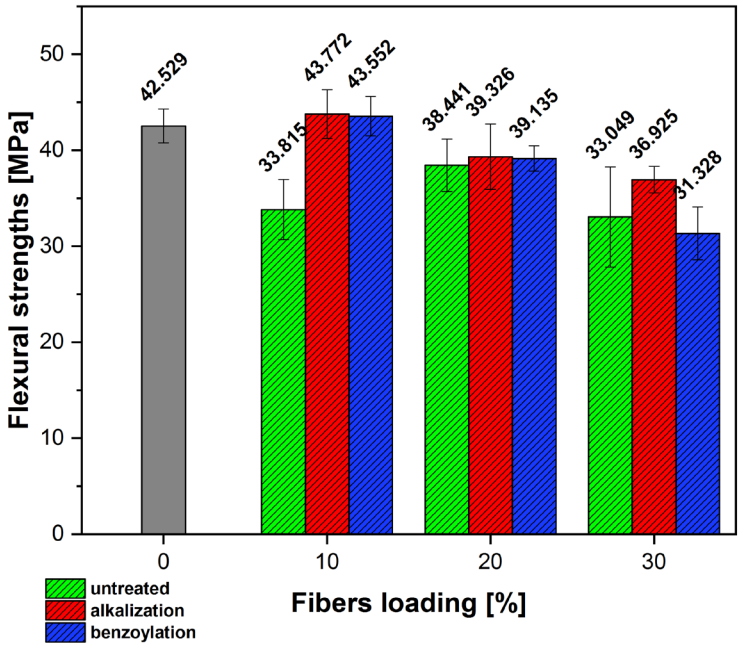

Figure IV. 8. The composite's Flexural strengths.

IV.1.5.2. Flexural modulus

According to the data presented in Figure IV.9, the flexural modulus of VPS is measured to be 2.897 GPa. It is observed that the flexural modulus experiences an increase following the integration of DPF. Compared to VPS, an increase of 0.93%, 17.81%, and 33.55% was seen in PS-10%UDPF, PS-20%UDPF, and PS-30%UDPF, respectively. The observed improvement is attributed to the higher stiffness of the cellulose fiber compared to the polymer matrix [8]. Bachitar's research [189] indicated that the flexural modulus of high-impact polystyrene (HIPS) composites reinforced with short sugar palm fibers increased in response to the addition of fiber loading.

Compared to composites of PS-UDPF with filler loadings of 10% and 20%, the flexural modulus of PS-ADPF composites with the same filler loadings exhibited increases of 7.07% and 3.57%, respectively. The observed improvement in adhesion between the matrix and fillers used in this study can be attributed to the removal of natural and manufactured impurities. In contrast to a 30% PS-UDPF composite, the flexural modulus of a 30% PS-ADPF composite exhibits a reduction of 13.44%. The PS-BDPF composite yielded comparable findings. The researchers have made a significant finding indicating that the fiber loading and ratio can be augmented until the crucial loading threshold is reached. Beyond this point, however, the flexural properties decrease [199].

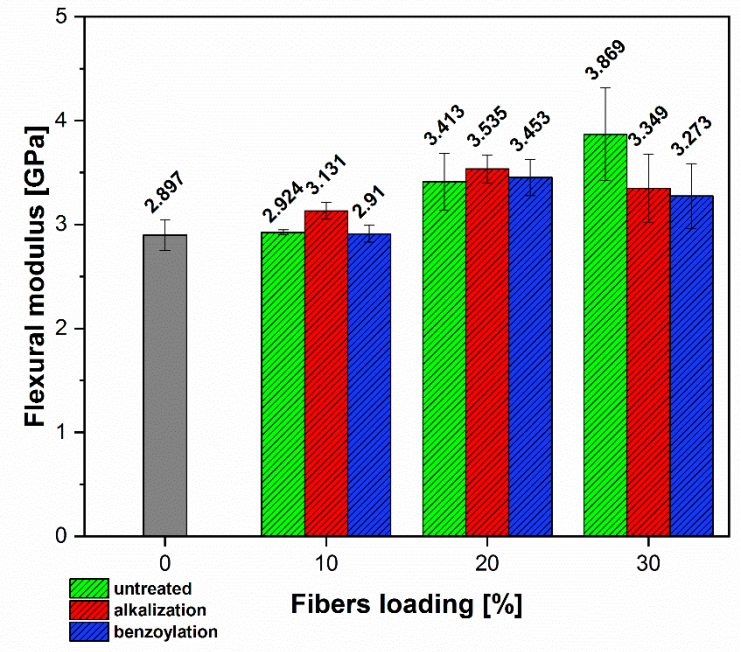

Figure IV. 9. The composite's Flexural modulus.

IV.1.5.3. The maximum deflection

The tensile test fracture point strain distribution is consistent (Figure IV.10). Therefore, readers should check the tensile test strain to avoid repeated interpretations.

It is important to note that fiber ratio and fiber processing affect tensile and flexural characteristics differently. According to Kotelnikova et al. [200], the tensile and flexural failure modes were caused.

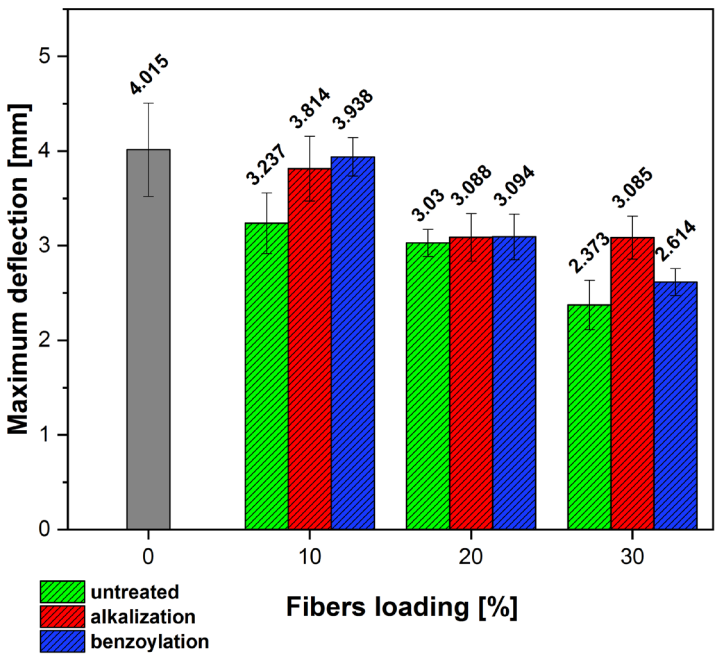

Figure IV. 10. The composite's maximum deflection.

IV.1.6. Thermogravimetric analysis

The present study analyzed the thermogravimetric profiles of virgin polystyrene (VPS) and PS-DPF composites with varying concentrations of raw and treated particulate filter (DPF) materials. The thermogravimetric analysis (TGA and DTGA) data for these composites are presented in Figure IV.11. The plots indicate that thermal degradation of all samples takes place within the temperature range of 30 to 620 ℃. Bachtiar et al. (2012) [189] conducted a study on the characterization of untreated short sugar palm fiber reinforced high-impact polystyrene (HIPS) composites, which had a comparable range finding.

The VPS exhibited a single stage of degradation. However, the composite of Polystyrene (PS) and DPF displayed four distinct phases of degradation (although this was not evident in all samples of PS-10%DPF). During the initial temperature range of 30-100°C, the derivative thermogravimetric (DTG) curve of composites has a less distinct and absent peak, which is not observed in the VPS. The observed phenomenon can be attributed to the decrease in moisture content within DPF, which did not demonstrate a substantial loss (less than 3 weight percent). The phenomenon of moisture loss is commonly observed in natural fabrics. This phenomenon is more conspicuous in composites with a filler concentration of 30% compared to those with a filler concentration of 10%. This is because a more significant concentration of dispersed phase filler leads to increased water retention, subsequently leading to a more substantial loss in weight. In this particular stage, it can be observed that the weight loss of composites incorporating BDPF is marginally lower compared to those containing PS-ADPF and PS-UDBF. The observed phenomenon can be attributed to the alkali surface treatment, which increases surface roughness and enhances the accessibility of hydroxyl groups. Conversely, the benzoyl treatment results in a reduction of the fiber's hydrophobic characteristics [23]. This supports the conclusions found by Tawakkal et al. (2014) [192] in their study on the thermal stability of composites made from PLA, kenaf, and thymol.

During the second phase of degradation, which occurs between temperatures of 180°C and 360°C, the composite materials PS-30 % UDPF, PS-30 % ADPF, and PS-30 % BDPF (as shown in Figure IV.11-b and f demonstrate their highest rate of decomposition at temperatures of 355°C, 335°C, and 304°C, respectively. The corresponding weight losses for these materials are measured at 11.53 %, 12.98 %, and 7.12 %, respectively. The observed phenomenon can be attributed to the degradation of hemicellulose, which occurs within a temperature range of 160 to 360 °C. Additionally, the high thermal stability of

cellulose, characterized by its crystalline structure, results in a decomposition temperature of 240–390 °C. Furthermore, lignin, with a degradation temperature ranging from 250 to 700 °C, also contributes to this phenomenon [138] and [131]. VPS does not logically exhibit this particular phase. Both of the treated composites, which consist of DPF-reinforced PS, exhibit lower temperatures at which the maximum rate of disintegration occurs within the specified temperature range. The observed phenomenon can be attributed to eliminating a fraction of lignin, as lignin tends to break down over a wider temperature range than cellulose.

The third stage, the major disintegration stage, is observed in VPS and PS-DPF composites within the temperature range of 360 °C to 460 °C. Two potential factors may contribute to this phenomenon. Firstly, the breakdown of DPF's cellulose II, α-cellulose, and lignin. Secondly, the deterioration of the polymer network structure and the formation of volatile oligomers [201]. These factors are believed to be the primary reasons for the significant loss of mass observed during the primary decomposition phase. The peaks in this stage occur at temperatures of 415, 422, and 426 °C, indicating the points of highest disintegration rate. These temperature values correspond to weight losses of 66.5%, 60.9%, and 53.6% for VPS, PS-10% UDPF, and PS-30% UDPF, respectively, as illustrated in Figure IV. a and d. In the present stage, adding UDPF reinforcements improves the thermal stability of PS-DPF composites by functioning as protective barriers that provide effective heat insulation [189]. The enhancement of thermal stability at this particular stage may be observed by increasing the filler loading from 10 to 30. This improvement can be attributed to the physical interlock mechanism, which restricts the thermal motion of polystyrene (PS) segments located near the surface of the diesel particulate filter (DPF) [202].

In contrast, the maximum decomposition rates for PS-10 %ADPF and PS-10% BDPF at this stage are recorded as 412 °C and 418 °C, respectively. These values correspond to weight losses of 66.32% and 63.17%, respectively, as depicted in Figure IV.-c and d.
The PS-30%ADPF and PS-30%BDPF exhibit a peak disintegration rate at temperatures of 420 and 422°C, resulting in weight losses of 55.32% and 56.22%, respectively. Both treatments exhibit a decrease in the decomposition temperature when compared to PS-30%UDPF. Removing impurities, such as pollutants, wax, and hemicellulose, from the surface of the fibers elucidates this phenomenon. The components above form a protective layer around the cellulose material, impeding its degradation process. Cellulose constitutes a significant proportion of the fibrous substance [203].

The fourth stage of deterioration, which occurs within the temperature range of 450 to 540 °C, is not universally observed in all samples exhibiting a broad DTGA peak. The primary cause of degradation at this stage is the deterioration of a non-cellulosic component, such as lignin, waxy material, or sugar mallards. The slow degradation of lignin renders it more resistant to disintegration than other organic constituents. Furthermore, the structure of the compound encompasses aromatic rings with several branches and substantial cross-linked molecules [138].

Based on an analysis of the residue weight at a temperature of 650°C, it is evident that VPS exhibits a lack of significant residue when compared to the PS-DPF composites. This observation aligns with the conclusions reached by Tawakkal et al. [192]. The data indicates a positive correlation between the proportion of treated or raw DPF and the residual, as the ratio climbs from 10% to 30%. As an illustration, when examining PS-10 % UDPF, a residue of 1.57 % is observed, but PS-30 % UDPF exhibits a residue of 13.57 %.

The formation of residue in the composite can be attributed to two factors. Firstly, the inclusion of cellulose in the DPF fibers, a type of lignocellulosic material known to generate char residue [192]. Secondly, the presence of lignin residue, which undergoes decomposition within the temperature range of 250 to 700 ˚C [1].

At a temperature of 650°C, the PS-30 % ADPF and PS-30 % BDPF residues are measured to be 5.67 % and 4.14 %, respectively. These values are lower than the residue of PS-30 % UDPF. The reduction of the final residue can be attributed to eliminating hemicelluloses and lignin during the processing of Saba [204].

The incorporation of DPF reinforcements has been found to enhance the heat resistance of materials, potentially leading to increased fire retardancy [192].

In conclusion, it can be asserted that the polystyrene samples comprising 30% untreated and treated fibers (as depicted in Figure IV.11-b and Figure IV.11-f) exhibit superior thermal stability compared to the VPS. Furthermore, a slight advantage is observed in the thermal stability of the untreated sample over the treated sample when considering the residues. The thermal stability of the composite is not considerably affected by the incorporation of 10% treated and untreated fibers. However, it is worth noting that the curves exhibit some overlap, which can be attributed to the minimal quantity of fibers present.

In comparison to metals, composites exhibit significant thermal degradation at temperatures over 210 °C, a range that is unattainable during the manufacturing process or in practical applications involving these composite materials [171].

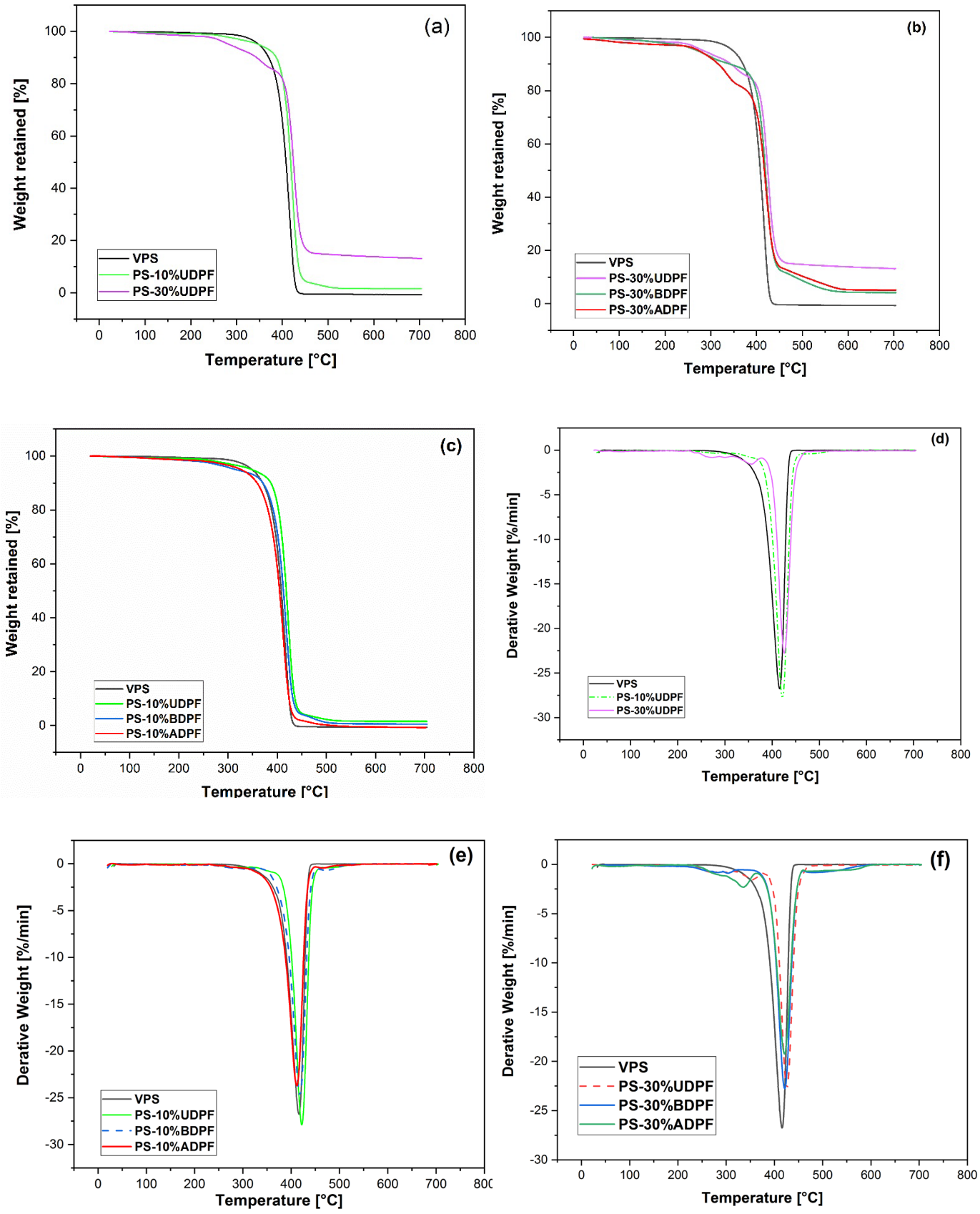

Figure IV. 11. TGA and DTGA curves of composite

IV.1.7. MIP analysis results

IV.1.7.1. Pore size distribution

Table IV.2 presents the values obtained through the use of MIP on untreated fibers (UDPF), virgin polystyrene (VPS), and PS-UDPF specimens, as depicted in Figure IV.12 and Figure IV.13 . The mercury intrusion volume is indicative of the overall open porosity, which exhibits an increase with the addition of UDPF due to the increased porosity of the fiber material. Specifically, the fiber material has a porosity of 18.5076%, whereas virgin polystyrene has a porosity of 4.6976%. The porosity of UDPF fibers can be attributed to the presence of high lumens in their cross-sectional morphologies [205]. The PS sample containing 30% UDPF exhibited the highest reported porosity values. The intrusion seen in the control specimen VPS was found to be lower compared to the intrusion observed in DPF-reinforced polystyrene.

Table IV. 2. Mercury intrusion porosimetry of UDPF test results.

Test index	UDPF	VPS	PS-10%UDPF	PS-20%UDPF	PS-30%UDPF
Total intrusion volume (mL/g)	0.3137	0.0453	0.0490	0.0775	0.0750
Median pore diameter (μm)	1.0372	0.0142	0.0167	0.0174	0.0201
Porosity (%)	18.5076	4.6976	5.2866	7.9155	7.9465

As the concentration of DPF rose, there was an observed rise in both the median pore size and porosity. The median pore sizes of VPS, PS-10%UDPF, PS-20%UDPF, and PS-30%UDPF are 0.0142, 0.0167, 0.0174, and 0.0201 μm, respectively. In general, it was observed that a finer pore structure was associated with reduced median pore diameter and porosity [206]. Consequently, the PS-DPF composite exhibited lower compaction and a more extensive pore network than VPS.

Figure 16 shows untreated date palm fiber pore size distribution and cumulative pore volume. The particle has pore size diameters ranging from 0.005μm to 6μm. The differential log intrusion curve shows that most pores had a diameter of 0.76 μm to 3 μm, with a noticeable peak at 1.35 μm.

Figure IV.13 shows the cumulative intrusion and log differential intrusion in polystyrene and untreated date palm fiber samples as a function of pore diameter. The PS-UDPF composite curves are higher than the virgin polystyrene curve, indicating a higher proportion of porosity. A larger fiber weight ratio increases pores, explaining the fall in tensile and flexural strengths with fiber load.

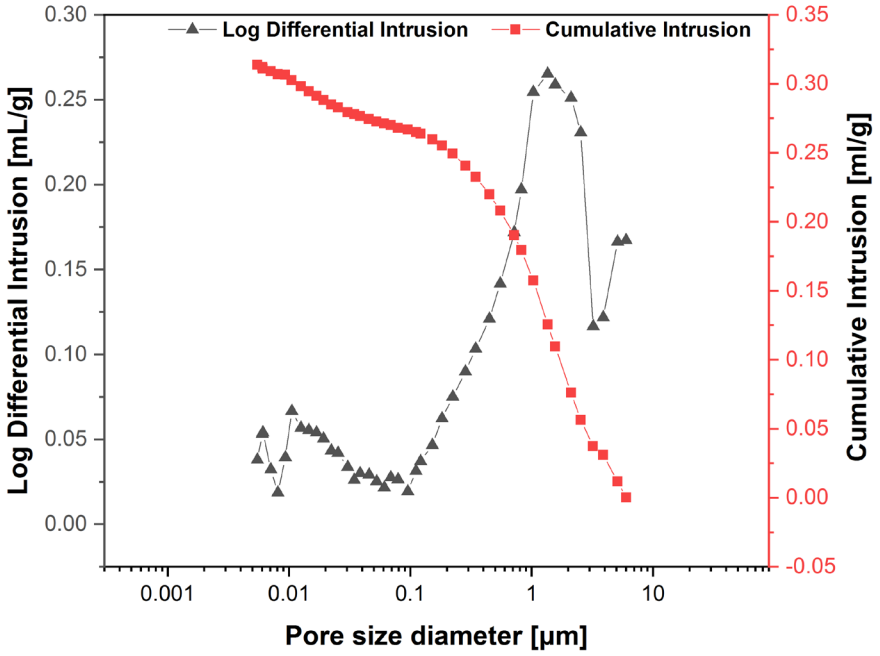

Figure IV. 12. UDPF pore size distribution and total pore volume.

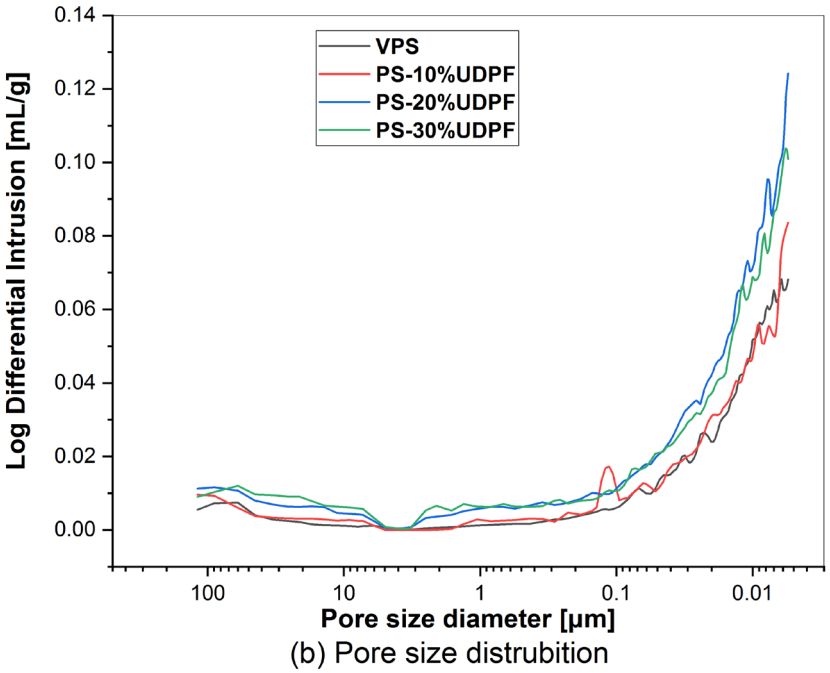

Figure IV. 13. MIP curves of PS-UDPF.

The data presented in Figure IV.13 indicates that the observed pores have diameters ranging from 0.01 μm to 0.1 μm. Pores larger than 0.1 μm exhibit a minimal presence and can be considered virtually absent. However, it is worth noting that PS-20% UDPF and PS-30% UDPF demonstrate larger pore sizes, indicating the presence of newly formed pores inside the material. This observation proves the limited bonding strength between the VPS material and UDPF. The obtained outcomes align with the observations made using scanning electron microscopy (SEM) micrographs.

IV.1.7.2. Results for Bulk Density

Figure IV.14 illustrates the changes in bulk density among the various samples. It is evident that the inclusion of both untreated and treated fibers resulted in a decrease in the bulk density of VPS, which was initially reported as 1019.7 kg/m3 (Table IV. 3). This reduction can be attributed to the fact that the fibers possess a lower density compared to the polystyrene-based resin. Our findings indicate that the bulk density of DPF ranges from 540 to 590 kg/m3, as shown in Table 3. These values are higher than those reported by Almi et al. [30], who observed a bulk density of approximately 411 kg/m^3 for DPF obtained from leaflets. A comparable pattern is observed in various prior studies, including the work of Praveena B et al. [207], who examined the impact of incorporating pineapple fibers into polyester resin. Conversely, Abu-Jdayil et al. [131] discovered an opposite trend when incorporating date pit powder into pure polystyrene, increasing composite density. This can be attributed to using a reinforcement material with a higher density than the matrix.

Furthermore, it has been observed that the augmentation of filler content is inversely proportional to the density of composites. Furthermore, increased fiber content inside the composite leads to elevated pore interiors due to the diminished adhesion between the fiber and the polymer. The unaddressed one substantiates this occurrence. In a study by Abu-Jdayil et al. [1], a comparable pattern was seen when the concentration of date palm seed fillers was augmented within the unsaturated polyester matrix.

The results obtained from samples composed of alkaline and benzoylated fibers exhibit a high degree of similarity. The enhanced adhesion between fillers and polymers reduces voids within the composite material, in contrast to PS-UDPF. Consequently, the treated composite exhibits a higher density compared to the untreated composite.

The density values of the PS-DPF composites exhibit a range of 982.4 kg/m3 for PS-30%UDPF samples to 1016.1 kg/m3 for PS-10%BDF composites. This is low or comparable to other materials suggested in Table 5 for thermal insulation and construction.

Table IV. 3. The thermophysical properties of PS-DPF and comparable substances.

Materials	**λ [W. m^{-1} K^{-1}]**	**ρ [kg.m^{-3}]**	**References**
VPS	0.1492	1019.7	This work
PS- DPF	0.1185-0.1392	864.3–972.2	This work
Gypsum neat	0.44	1130	Chikhi et al.[147]
HG/DPF (10%)	0.15–0.17	753	Chikhi et al.[147]
LPC	0.112–0.159	542–824	Masri et al.[2]
DPC	0.185	954	Haba et al.[208]
AlN/PS	0.189-0.418	/	Wu et al.[202]
PLA- DPWF	0.077-0.105	1200-1450	Al et al.[209]
DS-UPR	0.126 – 0.138	644-1200	Abu-Jdayil et al.[1]

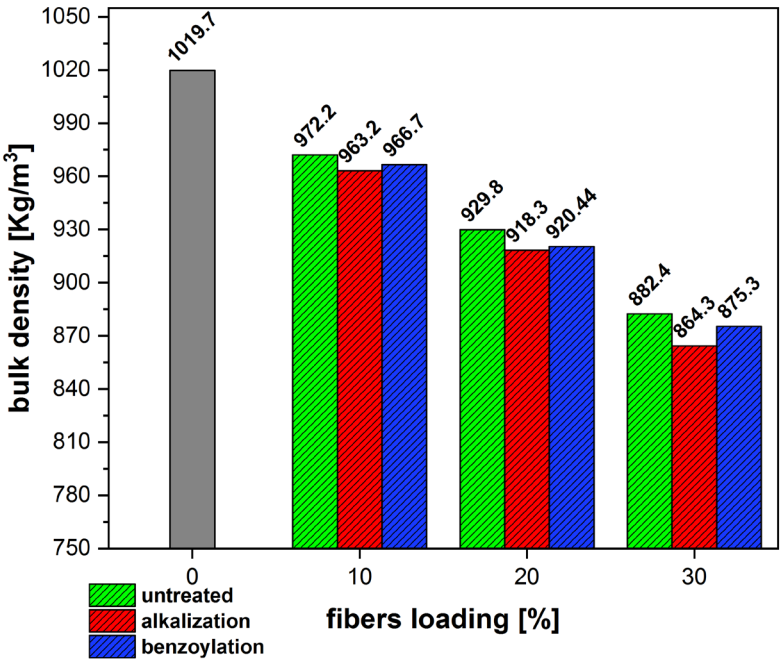

Figure IV. 14. Composites' bulk density.

IV.1.8. Results for Thermal conductivity

The thermal conductivity value of raw date palm fibers, as reported in Table 14, was measured to be 0.0895 W/m·K. The recorded value surpasses the findings of Agoudjil et al. [210], where they reported a thermal conductivity of 0.083 W/m·K for the petiole of the Deglet-Noor date palm cultivar. The observed variation in the specimen waste can likely be attributed to differences in regional factors and the extraction process. Additionally, the researchers conducted measurements on the electrical conductivity of solid materials. It has been established that thermal conductivity is influenced by the temperature [150].

In contrast, the thermal conductivities of ADPF and BDPF were measured to be 0.095 W/m.K and 0.0822 W/m.K, respectively. The results do not show a significant disparity in the thermal conductivity measurement. The observed phenomenon can be related to a slight alteration in the percentage of crystallinity of the fiber, as indicated in the X-ray diffraction (XRD) findings. The relationship between thermal conductivity and the degree of crystallinity has been established in previous studies by Basim Abu-Jdayil et al. [201], who mentioned that thermal conductivity increased with the degree of crystallinity.

Figure IV.15 illustrates the change in thermal conductivity of the prepared samples. The thermal conductivity of virgin polystyrene (VPS) was approximately 0.1492 W/m·K.

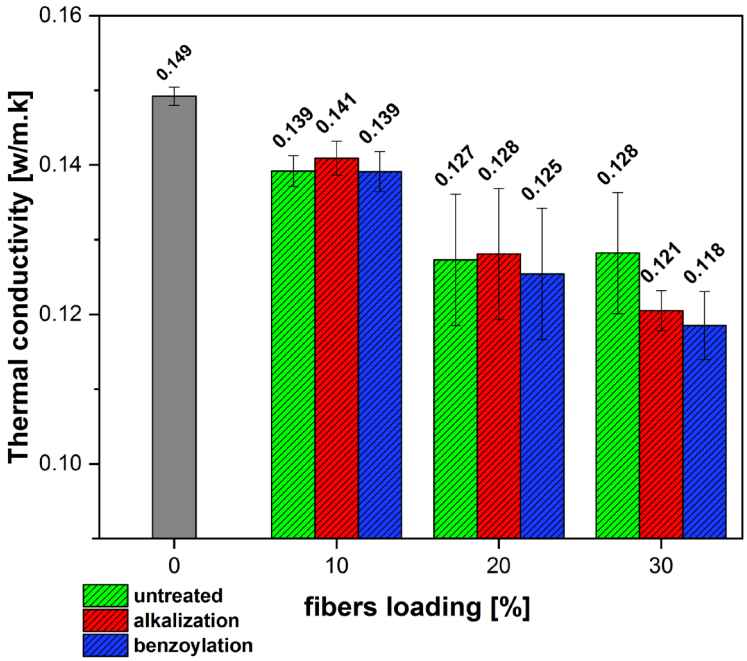

Figure IV. 15. Composites' Thermal conductivity.

It has been observed that the inclusion of fibers has a beneficial impact on the thermal insulation properties of resin-based polystyrene (VPS), reducing thermal conductivity. The observed phenomenon can be attributed to the disparity in thermal conductivity between fibers and VPS. Furthermore, as stated by Ighalo et al. [211], the decrease in density resulting from the inclusion of fibers leads to an increase in the number of pores inside the material, thereby reducing its thermal conductivity. Thereby, including excessive filler material within the matrix can fill the voids created by the pure polystyrene beads containing gases, leading to a subsequent increase in thermal conductivity, as observed in the case of PS-30%UDPF. This phenomenon can be attributed to the filler's substantially higher heat conductivity compared to air voids [1].

As an illustration, the PS-10%UDPF, PS-20%UDPF, and PS-30%UDPF exhibit reductions of 12.30%, 14.68%, and 13.57% correspondingly, in comparison to VPS. Haddadi et al. (2015) [212] observed comparable patterns in their investigation of vinyl resin white glue as a matrix with varying loadings of DPF. Furthermore, Boumhaout et al. [213] conducted a study that revealed that incorporating a higher quantity of DPF mesh into mortar results in an enhanced insulating performance, effectively reducing the thermal conductivity by up to 70%. This study also investigates the impact of integrating alkaline and benzoylated fibers on the thermal conductivity coefficient. Figure IV.14 illustrates that the thermal conductivity of PS-ADPF and PD-BDPF is greater than that of PS-UDPF when considering fibers of the same composition.

The observed rise can be attributed to removing hemicellulose by applying sodium hydroxide (NaOH) in the treatment process, resulting in an elevated cellulose ratio within the filler material. The cellulose in the treated filter (DPF) serves as a nucleating agent for the polymer, enhancing the crystallinity and resulting in elevated thermal conductivity. A direct relationship exists between the degree of crystallinity and the thermal conductivity, as supported by previous studies by Bai et al. 2018 [214]. Furthermore, the enhancement in heat conductivity compared to PS-UDPF might be attributed to the improved compatibility between the filler and matrix and the reduction of air gaps resulting from the treatments [1].

Samples with a greater treated fiber concentration of 30% exhibit a reduced thermal conductivity compared to samples prepared with PS-30%UDPF. The observed phenomenon can be attributed to a decrease in the concentration of fillers within the pores, resulting from

the treatment process due to the removal of hydrogen groups from the fibers. The previous discussion highlighted the effective dispersion of fibers within polystyrene resin.

During our investigation, a comparison was conducted to assess the impact of two distinct treatments on thermal conductivity. Generally speaking, it was observed that samples composed of benzoyl fibers exhibited a lower thermal conductivity than samples composed of alkaline fibers. As previously indicated, the reduced heat conductivity of BDPF compared to ADPF is the reason for this attribution.

In each instance, the range of thermal conductivity values (0.1185 to 0.1409W/m.K) exhibits minimal variance, indicating that the PS-DPF material demonstrates insulating characteristics.

The authors of this study claim that the LPC composite material, as described by Masri et al. [2], bears a striking resemblance to the PS-DPF material. Both composites have the same matrix and kind of filler, albeit with variations in filler loading, size, and treatment. The LPC thermal conductivity exhibits a range of values between 0.112 and 0.159. This range confirms the improved thermal insulation achieved by our research on this particular material. Furthermore, Ighalo et al. [211] formulated a polymer composite utilizing discarded rice husk and polystyrene materials. A thermal conductivity value ranging from 1.2 to 1.7 W/m·K was discovered, surpassing the results obtained in our study.

Assuming the context of thermal conductivity, heat transfer resistance can be defined as the inverse of a material's thermal conductivity. In this scenario, the collective resistance of a composite material can be calculated by summing the individual resistances of each constituent element, with their respective weights determined by their volume (or mass) percentages [215] equation (10)

$$\frac{1}{\lambda_{overall}} = \sum_{i=1}^{n} \frac{w_i}{\lambda_i}$$

Where w_i represents the weight fraction of component i and λ_i is the thermal conductivity, summed over all entering constituents of a composite.

Meanwhile, traditional construction walls consist of building blocks, concrete, and reinforced concrete, exhibiting an average thermal conductivity of 1.01W/m.K [215]. In an alternative scenario, if the wall is constructed using building blocks, concrete, and reinforced

concrete, and PS-30 % BDPF is used to form one-third of the wall's thickness, while the remaining two-thirds of the wall is made up of the aforementioned materials, then the parameter w_i remains unaffected.

$$\frac{1}{\lambda_{overall}} = \sum_{i=1}^{n} \frac{w_i}{\lambda_i} = \frac{(1/3)}{0.1185} + \frac{(2/3)}{1.01} = 3.473$$

This implies that the updated value of $\lambda_{overall}$ will be 0.2879 W/ m. K. Hence, when constructing a wall with a thickness equivalent to one-third of its total width, employing PS-30 % BDPF as the material, the resulting decrease in thermal conductivity may be estimated to be approximately 71.4%.

In the second instance, we will assess if PS-30% BDPF accounts for one-third of roofs produced from gypsum plaster, possessing a thermal conductivity value of 0.52 W/m.k [143]. If this condition is met, the roofs will have a thermal conductivity value of 0.52 W/m.k.

$$\frac{1}{\lambda_{overall}} = \sum_{i=1}^{n} \frac{w_i}{\lambda_i} = \frac{(1/3)}{0.1185} + \frac{(2/3)}{0.52} = 4.094$$

Consequently, the new value of λ_overall is determined to be 0.2442W/m.K. Therefore, by utilizing PS-30%BDPF material to build a wall with a thickness of one-third of the total wall thickness, the resultant decrease in the overall thermal conductivity will be approximately 53.03%.

IV.1.9. Cost-effectiveness

Evaluating the sustainability of composite materials reinforced with date palm fibers also considers the significant aspect of cost-efficiency. Tables IV.4 and IV.5 provided information on the unit costs of raw materials and the cost-efficiency of the PS-UDPF in the Biskra region of Algeria, respectively. Furthermore, it is vital to acknowledge that the investigation was carried out regarding the quantity of material utilized to produce two plaques (measuring 130x130x2.4 mm^3) for each formulation category. The PS-UDPF composite materials exhibited greater cost-effectiveness compared to the VPS. Consequently, utilizing these inexpensive or freely available waste materials has enhanced cost-efficiency. Upon conducting a comparative analysis of the overall expenses incurred by each group, it has been determined that a higher replacement rate of DPF for polystyrene leads to enhanced cost-effectiveness.

Preserving the environment and minimizing the consumption of natural resources, such as polystyrene, a petroleum derivative, are of utmost importance.

Table IV. 4. Unit costs of raw materials employed in PS-DPF composites materials.

Materials	**EPS**	**DPF**
Units cost (DZD/Kg)	336,22	13,45

Table IV. 5. Cost-efficiency of PS-DPF composite materials.

Samples formulation	**EPS**		**DPF**		**Total material costs (DZD)**
	Mass (g)	**Cost (DZD)**	**Mass (g)**	**Cost (DZD)**	
VPS	200	67,24	0	0	67,24
PS-10%UDPF	180	60,52	20	0,27	60.79
PS-20%UDPF	160	53,80	40	0,54	54,34
PS-30%UDPF	140	47,07	60	0,81	47,88

IV.2. SECOND WORK HYBRID BIOCOMPOSITE (GYPSUM/DPF/EPS)

IV.2.1. FTIR Results

Figure IV.16 illustrates the infrared spectra of NG, DPP, and EPS.

One may detect the presence of various peaks inside the NG sample. The bands detected at wavenumbers 3613 and 3548 cm^{-1} can be ascribed to the dimeric and characteristic polymeric stretching vibrations of the O-H bonds in crystalline water in CaSO4.2H2O. The observations above provide supporting evidence for the existence of gypsum and sulfate compounds within the analyzed sample [216]. The identification of the O-H vibrations of water in the original chemical composition of the binder, specifically calcium sulfate hemihydrate, can be deduced based on the peak detected at 1616 cm^{-1}[143]. The vibrational frequencies of alkyl thioketones (-C=S) in sulfur compounds have been shown to fall within the range of 1050-1150 cm^{-1} [217]. The gypsum specimen has a distinctive S-O bending

vibration, which has been determined through experimentation at a wavenumber of 594 cm^{-1}[143].

Significant and extensive O-H stretching can be identified from the peaks detected at around 3248 cm-1 in the context of fibers [167]. The identification of prominent peaks in the vicinity of 2913 and 2842 cm-1 indicates the possible presence of the alkane (C–H) functional group [175]. The identification of a peak at around 1737 cm^{-1} in the DPP spectra can be attributed to the carbonyl group C=O [183]. The presence of a peak at 1616 cm-1 in the spectrum can be ascribed to water absorption by the untreated palm fiber. This absorption is predominantly influenced by the fiber's hydrophilic properties, as documented in previous studies [157]. The peak that is prominently visible at around 1010 cm−1 is associated with the carbohydrate backbone of cellulose, as well as the C–OH stretching vibration of the lignin, cellulose, and hemicellulose backbones [4,153,218].

The Fourier Transform Infrared (FTIR) spectra of EPS had discernible peaks corresponding to the stretching vibrations of C-H bonds, notably at around 3021 cm−1 and 3066 cm−1. Furthermore, the spectra exhibited peaks characteristic of C-H2 stretching vibrations, with approximate values of 2913 cm^{-1} and 2842 cm^{-1} [219]. The stretching vibrations of the benzene ring are typically detected at around 1616 cm−1 and 1456 cm−1, whereas the bending vibrations manifest at approximately 758 cm^{-1} and 524 cm^{-1} [220].

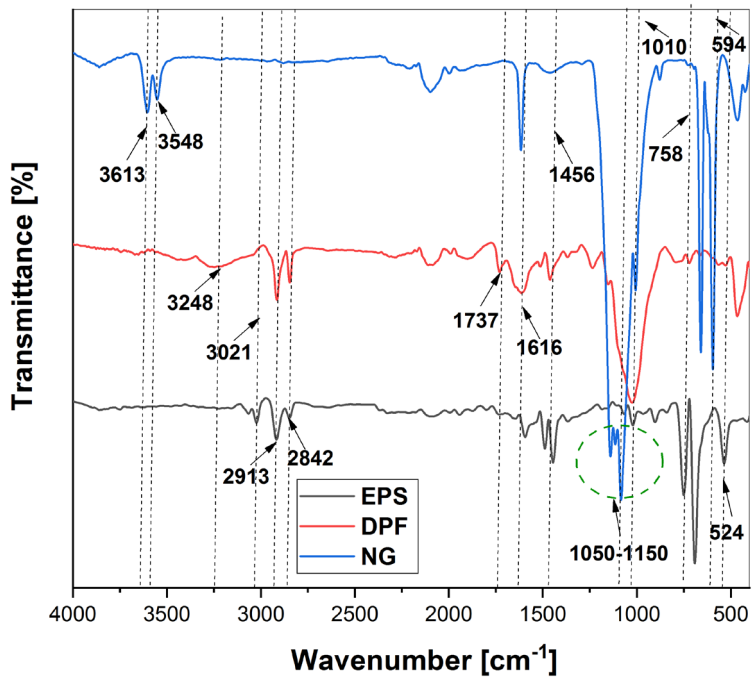

Figure IV. 16. FTIR spectra of NG, DPP, and EPS.

IV.2.2. DRX results

Figure IV.17-a, b, c, and d display the X-ray diffraction spectra of NG, DPP, G-EPS-15F, and polystyrene, respectively. The current study provides evidence that the gypsum plaster used has a distinct composition consisting of various minerals with differing levels of intensity:

-Quartz is a mineral characterized by its crystalline structure, primarily of silicon dioxide (SiO2) [221].

-Calcite is a mineral mainly composed of calcium carbonate (CaCO3). Sedimentary rocks, such as limestone and dolomite, are often strongly associated with geological formations such as stalactites and stalagmites [216].

-Dihydrate calcium sulfate, known as gypsum, is a mineral characterized by white or grayish coloration. It is naturally formed by evaporation of seawater or salt-laden groundwater. The source referenced as [216] states that the primary constituent of the substance is hydrated calcium sulfate.

Additionally, halite (NaCl) has been observed in the analyzed samples, concluding that the gypsum powder under investigation does not possess complete purity. Additional components, commonly known as contaminants, possess the capacity to influence the mechanical and thermophysical characteristics of the gypsum powder. The research findings indicate that the sample demonstrates a 28.42% amorphous content, while the remaining 71.58% is attributed to its degree of crystallinity.

Figure IV.17-b illustrates the X-ray diffraction pattern of DPP. This examination aimed to get qualitative data on the mineralogical composition of the biofiber under investigation. A comparative analysis was conducted using X-ray patterns of sugar palm fiber [222] and bamboo fiber [223], which confirmed that the apparent crystalline component in the fiber primarily consisted of cellulose. The examination indicates that the sample demonstrates a composition of 47.69% amorphous and 52.31% crystalline phases. The occurrence of two separate peaks at 2θ values of 16.8° and 21.7° can be ascribed to the existence of cellulose I and cellulose IV, both of which possess a monoclinic crystal structure [155]. The results of this investigation suggest that the fibers obtained from date palms exhibit a semi-crystalline structure.

The results of an X-ray diffraction analysis conducted on a polystyrene sample are presented in Figure 7-d. A solitary, broad diffraction peak was seen at a 2θ angle of 19.67°, a characteristic peak linked to polystyrene [224]. The observed peak indicates that the polystyrene sample exhibits high purity and lacks a crystalline structure. The researchers discovered that the degree of crystallinity was 29.91%, which is consistent with the results given by Huang et al. [225].

Figure IV.17-c depicts the X-ray diffraction (XRD) pattern of the composite samples G-EPS-15F. The observed trend suggests that the presence of DPP and EPS influences the crystallinity of the plaster. The decrease in peak intensities found in G-EPS-15F composites, in comparison to NG, indicates a decline in the crystallinity of the composite. This assertion is reinforced using equation (3), resulting in a computed value for the degree of crystallinity of 61.70%.

The calcium sulfate dihydrate and quartz peaks in pure gypsum, as shown in Figure IV.17-c, have intensities of 2628 and 1212, respectively, at around 14.7◦ and 50◦. On the other hand, the G-EPS-15F composite demonstrates peak intensities of 873 and 347, respectively. A decrease in the level of crystallinity leads to a proportional decrease in the mechanical characteristics of the composite material. El, Charai, and Channouf [221] identified a similar trend.

Table IV.17 displays the X-ray diffraction (XRD) analysis results for the materials under investigation.

Table IV. 6. Microstructural parameters from XRD-analysis for some studied samples.

Samples code	The area under the crystalline peaks, A_{Cryst}	Total area under the entire diffraction curve ($A_{Cryst} + A_{Amorph}$)	Degree of crystallinity, X_{Cryst} [%]	Amorphous ratio, X_{Am} [%]
NG	6912.09	9656,46	71.58	28.42
DPP	21235.59	40587,92	52.31	47.69
PS	5191,19	17353,43	29.91	70.09
G-EPS-15F	4724,96	7656,99	61.70	38.30

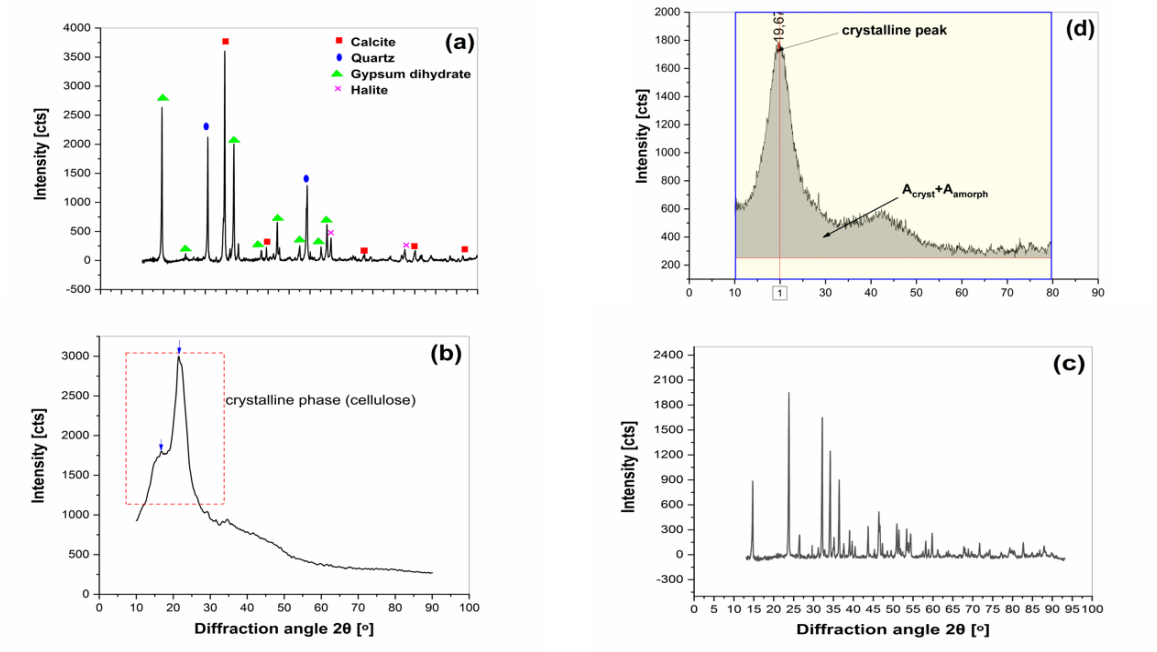

Figure IV. 17. X-ray diffractograms of (a) NG, (b) DPP, (c) G-EPS-15F, and (d) EPS.

4.2.3. Mechanical proprieties

Including EPS and date palm fibers in gypsum plaster reduced mechanical properties, as evidenced by the bending and compression test curves (Figure IV.18-a and Figure IV.18-b respectively). The observed fragile behavior suggests a potential compromise in structural integrity. Curves reveal an evolution in the fragile behavior of the gypsum plaster resulting from the different added particles. Further analysis and optimization may be necessary to enhance the composite's performance and address the identified mechanical limitations introduced by incorporating these waste materials. The behavior of the present composite is similar to that observed by R. Belakroum et al. [2] and Le et al.[52].

The mechanical parameters of compression strength (a), flexural strength (b), and Young's modulus (c) are depicted in Figure IV.18. The preliminary observation suggests that the incorporation of expanded polystyrene (EPS), fiber (F), or a combination of both leads to a significant reduction in the mechanical properties of the samples that were prepared. The compression strength of G-EPS, G-5F, and G-EPS-10F materials shows a decrease of 38.68%, 68.68%, and 76.25%, respectively, when compared to the compression strength of plain gypsum (NG), which has the most significant value of 7.79MPa. As explained in section 4.2.3, EPS, DPP, or both reduce density, causing mechanical properties to decline.

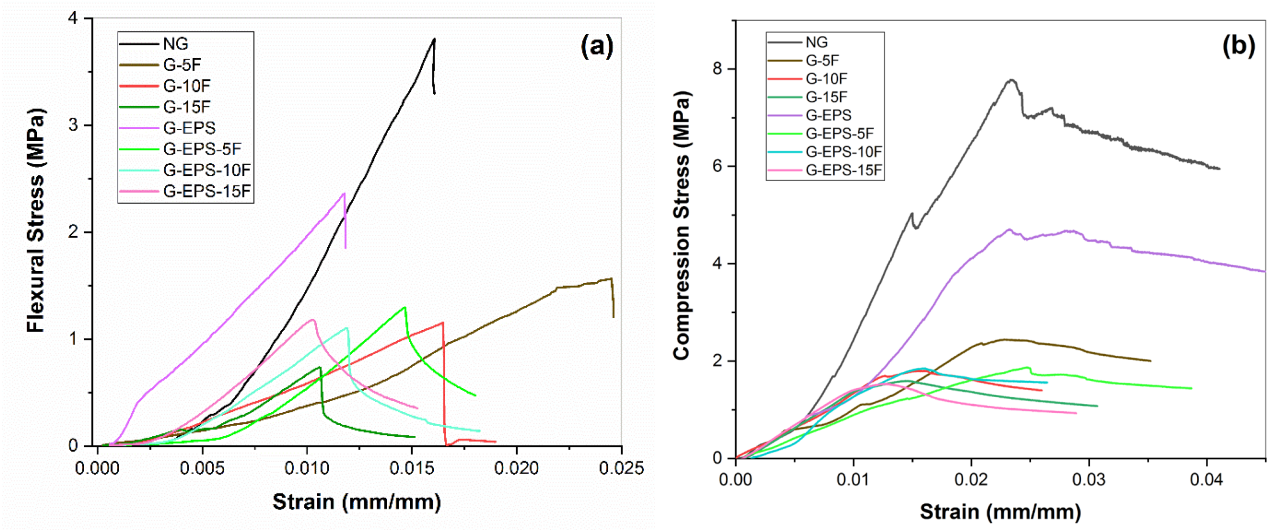

Figure IV. 18. Stress-Strain curves of (a) Three bending test (b) Compression test

Inclusion reduces compactness, increasing voids and faults in composite materials. Thus, internal coherence and interaction decrease across all components [226].

In contrast, the G-EPS sample composite exhibits enhanced mechanical properties compared to G-F and G-EPS-F. Compared to G-EPS, G-5F experiences a decrease in flexural strength of 32.35%, whereas G-EPS-5F experiences a decrease of 43.27%. It is worth noting that G-EPS demonstrates a flexural strength of 2.38MPa.The observed phenomena can be ascribed to the low weight percentage of EPS incorporated into the gypsum plaster at 0.3%. In comparison to samples NG, it is seen that G-EPS exhibits a significant reduction in compression strength by 38.68%, flexural strength by 37.20%, and Young's modulus by 16.44%, despite its comparatively low weight percentage of expanded polystyrene (EPS). The literature reports that Expanded Polystyrene (EPS) is characterized by a low density within the range of 15-35 kg.m-3, as indicated by references [18,224,227].

As a result, small quantities of EPS balls can fill a specified volume of a sample. Bouzit et al. (2021) [163] explain the reduction in mechanical proprieties by examining the presence of pores inside the EPS material and the gypsum plaster. The decrease in adhesion between expanded polystyrene (EPS) and gypsum plaster can be ascribed to the hydrophobic properties exhibited by EPS. The observation above has been documented by Semlali Aouragh Hassani et al. [226] and further corroborated by similar findings presented by Bicer et al.[228]. On the other side, empirical results demonstrate that an augmentation in the proportion of fiber from 5% to 15% decreases compression and flexural strength. As a demonstration, it is evident that the G-10F specimen displays a decline of 29.91% in compressive strength and a fall of 27.95% in flexural strength compared to the G-5F

specimen. The observed phenomena can be ascribed to the existence of amorphous substances on the outer surface of the fiber, leading to a non-uniform and coarse texture. As a result, this phenomenon reduces the interfacial adhesion between the fibers and the matrix, as indicated by previous research by Messaoud Boumaaza [229]. This phenomenon can be ascribed to the creation of filler aggregates, which arise from the establishment of strong hydrogen connections between them and the insufficient dispersion of fibers [11, 15].

Figure IV.18-c depicts a proportional correlation between the young modulus and the amount of fiber present. An increase in fiber content leads to a corresponding increase in the young modulus. As an example, it can be observed that the young modulus of G-15F is 154.75MPa, which is 57.19% and 31.71% higher than the young modulus of G-5F and G-10F, respectively.

The observed increase in rigidity can be ascribed to the inherent rigidity of the fibers, which surpasses that of gypsum plaster. A comparable pattern was noted in previous studies by Gellala et al. [142] and Benchouia et al. [4]. About the G-EPS-F samples, it is evident that these specimens demonstrate diminished levels of compression strengths, flexural strength, and Young's modulus in comparison to G-F. For example, the G-EPS-5F variant exhibits a decrease of 18.85%, 16.14%, and 1.71% in the attributes above compared to the G-5F variant. The observed decrease in [variable] can be attributed to the presence of voids resulting from including polystyrene balls within the gypsum matrix. The presence of these voids leads to a decrease in mass and an increase in structural imperfections inside the specimens. The fibers are expected to enhance stress transmission and inhibit the propagation of fractures by means of a bridging mechanism while simultaneously offering support for a portion of the applied load. In the present situation, the fibers demonstrate restricted load transfer capacities, accumulating stress at distinct locations inside the composite material.

The relatively slower rate of hydration in the composite materials can be attributed to this phenomenon. The decreased water content resulted in notable matrix contraction, reducing the adhesive potency between the fiber and matrix. Chikhi et al. [147] posit that a decrease in the adhesive strength between the fiber and matrix renders the fibers more susceptible to causing structural tears or disruptions within the system. Consequently, there is a decline in the mechanical properties of the system.

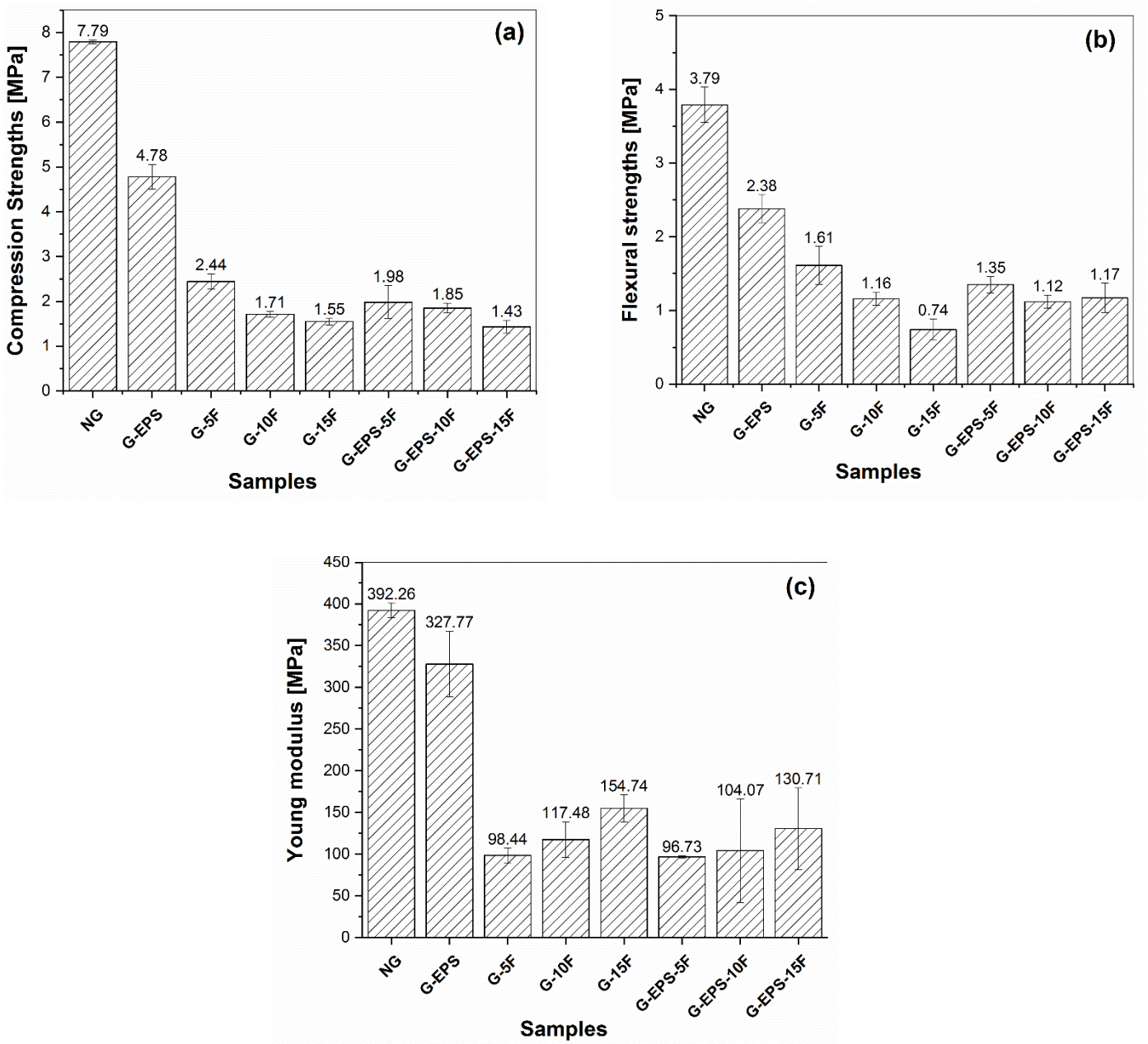

Figure IV. 19. Flexural strength (a), compressive strength (b), and Young modulus (c) as a function of expanded polystyrene and date palm fiber content.

The incorporation of Expanded Polystyrene (EPS), DPP, or a combination of both in gypsum results in a reduction of its mechanical qualities. Therefore, it is imperative to investigate viable solutions to improve these characteristics. Previous studies have extensively examined chemical interventions on the fibers as potential remedies Benchouia et al.[4]. Moreover, it is expected to enhance the manufacturing procedure. Including an extra important factor is of utmost importance, as supported by numerous studies, which emphasize the impact of variables such as fiber dimensions, alignment, and EPS content on the mechanical characteristics [142,230].

Plaster composites that incorporate Expanded Polystyrene (EPS), (DPP), or a combination of both demonstrate restricted mechanical properties while exhibiting a deficiency in structural integrity. Therefore, their utilization is predominantly appropriate for ornamental functions, interior plastering, or as thermal insulators in the field of construction, as emphasized in the research carried out by Braiek et al. [144] and Bicer et al. [137].

Figure IV.19 illustrates a collection of fractured samples obtained due to the three-point bending experiment. The provided figures depict the fracture characteristics of three distinct specimens, namely neat gypsum NG (Figure IV.19-a), sample G-EPS (Figure IV.19-b), and sample G-EPS-15F (Figure IV.19-c). The observation indicates that the gypsum NG and G-EPS samples underwent complete fracture, separating them. Nevertheless, the G-EPS-15F specimen, despite displaying indications of fracture and the existence of cracks (as denoted by the red line), maintained its structural integrity and did not undergo complete separation into two different entities. The observed phenomenon can be ascribed to the fact of the embedded fibers in the composite (Fig.25-b), which effectively impede the development and progression of cracks by means of a sewing mechanism. As a result, the fibers effectively preserve the structural integrity of the sample, so enabling the management of cracks prior to complete breakage. The observations above, as provided by Balti et al.[231] and Boumaaza et al. [229], exhibit congruence.

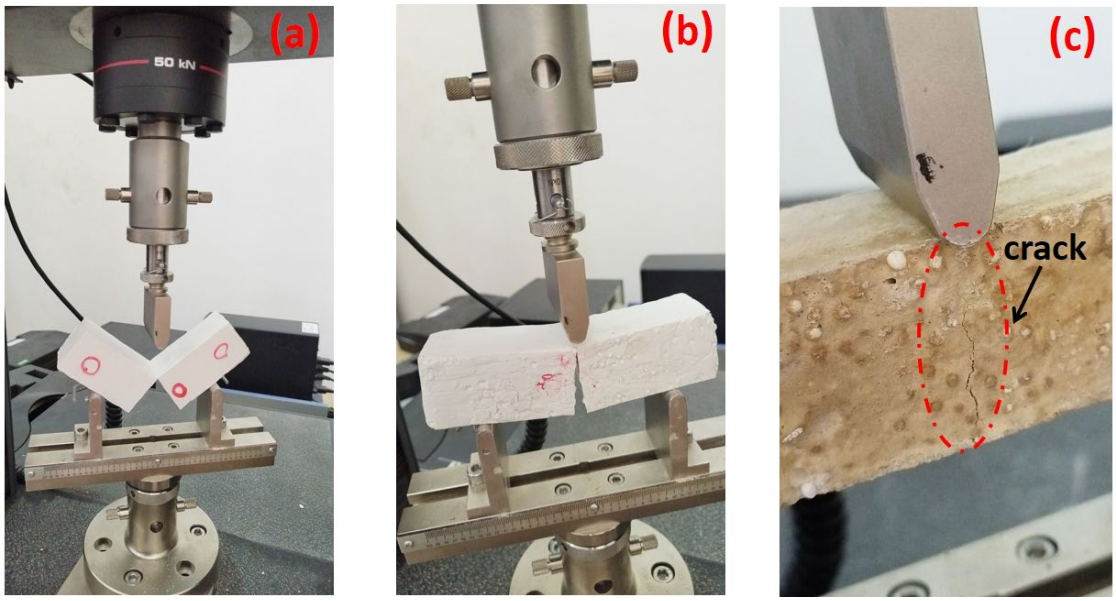

Figure IV. 20. Broken samples (a) NG, (b) G-EPS, and (c) G-EPS-15F following flexural test.

IV.2.4. Thermo-physical proprieties

Figure IV.20 demonstrates the influence of integrating EPS, DPP, or a combination of both on the thermal conductivity of the composite materials being studied. The matrix, in this case, is gypsum plaster. The main finding of interest is that the incorporation of vegetal waste (DPP), synthetic waste (EPS), or a combination of both results in a decrease in thermal conductivity in the generated samples in comparison to the reference sample (NG). For example, the thermal conductivity of G-EPS, G-5F, and G-EPS-10F demonstrates a respective reduction of 11.88%, 21.18%, and 28.47% when compared to neat gypsum (NG), which possesses the maximum thermal conductivity value of 0.425 W/m.K.

Drawing upon a comprehensive examination of numerous prior studies conducted within the identical domain of inquiry, the decrease in thermal conductivity can be ascribed to two fundamental variables. One crucial aspect to take into account is the notable discrepancy in thermal conductivity between the gypsum plaster employed (0.425 W/m.K, as depicted in Figure IV.20 and the thermal conductivity of the fibers (0.0895 W/m.K, as documented by Benchouia et al. [4], as well as the thermal conductivity range of expanded polystyrene (0.035–0.04 W/m.K, as indicated by G. Huanget al. [18] and Hung et al. Anh [227]. The findings and interpretations of the research conducted by Amara et al. (2017)[140], Chikhi (2016) [232], Braiek et al. (2017) [144], and Bouzit et al. (2021) [163] were found to be similar.

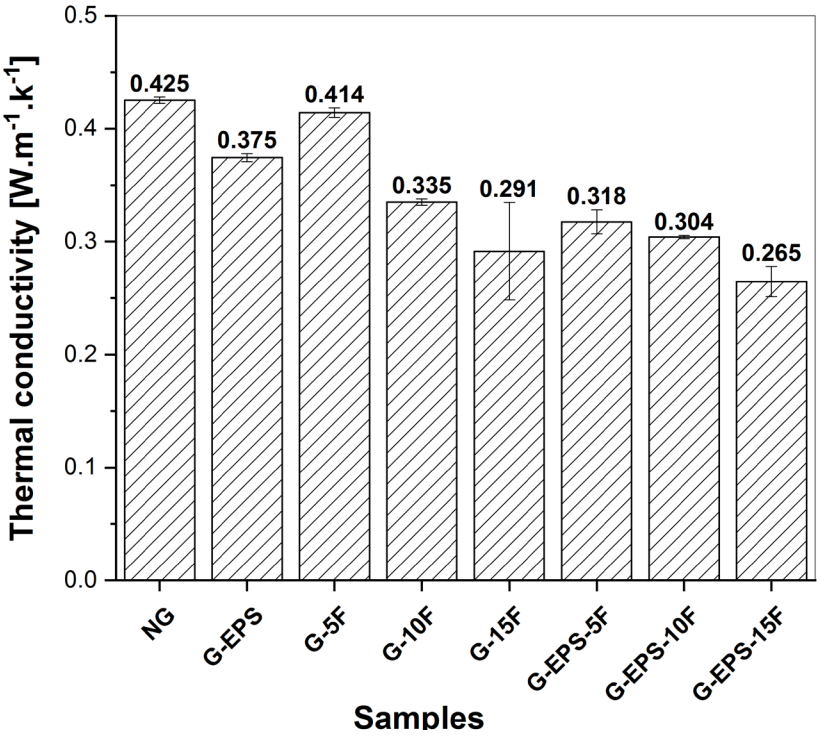

Figure IV. 21. The thermal conductivity of the composite samples.

Waste elements in gypsum plaster reduce composite material density, the second significant factor [13,137,143,230]. Belakroum et al. (2018) [10] found a correlation between composite density and heat conductivity. Figure IV.20 shows this.

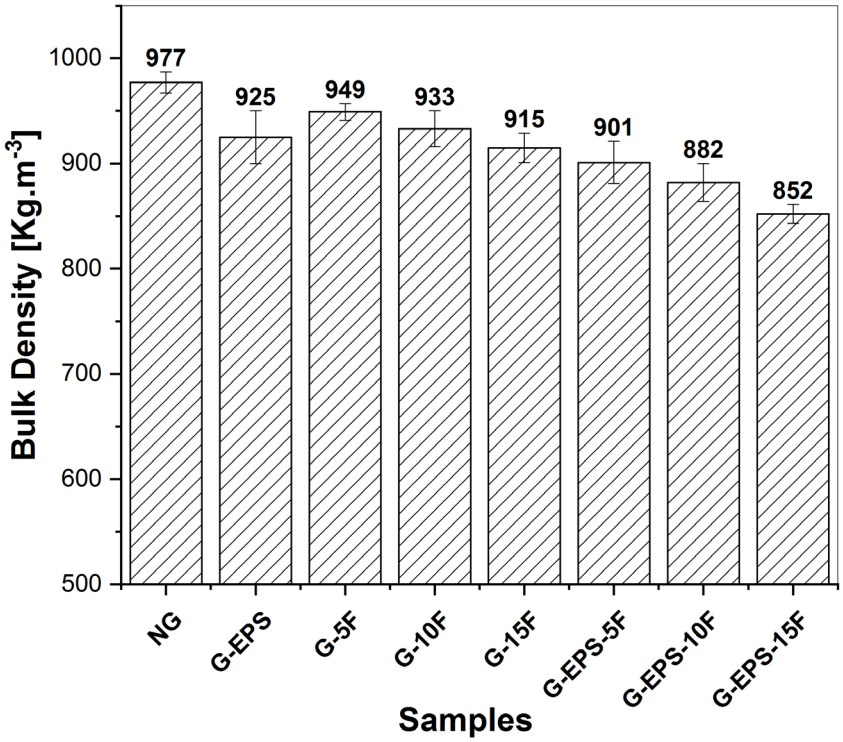

Figure IV. 22. The Bulk Density of the composite samples.

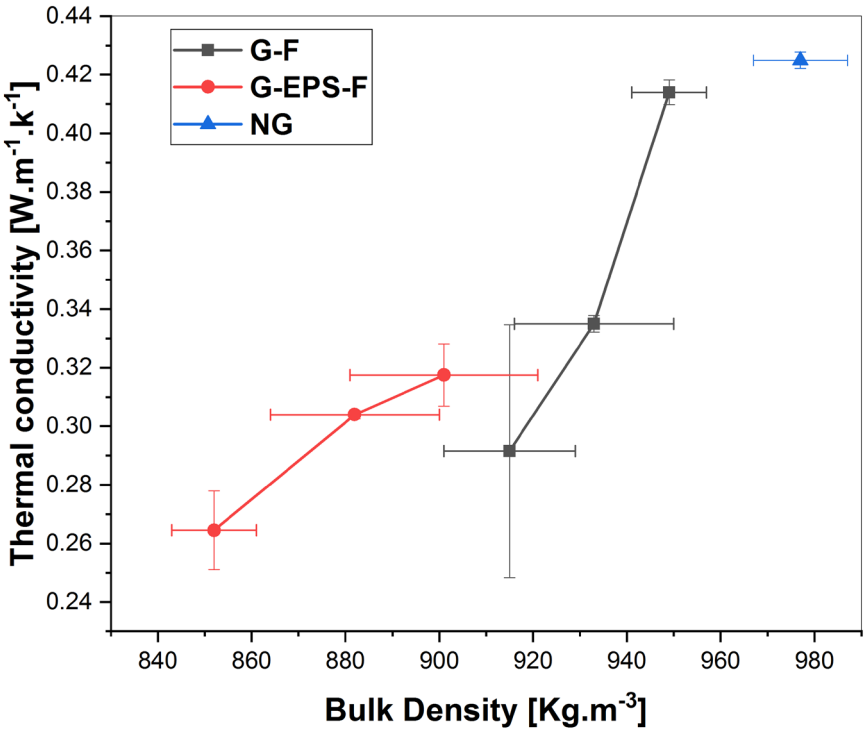

Figure IV. 23. Variation in thermal conductivity based on the bulk density of composites.

The impact of air gaps on the density of composites has been documented Figure IV.25, leading to a direct negative connection. This phenomenon results in an elevation in thermal resistance and a reduction in thermal conductivity. The observed pattern aligns with the outcomes of our research, as illustrated in Figure Figure IV.22, wherein a decrease in density is associated with a decrease in thermal conductivity.

The porous structure of Expanded Polystyrene (EPS), composed of air-filled beads (Fig25-e), is generally acknowledged by Bicer and Kar [137]. The reported range for the bulk density of EPS is 15-35 kg/m3 [227,233]. This range is associated with a drop in bulk density and subsequently affects the thermal conductivity of the manufactured composites. The observed pattern aligns with the research conducted by S. Bouzit et al.[163], wherein a non-linear reduction in the thermal conductivity of gypsum plaster was observed as the polystyrene content increased and the ball diameter decreased.

Additionally, it is essential to acknowledge that according to Benchouia et al. 's findings [4], date palm fibers have a lower bulk density of 590 kg/m3 in comparison to NG, which has a bulk density of 977 kg/m3 (as depicted in Figure IV.21). These fibrous materials can increase in size when they absorb water and can be mixed with gypsum. Notably, the moisture contained within the gypsum solution undergoes gradual evaporation throughout the 28-day drying period. This evaporation process contributes to the development of synthetic micro-pores inside the binding agents [137], in conjunction with the pre-existing EPS pores, throughout the drying phase of the specimens. The observed decrease in bulk density and thermal conductivity of the resultant composite depends on the DPF ratio, as indicated by a previous study by researchers [5,213]. In our specific case, Djoudi et al. [[171] and Gallala [142] have observed that the alignment and tight packing of small fiber lengths provide greater difficulty compared to larger fibers. Hence, while evaluating the explicit fiber content, it becomes evident that decreased fiber length leads to many voids within the material.

It reduces the material's thermal conductivity. We found 19.08% and 29.59% reductions in samples G-10F and G-15F compared to G-5F. Expanded Polystyrene (EPS) reduces thermal conductivity over time. G-EPS-5F and G-EPS-15F have 9.23% and 23.30% lower thermal conductivity than G-5F and G-15F. The above factors explain this tendency.

Figure IV.23 shows the volumetric thermal capacity (ρc) variation of composite material samples prepared for investigation. Pure gypsum plaster has the highest volumetric thermal

capacity at 1212.03 KJ/m3.K. However, EPS, DPP, or both lower volumetric thermal capacity. Samples with EPS and fiber have a lower volumetric thermal capacity than those with only fibers.

The G-EPS-15F samples demonstrate the lowest volumetric thermal capacity, measuring 946.94 KJ/m3.K. This measurement indicates a reduction of 21.87% in comparison to NG. The research conducted by Ouakarrouch et al. [143] revealed a significant decrease of approximately 16% in the volumetric thermal capacity. The aforementioned decrease in thermal conductivity was observed in the pure plaster sample, which initially had a value of 1550 kJ/m3.K. The composite material, consisting of P + 5% chicken feather waste, gradually declined in energy density until it reached a value of 1310 kJ/m^3.K. Moreover, the volumetric thermal capacity of the fabricated materials declined when the mass fraction of date palm fibers escalated from 5% to 15%. The utilization of date palm fibers has been found to have a two-fold impact, specifically a decrease in material densities and an improvement in thermal properties. Braiek et al. [144] also noted a similar finding, wherein they observed a decrease in the thermal capacity of the DPF/gypsum composite when the mass percentage of date palm fibers grew from 5% to 20%, ranging from 3.14% to 36.22%.

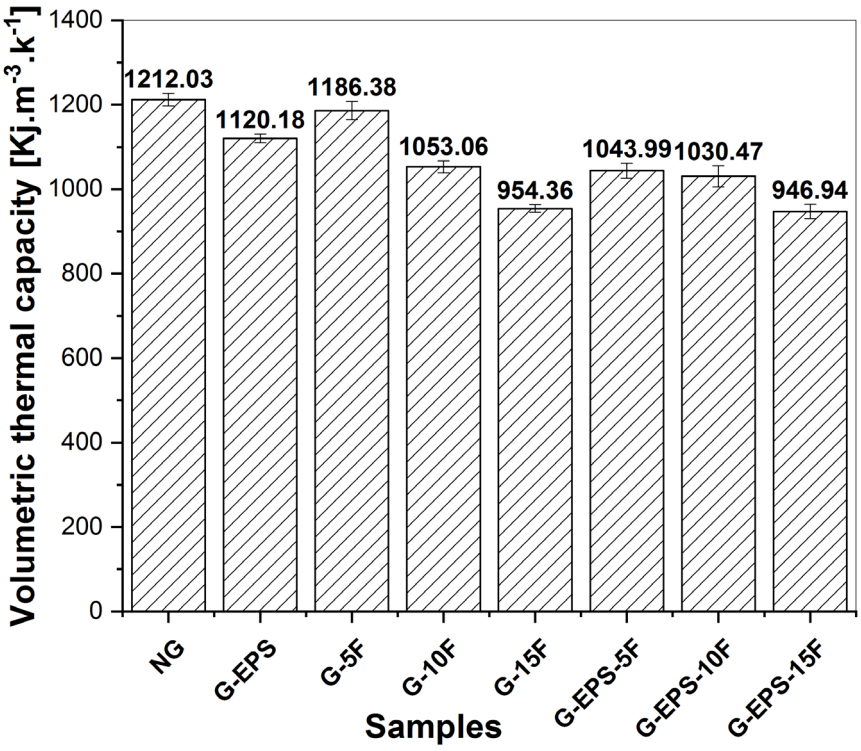

Figure IV. 24. Volumetric thermal capacity of the composite samples.

Thermal diffusivity is a key parameter that measures the rate of heat conduction within a material. The assessment of materials for building purposes is significantly influenced by this particular property [13]. The thermal diffusivity values derived from the computations are illustrated in Figure IV.24.

The addition of Expanded Polystyrene (EPS), (DPP), or a combination of both to the plaster material positively affects the reduction of thermal diffusivity in the composite. The most significant decrease, amounting to 20.34%, is observed in the case of G-EPS-15F. The decrease in heat diffusion can be ascribed to the increased porosity that arises from the inclusion of Expanded Polystyrene (EPS), DPP, or a combination of both in the composite material, along with the honeycomb structure of the fibers. This configuration is in opposition to the established direction of thermal energy transfer [141,221]. Ouakarrouch et al.[143]observed the same patterns in their study, wherein they found that the thermal diffusivity of pure gypsum plaster fell from 3.07 × 10−7 m2/s to 2.69 × 10−7 m2/s when combined with a composite of P + 5% chicken feathers waste. As a consequence, there was a calculated decrease of around 13%. In a study conducted by Braiek et al. [144], it was discovered that the application of 20% (DPP) to gypsum plaster resulted in a drop of 39.58% in the thermal diffusivity value.

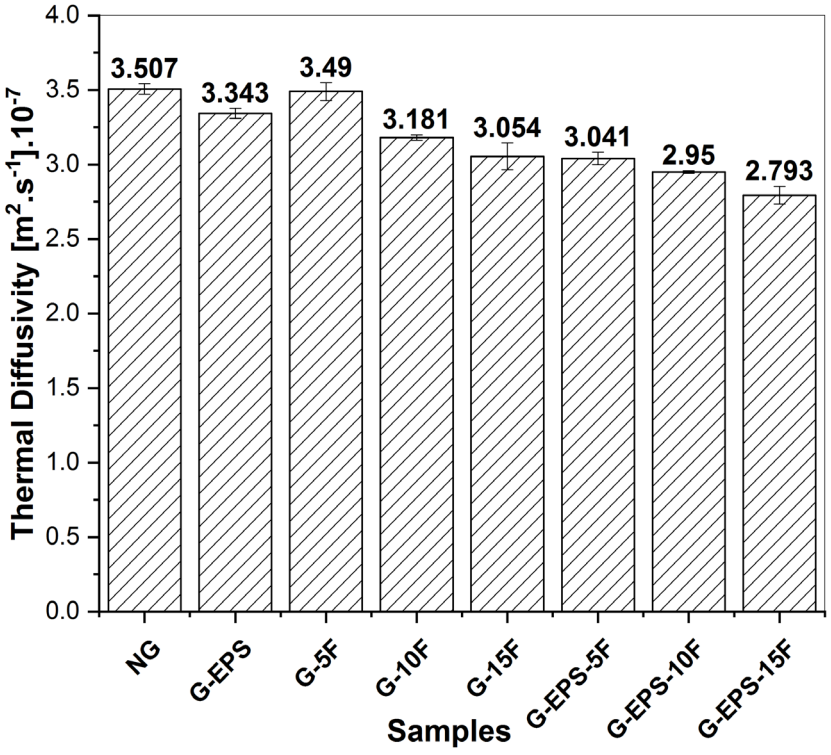

Figure IV. 25. Thermal diffusivity of the fabricated composite specimens.

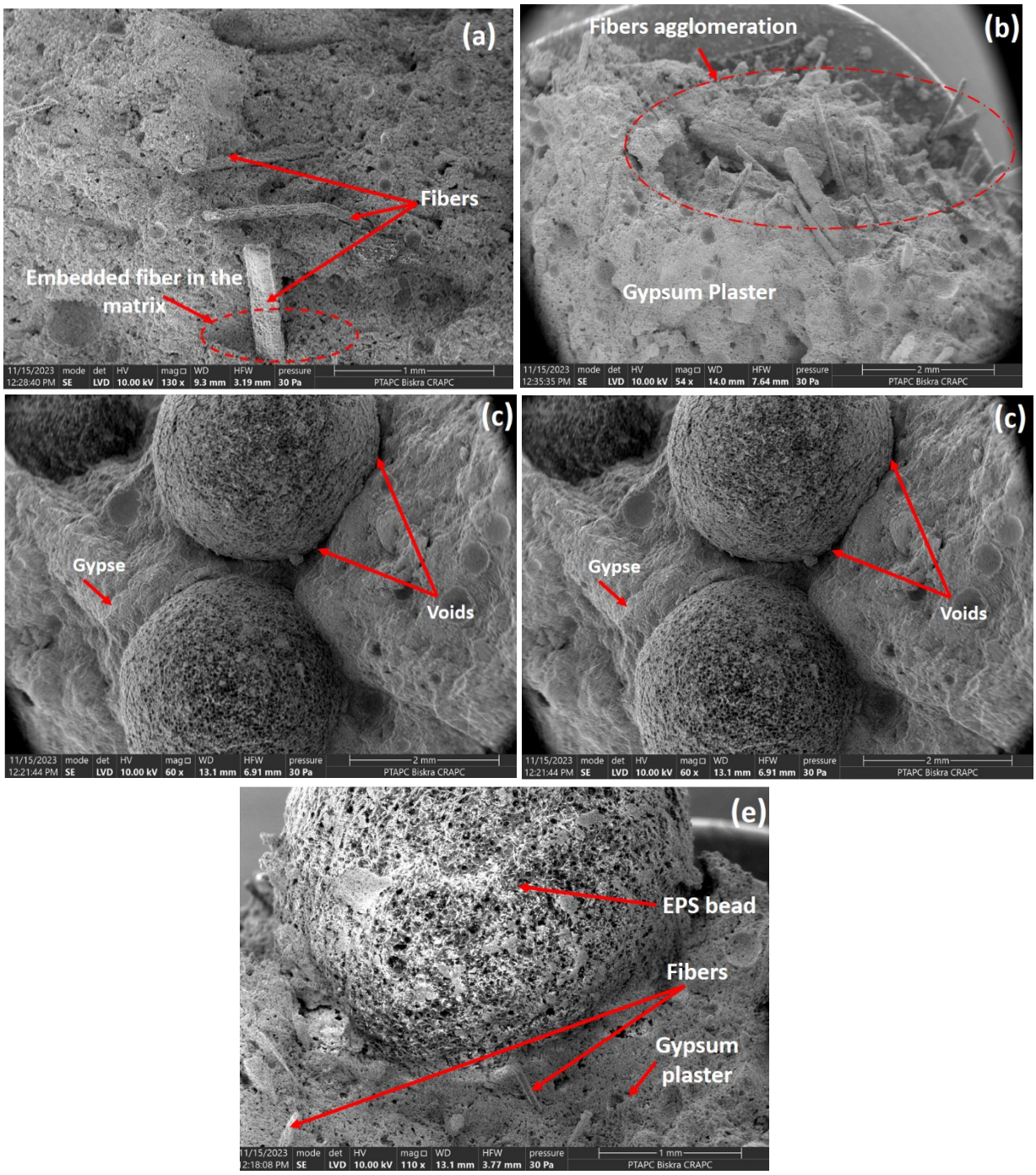

Figure IV. 26. SEM micrograph of composites samples (a) G-5F (b) G-15F (c) G-EPS (d) G-EPS-5F (e) G-EPS-15F.

Ismail et al. [234] have reported a significant correlation between moisture and thermal diffusivity, indicating that moisture substantially impacts thermal diffusivity. According to research findings, it has been observed that the thermal capacity of dried samples is higher compared to undried samples. However, the thermal diffusivity of dried samples shows a decrease of roughly 22%. This implies the need to assess the influence of moisture on the thermal properties of various materials. Hence, considering the notable discoveries in

thermal insulation, an insulating material must exhibit low conductivity and demonstrate the capacity to impede heat transfer efficiently.

IV.2.5. Comparative study

Table IV. 7 presents a comparative analysis of the mechanical and thermophysical properties of the biocomposite composed of gypsum reinforced with EPS, DPP, or a combination of both. This comparison includes similar composites developed by researchers for thermal insulation and building construction.

A difference in the results is seen, which can be attributed to the variance in the properties and attributes of the binder and reinforcement materials employed. Furthermore, it is essential to consider that several factors can influence the properties above. These factors include temperature variations, moisture content [227,234], chemical treatment [223], and the inherent manufacturing process.

Furthermore, other techniques exist for quantifying thermophysical properties, such as the steady-state Hot Plate approach and the flash method [235], which can yield divergent outcomes. The experimental results suggest that the composite examined in this study exhibits favorable mechanical and thermal properties when compared to other composites, as demonstrated in Table IV.07. It is worth noting that the density and thermal conductivity values obtained in this study are lower than those reported in previous works [142,228], Gellala et al. [142], Fatma et al.[13], charai et al. [236], and Ouakarrouch et al.[143]. In previous studies by Amara et al.[140] , S. Bouzi et al. [163], and Braiek et al.[144], the obtained results were slightly lower compared to the findings presented in our research.

The gypsum biocomposite based on EPS/DPP has promising characteristics as a feasible choice for developing economically efficient, reliable, and high-performing insulation materials.

Table IV. 7. A Comparison of the mechanical and thermophysical properties of the fabricated hyprid biocomposites to those of various building materials.

Materials	**Bulk Density [Kg.m^{-3}]**	**Thermal Conductivity [W.m^{-1}.k^{-1}]**	**Thermal diffusivity [m^2.s^{-1}] .10^{-}**	**Flexural Strength [MPa]**	**Compression strength [MPa]**	**References**
gypsum / EPS (20 %)	1088	0.335	/	/	3.05	Bicer et al.[228]
gypsum /15% date palm fibers (DPF)	861.86	0.213 ± 0.013	2.563 ± 0.047	/	/	Braiek *et al.* [144]
Lime/20% DPF	≃950	0.201	/	/	0.6	Belakroum *et al.* [10]
Plaster / 17% DPFW	1415.15	0.52	/	≃6	≃13.5	Gallala *et al.* [142]
Gypsum/10%EPS (d=3mm)	810-840	0.209	/	≃2.5	≃5.7	Bouzit *et al.*[163]
Gypsum/5% chicken feathers waste	1049.0	0.309	2.69	/	/	Ouakarrouch *et al.*(2020)[143]
Gypsum/1.5% doum palm fibers	1132	0.31	2.9	1.62	3.29±0.12	Fatma *et al.* [13]
gypsum plaster / with 10% DPF	825.233	0.232	3.417	/	/	Amara *et al.* [140]
(Sand, cement)/ (0%-10%) Alfa plant	1338-1682	0.46–0.19	/	0.54–4.16	0.66-19.44	Charai *et al.* [236]
Gypsum/ (EPS and/or DPP)	**852-977**	**0.2645-0.425**	**2.79-3.51**	**0.74-3.79**	**1.55-7.79**	**This work**

Conclusion

This chapter presented the findings of two biocomposite materials developed from waste plant compounds for thermal insulation applications. For the PS-DPF composite, filler loading and chemical treatments were found to significantly influence properties like strength and thermal stability. The second composite, gypsum plaster reinforced with EPS and DPP, showed reduced mechanical strength but improved thermal properties. These findings suggest that these biocomposites have potential for eco-friendly construction practices, but further research is needed to fully assess their suitability.

GENERAL CONCLUSION

GENERAL CONCLUSION

To promote waste materials in civil and mechanical engineering, specifically in thermal insulation, two new biocomposite materials based on waste plant compounds are being developed and studied. The first composite is the date palm leaflet fibers DPF reinforced polystyrene, the fibers derived from date palm leaflets obtained from the Deglet Noor species gathered from a palm oasis in the Horaya district of Biskra, situated in the southeastern part of Algeria; the matrix was obtained from melting the polystyrene. The second biocomposite is based on gypsum plaster reinforced with expanded polystyrene EPS and/ or date palm petiole fiber (DPP). Different physical, mechanical, thermal, and morphological tests were carried out to characterize both elaborated composites.

The first composite, based on date palm waste and polystyrene PS-DPF, uses the fibers of the date palm leaflets as reinforcement. In this work, we studied the effect of two parameters in the measured proprieties; the first, the initial variable was the filler loading (10%, 20%, and 30%). The second factor was subjecting the fibers to two chemical treatments: one with sodium hydroxide and the other with chloride benzoyl to enhance the compatibility and bonding of the fibers with the polymer.

Les results of scanning electron microscopy (SEM) micrographs revealed that the filler dispersion and its interfacial interactions with the matrix were enhanced due to reducing the presence of OH groups on the fibers. This finding was confirmed by Fourier transform infrared spectroscopy analysis (FTIR). X-ray diffraction (XRD) investigations show that ADPF exhibits the highest level of crystallinity index. The PS-DPF composites demonstrated good tensile strength ranging from 14 to 27 MPa, flexural strength ranging from 31 to 44 MPa, and yung modulus ranging from 2.9 to 5.9 GPa. The findings indicated that using alkaline and benzoylated treatments enhances the tensile and flexural strength but causes a minor reduction in the elasticity modulus. Both chemical treatments exhibited a comparable effect on these characteristics. The Thermogravimetric analysis (TGA) findings showed that PS samples packed with 30% untreated and treated fibers exhibit the highest level of thermal stability compared to VPS. There is a slight advantage for the untreated sample when considering residues. The composites exhibited a low thermal conductivity (λ) ranging from 0.118 to 0.141 W/m.K at 18◦C. The variation in thermal conductivity was not consistent with the changes in bulk density (ρ), which ranged from 860 to 980 kg/m3 and decreased with the addition of fibers. Furthermore, substituting one-third of traditional

building materials with a PS-DPF composite has demonstrated potential for various uses, particularly in thermal insulation, resulting in a notable decrease in thermal conductivity by as much as 50%. Composite materials have demonstrated their potential as thermal insulators, promoting the regular utilization of waste in nations' production dates.

For the second studied biocomposite material, the objective was to investigate the potential application of Date palm petiole fibers (DPP), expanded polystyrene waste (EPS), or a combination of both as aggregates for the development of a lightweight gypsum plaster hybrid bio-composite. The aim was to enhance the mechanical and thermophysical properties of the composite. To determine the most effective mass ratio of inclusion for creating thermally insulating building materials that can resist mechanically. A total of eight gypsum-based mixtures were formulated. These mixtures had varying amounts of DPP (0%, 5%, 10%, and 15% by weight) and were tested both with and without EPS. The mixtures were then subjected to experimental analysis to assess their properties. The X-ray diffraction (XRD) analysis reveals that the crystallinity percentages of neat gypsum plaster (NGP), EPS, and DPP are 71.58%, 29.91%, and 52.93%, respectively. The compression strengths, flexural strengths, and young modulus indicate that the incorporation of either EPS, DPP, or both severely diminishes the mechanical properties of the produced samples. The biocomposites exhibited reduced thermal conductivity (λ) ranging from 0.265 to 0.414 W/(m.K) at 24°C, as well as lower bulk density (ρ) ranging from 852 to 925 kg/m3, in comparison, the reference NGP samples had a thermal conductivity of 0.425 W/(m.K) and a bulk density of 977 kg/m3. According to a comparative study and based on this analysis, it is recommended to use the samples as internal plaster, insulation plaster, infill, and decorating material due to their inferior mechanical and thermal qualities compared to traditional gypsum plasters. Two notable advantages can be obtained by employing this plaster and decorative material. Initially, an evaluation will be conducted on the waste EPS and DPP, resulting in the mitigation of environmental contamination. Furthermore, the material will actively assist in saving energy in the heating and cooling operations of buildings.

In conclusion, our investigation into thermal comfort within constructions insulated with various materials has provided valuable insights into their performance. We meticulously measured thermal conductivity, thermal diffusivity, and mechanical properties throughout our study to assess insulation effectiveness and structural integrity. However, it is essential to acknowledge that due to equipment availability constraints, we could not measure several

other critical parameters essential for a comprehensive evaluation of thermal comfort. These include indoor temperature variations, relative humidity levels, mean radiant temperature, air velocity, surface temperatures, energy consumption patterns, and indoor air quality. The absence of these measurements limited the depth of our analysis. Nonetheless, our findings underscore the importance of further research endeavors equipped with advanced sensors and monitoring tools to capture a broader spectrum of data, thereby refining our understanding of thermal comfort in insulated constructions. These are some of the avenues that the LGM (Laboratory of Mechanical Engineering) intends to develop in pursuing this work.

REFERENCES

REFERENCES

[1] B. Abu-Jdayil, A.-H.I. Mourad, A. Hussain, H. Al Abdallah, Thermal insulation and mechanical characteristics of polyester filled with date seed wastes, Constr. Build. Mater. 315 (2022) 125805. https://doi.org/10.1016/j.conbuildmat.2021.125805.

[2] T. Masri, H. Ounis, L. Sedira, A. Kaci, A. Benchabane, Characterization of new composite material based on date palm leaflets and expanded polystyrene wastes, Constr. Build. Mater. 164 (2018) 410–418. https://doi.org/10.1016/j.conbuildmat.2017.12.197.

[3] M. Chikhi, N. Metidji, F. Mokhtari, N.K. Merzouk, Numerical investigation of porous materials composites reinforced with natural fibers, IOP Conf. Ser. Mater. Sci. Eng. 350 (2018). https://doi.org/10.1088/1757-899X/350/1/012003.

[4] H.E. Benchouia, B. Guerira, M. Chikhi, H. Boussehel, C. Tedeschi, An experimental evaluation of a new eco-friendly insulating material based on date palm fibers and polystyrene, J. Build. Eng. 65 (2023) 105751. https://doi.org/10.1016/j.jobe.2022.105751.

[5] L. Boukhattem, M. Boumhaout, H. Hamdi, B. Benhamou, F. Ait Nouh, Moisture content influence on the thermal conductivity of insulating building materials made from date palm fibers mesh, Constr. Build. Mater. 148 (2017) 811–823. https://doi.org/10.1016/j.conbuildmat.2017.05.020.

[6] R. Chaari, M. Khlif, H. Mallek, C. Bradai, C. Lacoste, H. Belguith, H. Tounsi, P. Dony, Enzymatic treatments effect on the poly (butylene succinate)/date palm fibers properties for bio-composite applications, Ind. Crops Prod. 148 (2020) 112270. https://doi.org/10.1016/j.indcrop.2020.112270.

[7] W. Hittini, B. Abu-Jdayil, A.H. Mourad, Development of date pit–polystyrene thermoplastic heat insulator material: Mechanical properties, J. Thermoplast. Compos. Mater. 34 (2021) 472–489. https://doi.org/10.1177/0892705719847242.

[8] M. Poletto, A.J. Zattera, Mechanical and dynamic mechanical properties of polystyrene composites reinforced with cellulose fibers, J. Thermoplast. Compos. Mater. 30 (2017) 1242–1254. https://doi.org/10.1177/0892705715619967.

[9] G.L. Devnani, Recent Trends in the Surface Modification of Natural Fibers for the

Preparation of Green Biocomposite, Springer Singapore, 2021. https://doi.org/10.1007/978-981-15-9643-8_10.

[10] R. Belakroum, A. Gherfi, M. Kadja, C. Maalouf, M. Lachi, N. El Wakil, T.H. Mai, Design and properties of a new sustainable construction material based on date palm fibers and lime, Constr. Build. Mater. 184 (2018) 330–343. https://doi.org/10.1016/j.conbuildmat.2018.06.196.

[11] A. George, A. Sulyman, A. Abdulkareem, Preparation and properties of wood dust (isoberlinia doka) reinforced polystyrene composites, Polym. Bull. (2021). https://doi.org/10.1007/s00289-021-03718-6.

[12] A.G. Adeniyi, D.V. Onifade, S.A. Abdulkareem, M.K. Amosa, J.O. Ighalo, Valorization of Plantain Stalk and Polystyrene Wastes for Composite Development, J. Polym. Environ. 28 (2020) 2644–2651. https://doi.org/10.1007/s10924-020-01796-7.

[13] N. Fatma, L. Allègue, M. Salem, R. Zitoune, M. Zidi, The effect of doum palm fibers on the mechanical and thermal properties of gypsum mortar, J. Compos. Mater. 53 (2019) 2641–2659. https://doi.org/10.1177/0021998319838319.

[14] Singh, S., & Kumar, D. (Eds.). (2022). Fabrication and Machining of Advanced Materials and Composites: Opportunities and Challenges (1st ed.). CRC Press. https://doi.org/10.1201/9781003327370

[15] Georges, F. S. C. A. C. (2021). Effects of water absorption on the behavior of composite materials reinforced with natural fibers: characterization and numerical simulation (Doctoral dissertation, Nantes).

[16] H. Boussehel, Etude des moyens de stabilisation des composites à base de polystyrène, (2018). PhD thesis, University of Mohamed Khider - Biskra, Biskra

[17] S.T. Pinho, R. Darvizeh, P. Robinson, C. Schuecker, P.P. Camanho, Material and structural response of polymer-matrix fibre-reinforced composites, J. Compos. Mater. 46 (2012) 2313–2341. https://doi.org/10.1177/0021998312454478.

[18] S. Huang, Q. Fu, L. Yan, B. Kasal, Characterization of interfacial properties between fibre and polymer matrix in composite materials – A critical review, J. Mater. Res. Technol. 13 (2021) 1441–1484. https://doi.org/10.1016/j.jmrt.2021.05.076.

[19] S. Sethi, B.C. Ray, Environmental effects on fibre reinforced polymeric composites: Evolving reasons and remarks on interfacial strength and stability, Adv. Colloid Interface Sci. 217 (2015) 43–67. https://doi.org/10.1016/j.cis.2014.12.005.

[20] M. Mohammed, M.S.M. Rasidi, A.M. Mohammed, R. Rahman, A.F. Osman, T. Adam, B.O. Betar, O.S. Dahham, Interfacial Bonding Mechanisms of Natural Fibre-Matrix Composites: An Overview, BioResources 17 (2022) 7031–7090. https://doi.org/10.15376/BIORES.17.4.MOHAMMED.

[21] A. Oushabi, S. Sair, F. Oudrhiri Hassani, Y. Abboud, O. Tanane, A. El Bouari, The effect of alkali treatment on mechanical, morphological and thermal properties of date palm fibers (DPFs): Study of the interface of DPF–Polyurethane composite, South African J. Chem. Eng. 23 (2017) 116–123. https://doi.org/10.1016/j.sajce.2017.04.005.

[22] W. Liu, J. Huang, N. Wang, S. Lei, The influence of moisture content on the interfacial properties of natural palm fiber–matrix composite, Wood Sci. Technol. 49 (2015) 371–387. https://doi.org/10.1007/s00226-015-0702-3.

[23] J. Neto, H. Queiroz, R. Aguiar, R. Lima, D. Cavalcanti, M.D. Banea, A review of recent advances in hybrid natural fiber reinforced polymer composites, J. Renew. Mater. 10 (2022) 561–589. https://doi.org/10.32604/jrm.2022.017434.

[24] Yasemin, F. Selli, Ü.H. Erdoğan, M. Atagür, M.Ö. Seydibeyoğlu, A review on alternative raw materials for sustainable production: novel plant fibers, Springer Netherlands, 2022. https://doi.org/10.1007/s10570-022-04597-4.

[25] S.K. Ramamoorthy, M. Skrifvars, A. Persson, A review of natural fibers used in biocomposites: Plant, animal and regenerated cellulose fibers, Polym. Rev. 55 (2015) 107–162. https://doi.org/10.1080/15583724.2014.971124.

[26] A. Karimah, M.R. Ridho, S.S. Munawar, D.S. Adi, Ismadi, R. Damayanti, B. Subiyanto, W. Fatriasari, A. Fudholi, A review on natural fibers for development of eco-friendly bio-composite: characteristics, and utilizations, J. Mater. Res. Technol. 13 (2021) 2442–2458. https://doi.org/10.1016/j.jmrt.2021.06.014.

[27] K. Dietrich, M.J. Dumont, V. Orsat, L.F. Del Rio, Consumption of sugars and inhibitors of softwood hemicellulose hydrolysates as carbon sources for polyhydroxybutyrate (PHB) production with Paraburkholderia sacchari IPT 101,

Cellulose 26 (2019) 7939–7952. https://doi.org/10.1007/s10570-019-02664-x.

[28] I. Cesarino, Yet another twist in lignin biosynthesis: Is there a specific alcohol dehydrogenase for H-lignin production?, Plant Physiol. 189 (2022) 1884–1886. https://doi.org/10.1093/plphys/kiac249.

[29] U.M. Khider -Biskra, A. Moummi, A. Benchabane, H. Benmoussa, F. Khaldi, M. Hecini, A. Chine, Contribution au développement des matériaux de construction à .(base des sous-produits du palmier dattier, (2018

[30] ALMI, K. (2018). Développement et caractérisation de matériaux à base du bois de palmier dattier adaptés aux applications de développement durable en Algérie (Doctoral dissertation, Université Mohamed Khider BISKRA).

[31] T. Gurunathan, S. Mohanty, S.K. Nayak, A review of the recent developments in biocomposites based on natural fibres and their application perspectives, Compos. Part A Appl. Sci. Manuf. 77 (2015) 1–25. https://doi.org/10.1016/j.compositesa.2015.06.007.

[32] S.O. Amiandamhen, M. Meincken, L. Tyhoda, Natural fibre modification and its influence on fibre-matrix interfacial properties in biocomposite materials, Fibers Polym. 21 (2020) 677–689.

[33] Hollaway, L. C. (2003). The evolution of and the way forward for advanced polymer composites in the civil infrastructure. Construction and Building Materials, 17(6-7), 365-378.

[34] S. Taj, M.A. Munawar, S. Khan, Natural fiber-reinforced polymer composites, Proceedings-Pakistan Acad. Sci. 44 (2007) 129.

[35] Montrose, G. (2021). Maîtrise de l'Energie dans les bâtiments en Climat Tropical Humide: étude des matériaux biosourcés d'origine végétale pour l'efficacité énergétique et le confort thermique (Doctoral dissertation, Antilles).

[36] C.H. Lee, A. Khalina, S.H. Lee, Importance of interfacial adhesion condition on characterization of plant-fiber-reinforced polymer composites: A review, Polymers (Basel). 13 (2021) 1–22. https://doi.org/10.3390/polym13030438.

[37] S.Z. Rogovina, E. V. Prut, A.A. Berlin, Composite Materials Based on Synthetic Polymers Reinforced with Natural Fibers, Polym. Sci. - Ser. A 61 (2019) 417–438.

https://doi.org/10.1134/S0965545X19040084.

[38] M.M. Abe, J.R. Martins, P.B. Sanvezzo, J.V. Macedo, M.C. Branciforti, P. Halley, V.R. Botaro, M. Brienzo, Advantages and disadvantages of bioplastics production from starch and lignocellulosic components, Polymers (Basel). 13 (2021). https://doi.org/10.3390/polym13152484.

[39] M.Y. Yuhazri, A.J. Zulfikar, A. Ginting, Fiber Reinforced Polymer Composite as a Strengthening of Concrete Structures: A Review, IOP Conf. Ser. Mater. Sci. Eng. 1003 (2020). https://doi.org/10.1088/1757-899X/1003/1/012135.

[40] DJOUDI, T. (2019). Elaboration et caractérisation de composites bio-sourcés à base de fibres de palmier dattier (Doctoral dissertation, Université Mohamed Khider-Biskra).

[41] Erden, S., & Ho, K. (2017). Fiber reinforced composites. In Fiber technology for fiber-reinforced composites (pp. 51-79). Woodhead Publishing.

[42] R. Hsissou, R. Seghiri, Z. Benzekri, M. Hilali, M. Rafik, A. Elharfi, Polymer composite materials: A comprehensive review, Compos. Struct. 262 (2021) 0–3. https://doi.org/10.1016/j.compstruct.2021.113640.

[43] B. John, C.P.R. Nair, Thermosetting polymer based syntactic foams: an overview, Handb. Thermoset Plast. (2022) 801–832.

[44] D.N. Trivedi, N. V Rachchh, Graphene and its application in thermoplastic polymers as nano-filler-A review, Polymer (Guildf). 240 (2022) 124486.

[45] Osswald, T. A., Baur, E., & Rudolph, N. (2019). Plastics handbook: the resource for plastics engineers. Carl Hanser Verlag GmbH Co KG.

[46] S. Sajan, D. Philip Selvaraj, A review on polymer matrix composite materials and their applications, Mater. Today Proc. 47 (2021) 5493–5498. https://doi.org/10.1016/j.matpr.2021.08.034.

[47] Ali, M. (2023). The Mechanical Characterization of TRM composite materials for structural applications (Doctoral dissertation, Politecnico di Torino).

[48] A. Mortensen, J. Llorca, Metal matrix composites, Annu. Rev. Mater. Res. 40 (2010) 243–270. https://doi.org/10.1146/annurev-matsci-070909-104511.

[49] T.-D. Ngo, Introduction to composite materials, Compos. Nanocomposite Mater. Knowl. to Ind. Appl. (2020).

[50] Chikhi, M. (2013). Métrologie et modélisation des transferts dans les composites naturels à faible cout pour l'isolation thermique dans les panneaux solaires (Doctoral dissertation, UB1).

[51] Ramírez Hernández, M. M. (2004). Funcionalidad familiar en adolescentes de preparatoria (Doctoral dissertation, Universidad Autónoma de Nuevo León).

[52] G. Promis, A. Gabor, P. Hamelin, Analytical modeling of the bending behavior of textile reinforced mineral matrix composite beams, Compos. Struct. 93 (2011) 792–801. https://doi.org/10.1016/j.compstruct.2010.08.002.

[53] MANOCHA, Lalit M. High performance carbon-carbon composites. Sadhana, 2003, vol. 28, p. 349-358.

[54] J. Zhang, G. Lin, U. Vaidya, H. Wang, Past, present and future prospective of global carbon fibre composite developments and applications, Compos. Part B Eng. (2022) 110463.

[55] L. Mohammed, M.N.M. Ansari, G. Pua, M. Jawaid, M.S. Islam, A Review on Natural Fiber Reinforced Polymer Composite and Its Applications, Int. J. Polym. Sci. 2015 (2015). https://doi.org/10.1155/2015/243947.

[56] G. Marsh, A. Jacob, Trends in marine composites, Reinf. Plast. 51 (2007). https://doi.org/10.1016/S0034-3617(07)70054-1.

[57] D.Z. Tang, The application of carbon fiber materials in sports equipment, Appl. Mech. Mater. 443 (2014) 613–616. https://doi.org/10.4028/www.scientific.net/AMM.443.613.

[58] D.D.L. Chung, Composite materials: functional materials for modern technologies, Springer Science & Business Media, 2003.

[59] N. Hu, Composites and their properties, BoD–Books on Demand, 2012.

[60] M. Nagalakshmaiah, S. Afrin, R.P. Malladi, M. Robert, M.A. Ansari, A. Svedberg, Biocomposites : present trends and challenges for the future, (2019) 197–215. https://doi.org/10.1016/B978-0-08-102177-4.00009-4.

[61] R.R. Krueger, J.M. Al-Khayri, S.M. Jain, D. V Johnson, Introduction: The Date Palm Legacy, in: Date Palm, CABI GB, 2023: pp. 1–21.

[62] A. Kriker, S. Abbani, M. Bouziane, A. Mokhtari, A. Mekhermeche, H. Chaib, F. Hafsi, Date Palm Fiber Composites in Hot-Dry Construction and Building, Date Palm Fiber Compos. Process. Prop. Appl. (2020) 323–356.

[63] A.A. Jaradat, Biodiversity, genetic diversity, and genetic resources of date palm, Date Palm Genet. Resour. Util. Vol. 1 Africa Am. (2015) 19–71.

[64] MADR, Statistique agricole: superficie et production,République Algérienne Démocratique et Populaire Ministère de l ' Agriculture et du Développement Rural, (2021) 1–87.

[65] W.J. Baker, J. Dransfield, Field Guide to the Palms of New Guinea, (2006) 108 (book).

[66] M.L. Robinson, B. Brown, C.F. Williams, The date palm in southern Nevada, Univ. Nevada Coop. Ext. 23 (2012) 1–26.

[67] A. El Hadrami, J.M. Al-Khayri, Socioeconomic and traditional importance of date palm, Emirates J. Food Agric. 24 (2012) 371.

[68] S.C. Mason, The Minimum Temperature for Growth of the Date Palm and the Absence of a Resting Period: Partial Thermostasy of the Growth Center of the Date Palm. The Inhibitive Effect of Direct Sunlight on the Growth of the Date Palm, US Government Printing Office, 1925.

[69] L.I. El-Juhany, Degradation of date palm trees and date production in Arab countries: causes and potential rehabilitation, Aust. J. Basic Appl. Sci. 4 (2010) 3998–4010.

[70] O.Y. Alothman, H.M. Shaikh, B.A. Alshammari, M. Jawaid, Structural, morphological and thermal properties of nano filler produced from date palm-based micro fibers (Phoenix dactylifera L.), J. Polym. Environ. (2021) 1–9.

[71] A. Kriker, G. Debicki, A. Bali, M.M. Khenfer, M. Chabannet, Mechanical properties of date palm fibres and concrete reinforced with date palm fibres in hot-dry climate, Cem. Concr. Compos. 27 (2005) 554–564. https://doi.org/10.1016/j.cemconcomp.2004.09.015.

[72] A. Oushabi, S. Sair, Y. Abboud, O. Tanane, A. El Bouari, Natural thermal-insulation materials composed of renewable resources: Characterization of local date palm fibers (LDPF), J. Mater. Environ. Sci. 6 (2015) 3395–3402.

[73] M. Asim, M. Jawaid, A. Khan, A.M. Asiri, M.A. Malik, Effects of Date Palm fibres loading on mechanical, and thermal properties of Date Palm reinforced phenolic composites, J. Mater. Res. Technol. 9 (2020) 3614–3621.

[74] K. Riahi, B. Ben, A. Ben, A. Ben, M. Habib, Biosorption characteristics of phosphates from aqueous solution onto Phoenix dactylifera L . date palm fibers, 170 (2009) 511–519. https://doi.org/10.1016/j.jhazmat.2009.05.004.

[75] B. Agoudjil, A. Benchabane, A. Boudenne, L. Ibos, M. Fois, Renewable materials to reduce building heat loss: Characterization of date palm wood, Energy Build. 43 (2011) 491–497. https://doi.org/10.1016/j.enbuild.2010.10.014.

[76] S. Pilla, Engineering applications of bioplastics and biocomposites-An overview, Handb. Bioplastics Biocomposites Eng. Appl. (2011) 1–15.

[77] I. Taha, L. Steuernagel, G. Ziegmann, Optimization of the alkali treatment process of date palm fibres for polymeric composites, Compos. Interfaces 14 (2007) 669–684.

[78] I. Taha, L. Steuernagel, G. Ziegmann, Optimization of the alkali treatment process of date palm fibres for polymeric composites, Compos. Interfaces 14 (2007) 669–684. https://doi.org/10.1163/156855407782106528.

[79] M.E. Ali, A. Alabdulkarem, On thermal characteristics and microstructure of a new insulation material extracted from date palm trees surface fibers, Constr. Build. Mater. 138 (2017) 276–284. https://doi.org/10.1016/j.conbuildmat.2017.02.012.

[80] M. Midani, Date palm fibre composites: a novel and sustainable material for the aerospace industry, JEC Compos Mag 54 (2017) 45–47.

[81] R.J. De Dear, G.S. Brager, Thermal comfort in naturally ventilated buildings: revisions to ASHRAE Standard 55, Energy Build. 34 (2002) 549–561.

[82] A. Mukhtar, M.Z. Yusoff, K.C. Ng, The potential influence of building optimization and passive design strategies on natural ventilation systems in underground buildings: The state of the art, Tunn. Undergr. Sp. Technol. 92 (2019) 103065.

[83] W. Rattanongphisat, W. Rordprapat, Strategy for Energy Efficient Buildings in Tropical Climate, Energy Procedia 52 (2014) 10–17. https://doi.org/https://doi.org/10.1016/j.egypro.2014.07.049.

[84] N. Aste, A. Angelotti, M. Buzzetti, The influence of the external walls thermal inertia on the energy performance of well insulated buildings, Energy Build. 41 (2009) 1181–1187.

[85] K. Pasupathy, S. Ramakrishnan, J. Sanjayan, Enhancing the properties of foam concrete 3D printing using porous aggregates, Cem. Concr. Compos. 133 (2022) 104687.

[86] M.K. Nematchoua, J.C.V. Noelson, I. Saadi, H. Kenfack, A.-Z.F.R. Andrianaharinjaka, D.F. Ngoumdoum, J.B. Sela, S. Reiter, Application of phase change materials, thermal insulation, and external shading for thermal comfort improvement and cooling energy demand reduction in an office building under different coastal tropical climates, Sol. Energy 207 (2020) 458–470.

[87] L. Aditya, T.M.I. Mahlia, B. Rismanchi, H.M. Ng, M.H. Hasan, H.S.C. Metselaar, O. Muraza, H.B. Aditiya, A review on insulation materials for energy conservation in buildings, Renew. Sustain. Energy Rev. 73 (2017) 1352–1365.

[88] S.B. Sadineni, S. Madala, R.F. Boehm, Passive building energy savings: A review of building envelope components, Renew. Sustain. Energy Rev. 15 (2011) 3617–3631.

[89] A.P. Nelson, Université des Antilles « Etude de Matériaux Biosourcés pour l ' Isolation Thermique des Bâtiments en Climat Tropical Humide »., (2020) 1–156.

[90] F. Asdrubali, F. D'Alessandro, S. Schiavoni, A review of unconventional sustainable building insulation materials, Sustain. Mater. Technol. 4 (2015) 1–17. https://doi.org/10.1016/j.susmat.2015.05.002.

[91] H. Engels, H. Pirkl, R. Albers, R.W. Albach, J. Krause, A. Hoffmann, H. Casselmann, J. Dormish, Polyurethanes: Versatile materials and sustainable problem solvers for today's challenges, Angew. Chemie Int. Ed. 52 (2013) 9422–9441.

[92] M.S. Al-Homoud, Performance characteristics and practical applications of common building thermal insulation materials, Build. Environ. 40 (2005) 353–366.

[93] A.M. Omer, Energy use and environmental impacts: A general review, J. Renew.

Sustain. Energy 1 (2009).

[94] X. Zhou, F. Zheng, H. Li, C. Lu, An environment-friendly thermal insulation material from cotton stalk fibers, Energy Build. 42 (2010) 1070–1074.

[95] H. Omrany, A. Ghaffarianhoseini, A. Ghaffarianhoseini, K. Raahemifar, J. Tookey, Application of passive wall systems for improving the energy efficiency in buildings: A comprehensive review, Renew. Sustain. Energy Rev. 62 (2016) 1252–1269.

[96] L.-S. Wang, P. Ma, E. Hu, D. Giza-Sisson, G. Mueller, N. Guo, A study of building envelope and thermal mass requirements for achieving thermal autonomy in an office building, Energy Build. 78 (2014) 79–88.

[97] S. Schiavoni, F. Bianchi, F. Asdrubali, Insulation materials for the building sector: A review and comparative analysis, Renew. Sustain. Energy Rev. 62 (2016) 988–1011.

[98] S. Khedache, S. Makhlouf, D. Djefel, G. Lefebvre, L. Royon, Preparation and thermal characterization of composite “Paraffin/Red Brick” as a novel form-stable of phase change material for thermal energy storage, Int. J. Hydrogen Energy 40 (2015) 13771–13776.

[99] F. Amirifard, S.A. Sharif, F. Nasiri, Application of passive measures for energy conservation in buildings–a review, Adv. Build. Energy Res. 13 (2019) 282–315.

[100] G.Y. Yun, K. Steemers, N. Baker, Natural ventilation in practice: linking facade design, thermal performance, occupant perception and control, Build. Res. Inf. 36 (2008) 608–624.

[101] G. Evola, F. Gullo, L. Marletta, The role of shading devices to improve thermal and visual comfort in existing glazed buildings, Energy Procedia 134 (2017) 346–355.

[102] I. de l’Energie et de l’Environnement de la F. (IEPF), Efficacite energetique de la climatisation en region tropicale Tome1: Conception des nouveaux bâtiments, 2001.

[103] Haïti, G. (2010). État et perspectives de l’Environnement. PNUE/Ministère de l’environnement/Université Quisqueya) http://www. pnuma. org/deat1/pdf/GEO_Haiti2010% 28web, 29.

[104] F. Garde, T. Mara, A.P. Lauret, H. Boyer, R. Celaire, Bringing simulation to implementation: presentation of a global approach in the design of passive solar

buildings under humid tropical climates, Sol. Energy 71 (2001) 109–120.

[105] luciechever, RTAA 2016 Fiche d'application Ventilation naturelle de confort thermique, (2016) 1–14.

[106] T. Joffroy, A. Misse, R. Celaire, L. Rakotomalala, Architecture bioclimatique et efficacité énergétique des bâtiments au Sénégal, (2017).

[107] Townsville City Council, Guide 3 Shading Out the Heat, (2016). www.townsville.qld.gov.au.

[108] A.I. Omar, D. David, E. Vergnault, J. Virgone, A.I. Idriss, A new set of indicators to evaluate the bioclimatic performance of air conditioned buildings in a hot and humid climate, J. Build. Eng. 31 (2020) 101350. https://doi.org/https://doi.org/10.1016/j.jobe.2020.101350.

[109] A. Kumar, B.M. Suman, Experimental evaluation of insulation materials for walls and roofs and their impact on indoor thermal comfort under composite climate, Build. Environ. 59 (2013) 635–643. https://doi.org/https://doi.org/10.1016/j.buildenv.2012.09.023.

[110] K.F. Fong, C.K. Lee, Towards net zero energy design for low-rise residential buildings in subtropical Hong Kong, Appl. Energy 93 (2012) 686–694.

[111] M. Ibrahim, K. Nocentini, M. Stipetic, S. Dantz, F.G. Caiazzo, H. Sayegh, L. Bianco, Multi-field and multi-scale characterization of novel super insulating panels/systems based on silica aerogels: Thermal, hydric, mechanical, acoustic, and fire performance, Build. Environ. 151 (2019) 30–42.

[112] D.I. Kolaitis, E. Malliotakis, D.A. Kontogeorgos, I. Mandilaras, D.I. Katsourinis, M.A. Founti, Comparative assessment of internal and external thermal insulation systems for energy efficient retrofitting of residential buildings, Energy Build. 64 (2013) 123–131.

[113] B.P. Jelle, Traditional, state-of-the-art and future thermal building insulation materials and solutions–Properties, requirements and possibilities, Energy Build. 43 (2011) 2549–2563.

[114] V. Kočí, J. Maděra, R. Černý, Exterior thermal insulation systems for AAC building envelopes: Computational analysis aimed at increasing service life, Energy Build. 47

(2012) 84–90.

[115] C. Xu, S. Li, K. Zou, Study of heat and moisture transfer in internal and external wall insulation configurations, J. Build. Eng. 24 (2019) 100724.

[116] N. Mendes, F.C. Winkelmann, R. Lamberts, P.C. Philippi, Moisture effects on conduction loads, Energy Build. 35 (2003) 631–644.

[117] A. Boudenne, L. Ibos, E. Gehin, Y. Candau, A simultaneous characterization of thermal conductivity and diffusivity of polymer materials by a periodic method, J. Phys. D. Appl. Phys. 37 (2003) 132.

[118] T. Jami, S.R. Karade, L.P. Singh, A review of the properties of hemp concrete for green building applications, J. Clean. Prod. 239 (2019) 117852.

[119] O. Onuaguluchi, N. Banthia, Plant-based natural fibre reinforced cement composites: A review, Cem. Concr. Compos. 68 (2016) 96–108.

[120] K. Bilba, M.-A. Arsene, A. Ouensanga, Study of banana and coconut fibers: Botanical composition, thermal degradation and textural observations, Bioresour. Technol. 98 (2007) 58–68.

[121] Nikolopoulou, M. (2011). Outdoor thermal comfort. J. Frontiers in bioscience, 3(1), 1552-1568.

[122] J. Zhang, J. Lu, W. Deng, P. Beccarelli, I.Y.F. Lun, Thermal comfort investigation of rural houses in China: A review, Build. Environ. (2023) 110208.

[123] K. Karyono, B.M. Abdullah, A.J. Cotgrave, A. Bras, The adaptive thermal comfort review from the 1920s, the present, and the future, Dev. Built Environ. 4 (2020) 100032.

[124] L. Ba, I. El Abbassi, C.S.E. Kane, A.M. Darcherif, M. Ndongo, The challenges of local and bio-sourced materials on thermal performance: Review, classification and opportunity, Int. J. Eng. Res. Africa 47 (2020) 85–101. https://doi.org/10.4028/www.scientific.net/JERA.47.85.

[125] A. Tarafdar, V.K. Gaur, N. Rawat, P.R. Wankhade, G.K. Gaur, M.K. Awasthi, N.A. Sagar, R. Sirohi, Advances in biomaterial production from animal derived waste, Bioengineered 12 (2021) 8247–8258.

[126] S. Gautam, M. Verma, R. Chauhan, S. Aghara, N. Goyal, Reviewing thermal conductivity aspects of solar salt energy storage, Energy Adv. (2023).

[127] B. Almuallim, W.S.W. Harun, I.J. Al Rikabi, H.A. Mohammed, Thermally conductive polymer nanocomposites for filament-based additive manufacturing, J. Mater. Sci. 57 (2022) 3993–4019.

[128] Y. Wang, S. Zhang, D. Wang, Y. Liu, Experimental study on the influence of temperature and humidity on the thermal conductivity of building insulation materials, Energy Built Environ. 4 (2023) 386–398.

[129] M. Kňažková, F. Hrbáček, Interannual variability of soil thermal conductivity and moisture on the Abernethy Flats (James Ross Island) during thawing seasons 2015–2023, CATENA 234 (2024) 107640.

[130] A. Salazar, On thermal diffusivity, Eur. J. Phys. 24 (2003) 351–358. https://doi.org/10.1088/0143-0807/24/4/353.

[131] B. Abu-Jdayil, W. Hittini, A.H. Mourad, Development of date pit-polystyrene thermoplastic heat insulator material: Physical and thermal properties, Int. J. Polym. Sci. 2019 (2019). https://doi.org/10.1155/2019/1697627.

[132] A.S. Singha, R.K. Rana, Natural fiber reinforced polystyrene composites: Effect of fiber loading, fiber dimensions and surface modification on mechanical properties, Mater. Des. 41 (2012) 289–297. https://doi.org/10.1016/j.matdes.2012.05.001.

[133] M.F. Zafar, M.A. Siddiqui, Effect of filler loading and size on the mechanical and morphological behaviour of natural fibre-reinforced polystyrene composites, Adv. Mater. Process. Technol. 00 (2020) 1–13. https://doi.org/10.1080/2374068X.2020.1793261.

[134] M. Raza, H. Al Abdallah, M. Kozal, A. Al Khaldi, T. Ammar, B. Abu-Jdayil, Development and characterization of Polystyrene–Date palm surface fibers composites for sustainable heat insulation in construction, J. Build. Eng. 75 (2023) 106982. https://doi.org/https://doi.org/10.1016/j.jobe.2023.106982.

[135] N.I. Cherkashina, Z.V. Pavlenko, D.V. Pushkarskaya, L.V. Denisova, S.N. Domarev, D.A. Ryzhikh, Synthesis and Properties of Polystyrene Composite Material with Hazelnut Shells, Polymers (Basel). 15 (2023).

https://doi.org/10.3390/polym15153212.

[136] A. Mohammed, D.N. Rao, Investigation on mechanical properties of flax fiber/expanded polystyrene waste composites, Heliyon 9 (2023) e13310. https://doi.org/10.1016/j.heliyon.2023.e13310.

[137] A. Bicer, F. Kar, Thermal and mechanical properties of gypsum plaster mixed with expanded polystyrene and tragacanth, Therm. Sci. Eng. Prog. 1 (2017) 59–65. https://doi.org/10.1016/j.tsep.2017.02.008.

[138] G.R. Mohamed, R.K. Mahmoud, I.S. Fahim, M. Shaban, H.M. Abd El-Salam, H.M. Mahmoud, Bio-composite Thermal Insulation Materials Based on Banana Leaves Fibers and Polystyrene: Physical and Thermal Performance, J. Nat. Fibers 00 (2021) 1–16. https://doi.org/10.1080/15440478.2020.1870628.

[139] A. Désiré Omgba Betené, F. Martoïa, P.J.J. Dumont, F. Ebanda Betené, A. Ateba, Gypsum plaster composites reinforced with tropical fibre bundles extracted from Rhecktophyllum camerunense and Ananas comosus plants: Microstructure and mechanical performance, Constr. Build. Mater. 392 (2023). https://doi.org/10.1016/j.conbuildmat.2023.131815.

[140] I. Amara, A. Mazioud, I. Boulaoued, A. Mhimid, Experimental study on thermal properties of bio-composite (gypsum plaster reinforced with palm tree fibers) for building insulation, Int. J. Heat Technol. 35 (2017) 576–584. https://doi.org/10.18280/ijht.350314.

[141] A. Djoudi, M.M. Khenfer, Bali, Effect of the addition of date palm fibers on thermal properties of plaster concrete: Experimental study and modeling, J. Adhes. Sci. Technol. 28 (2014) 2100–2111. https://doi.org/10.1080/01694243.2014.948363.

[142] W. Gallala, H.M.M. Khater, M. Souilah, K. Nouri, M. Ben Regaya, M.E. Gaied, Production of low-cost biocomposite made of palm fibers waste and gypsum plaster, Rev. Int. Contam. Ambient. 36 (2020) 475–483. https://doi.org/10.20937/RICA.53541.

[143] M. Ouakarrouch, K. El Azhary, N. Laaroussi, M. Garoum, F. Kifani-Sahban, Thermal performances and environmental analysis of a new composite building material based on gypsum plaster and chicken feathers waste, Therm. Sci. Eng. Prog. 19 (2020) 100642. https://doi.org/10.1016/j.tsep.2020.100642.

[144] A. Braiek, M. Karkri, A. Adili, L. Ibos, S. Ben Nasrallah, Estimation of the thermophysical properties of date palm fibers/gypsum composite for use as insulating materials in building, Energy Build. 140 (2017) 268–279. https://doi.org/10.1016/j.enbuild.2017.02.001.

[145] T. Mutuk, K. Arpacioğlu, S. Alişir, G. Demir, Thermal and mechanical evaluation of natural fibers reinforced gypsum plaster composite, J. Met. Mater. Miner. 33 (2023) 116–123. https://doi.org/10.55713/jmmm.v33i1.1669.

[146] N. Abir, A.B. Siddique, H.A. Begum, M.A. Gafur, A.N. Khan, M.A. Mahmud, Effect of fibre loading on mechanical properties of jute fibre bundle reinforced gypsum composites, Heliyon 9 (2023) e18147. https://doi.org/10.1016/j.heliyon.2023.e18147.

[147] M. Chikhi, B. Agoudjil, A. Boudenne, A. Gherabli, Experimental investigation of new biocomposite with low cost for thermal insulation, Energy Build. 66 (2013) 267–273. https://doi.org/10.1016/j.enbuild.2013.07.019.

[148] M. Charai, M.O. Mghazli, S. Channouf, A. El hammouti, P. Jagadesh, L. Moga, A. Mezrhab, Lightweight waste-based gypsum composites for building temperature and moisture control using coal fly ash and plant fibers, Constr. Build. Mater. 393 (2023) 132092. https://doi.org/https://doi.org/10.1016/j.conbuildmat.2023.132092.

[149] K. Kharrati, M. Salhi, J. Sliman, R. Abdeljabar, Thermomechanical and Physical Properties of Plaster Concrete Reinforced with Natural Fibers, Mech. Adv. Compos. Struct. 10 (2023) 295–308. https://doi.org/10.22075/macs.2023.28849.1447.

[150] A. Alabdulkarem, M. Ali, G. Iannace, S. Sadek, R. Almuzaiqer, Thermal analysis, microstructure and acoustic characteristics of some hybrid natural insulating materials, Constr. Build. Mater. 187 (2018) 185–196. https://doi.org/10.1016/j.conbuildmat.2018.07.213.

[151] S. Amroune, A. Bezazi, A. Dufresne, F. Scarpa, A. Imad, Investigation of the Date Palm Fiber for Green Composites Reinforcement: Thermo-physical and Mechanical Properties of the Fiber, J. Nat. Fibers 18 (2021) 717–734. https://doi.org/10.1080/15440478.2019.1645791.

[152] A. Bezazi, S. Amroune, F. Scarpa, A. Dufresne, A. Imad, Investigation of the date palm fiber for green composites reinforcement: Quasi-static and fatigue characterization of the fiber, Ind. Crops Prod. 146 (2020) 112135.

https://doi.org/10.1016/j.indcrop.2020.112135.

[153] F.Z. Semlali Aouragh Hassani, K. El Bourakadi, N. Merghoub, A. el kacem Qaiss, R. Bouhfid, Effect of chitosan/modified montmorillonite coating on the antibacterial and mechanical properties of date palm fiber trays, Int. J. Biol. Macromol. 148 (2020) 316–323. https://doi.org/10.1016/j.ijbiomac.2020.01.092.

[154] H. Khakpour, M.R. Ayatollahi, A. Akhavan-Safar, L.F.M. da Silva, Mechanical properties of structural adhesives enhanced with natural date palm tree fibers: Effects of length, density and fiber type, Compos. Struct. 237 (2020) 111950. https://doi.org/10.1016/j.compstruct.2020.111950.

[155] Y. Bellatrache, L. Ziyani, A. Dony, M. Taki, S. Haddadi, Effects of the addition of date palm fibers on the physical, rheological and thermal properties of bitumen, Constr. Build. Mater. 239 (2020) 117808. https://doi.org/10.1016/j.conbuildmat.2019.117808.

[156] K. Almi, A. Benchabane, S. Lakel, A. Kriker, Potential utilization of date palm wood as composite reinforcement, J. Reinf. Plast. Compos. 34 (2015) 1231–1240. https://doi.org/10.1177/0731684415588356.

[157] H. Boussehel, D.E. Mazouzi, N. Belghar, B. Guerira, M. Lachi, Effect of chemicals treatments on the morphological, mechanical, thermal and water uptake properties of polyvinyl chloride/ palm fibers composites, Rev. Des Compos. Des Mater. Av. 29 (2019) 1–8. https://doi.org/10.18280/rcma.290101.

[158] A. Abdal-Hay, N.P.G. Suardana, D.Y. Jung, K.S. Choi, J.K. Lim, Effect of diameters and alkali treatment on the tensile properties of date palm fiber reinforced epoxy composites, Int. J. Precis. Eng. Manuf. 13 (2012) 1199–1206. https://doi.org/10.1007/s12541-012-0159-3.

[159] M. Lahouioui, R. Ben Arfi, M. Fois, L. Ibos, A. Ghorbal, Investigation of Fiber Surface Treatment Effect on Thermal, Mechanical and Acoustical Properties of Date Palm Fiber-Reinforced Cementitious Composites, Waste and Biomass Valorization 11 (2020) 4441–4455. https://doi.org/10.1007/s12649-019-00745-3.

[160] F.M. AL-Oqla, M.T. Hayajneh, M.M. Al-Shrida, Mechanical performance, thermal stability and morphological analysis of date palm fiber reinforced polypropylene composites toward functional bio-products, Cellulose 29 (2022) 3293–3309.

https://doi.org/10.1007/s10570-022-04498-6.

[161] M. Ali, Epoxy–Date Palm Fiber Composites: Study on Manufacturing and Properties, Int. J. Polym. Sci. 2023 (2023) 5670293. https://doi.org/10.1155/2023/5670293.

[162] Fiche technique sunchem.pdf, user manual SARL POLYMOST sétif. Algeria.

[163] S. Bouzit, F. Merli, M. Sonebi, C. Buratti, M. Taha, Gypsum-plasters mixed with polystyrene balls for building insulation: Experimental characterization and energy performance, Constr. Build. Mater. 283 (2021) 122625. https://doi.org/10.1016/j.conbuildmat.2021.122625.

[164] K. Almi, S. Lakel, A. Benchabane, A. Kriker, Characterization of date palm wood used as composites reinforcement, Acta Phys. Pol. A 127 (2015) 1072–1074. https://doi.org/10.12693/APhysPolA.127.1072.

[165] H. Boussehel, A. Meghezzi, N. Nebbache, S. Maou, M. Slimani, A. Loucif, The effect of alkali treatment on the mechanical and water absorption characteristics of olive stone flour reinforced polystyrene composites, Res. J. Pharm. Biol. Chem. Sci. 7 (2016) 26–33.

[166] S.N.A. Safri, M.T.H. Sultan, N. Saba, M. Jawaid, Effect of benzoyl treatment on flexural and compressive properties of sugar palm/glass fibres/epoxy hybrid composites, Polym. Test. 71 (2018) 362–369. https://doi.org/10.1016/j.polymertesting.2018.09.017.

[167] S.M. Izwan, S.M. Sapuan, M.Y.M. Zuhri, A.R. Mohamed, Effects of Benzoyl Treatment on NaOH Treated Sugar Palm Fiber: Tensile, Thermal, and Morphological Properties, J. Mater. Res. Technol. 9 (2020) 5805–5814. https://doi.org/10.1016/j.jmrt.2020.03.105.

[168] S.T. Method, Standard Test Method for Tensile Properties of Polymer Matrix Composite Materials 1, 15 (2002).

[169] ASTM INTERNATIONAL, Standard Test Methods for Flexural Properties of Unreinforced and Reinforced Plastics and Electrical Insulating Materials. D790, Annu. B. ASTM Stand. (2002) 1–12.

[170] A.A. Akl, A.S. Hassanien, Comparative microstructural studies using different methods: Effect of Cd-addition on crystallography, microstructural properties, and

crystal imperfections of annealed nano-structural thin CdxZn1-xSe films, Phys. B Condens. Matter 620 (2021) 413267. https://doi.org/10.1016/j.physb.2021.413267.

[171] T. Djoudi, M. Hecini, D. Scida, Y. Djebloun, H. Djemai, Physico-Mechanical Characterization of Composite Materials Based on Date Palm Tree Fibers, J. Nat. Fibers 18 (2021) 789–802. https://doi.org/10.1080/15440478.2019.1658251.

[172] P. Guise, C. Grattoni, Q.J. Fisher, A. Schiffer, Stress Sensitivity of Mercury, Int. Symp. Ofthe Soc. Core Anal. Held Vienna, Austria, 27-30 August 2017 (2017) 1–12.

[173] G. RonglinZhang, P. Liu, L. Ma, Z. Yang, H. Chen, H.X. Zhu, H. Xiao, J. Li, Research on the Corrosion/Permeability/Frost Resistance of Concrete by Experimental and Microscopic Mechanisms Under Different Water–Binder Ratios, Int. J. Concr. Struct. Mater. 14 (2020). https://doi.org/10.1186/s40069-019-0382-8.

[174] S.M. Hassan, Use of Mercury Intrusion Porosimetry (MIP) Technique to Measure the Porosity of Anodes in Solid Oxide Fuel Cell (SOFC), Chem. Mater. Res. 7 (2015) 14–20.

[175] H. Aouat, D. Hammiche, A. Boukerrou, H. Djidjelli, Y. Grohens, I. Pillin, Materials Today : Proceedings Effects of interface modification on composites based on olive husk flour, Mater. Today Proc. 36 (2021) 94–100. https://doi.org/10.1016/j.matpr.2020.05.459.

[176] R. Bodîrlău, C.A. Teacă, Fourier transform infrared spectroscopy and thermal analysis of lignocellulose fillers treated with organic anhydrides, Rom. Reports Phys. 54 (2009) 93–104.

[177] L.Y. Mwaikambo, M.P. Ansell, Chemical modification of hemp, sisal, jute, and kapok fibers by alkalization, J. Appl. Polym. Sci. 84 (2002) 2222–2234. https://doi.org/10.1002/app.10460.

[178] A. Hachaichi, B. Kouini, L.K. Kian, M. Asim, M. Jawaid, Extraction and Characterization of Microcrystalline Cellulose from Date Palm Fibers using Successive Chemical Treatments, J. Polym. Environ. 29 (2021) 1990–1999. https://doi.org/10.1007/s10924-020-02012-2.

[179] Kethiri, M. A., Chikhi, M., Tedeschi, C., & Belghar, N. (2022). The Characterization of the Date Palm Tree Leaflet for Using That as Green Materials for Building House.

Materials Circular Economy, 4(1), 16.

[180] A. Alawar, A.M. Hamed, K. Al-Kaabi, Date palm tree fiber as polymeric matrix reinforcement, DPF-polypropylene composite characterization, Adv. Mater. Res. 47-50 PART (2008) 193–196. https://doi.org/10.4028/www.scientific.net/amr.47-50.193.

[181] F. Delzendehrooy, M.R. Ayatollahi, A. Akhavan-Safar, L.F.M. da Silva, Strength improvement of adhesively bonded single lap joints with date palm fibers: Effect of type, size, treatment method and density of fibers, Compos. Part B Eng. 188 (2020) 107874. https://doi.org/10.1016/j.compositesb.2020.107874.

[182] P.K. Jena, J.R. Mohanty, S. Nayak, Effect of Surface Modification of Vetiver Fibers on Their Physical and Thermal Properties, J. Nat. Fibers 00 (2020) 1–12. https://doi.org/10.1080/15440478.2020.1726249.

[183] N. Kumar, A. Singh, K. Debnath, Influence of surface modification on the performance of borassus fruit fiber composites, Emerg. Mater. Res. 9 (2020) 686–694. https://doi.org/10.1680/jemmr.19.00067.

[184] P.A. Sreekumar, S.P. Thomas, J. marc Saiter, K. Joseph, G. Unnikrishnan, S. Thomas, Effect of fiber surface modification on the mechanical and water absorption characteristics of sisal/polyester composites fabricated by resin transfer molding, Compos. Part A Appl. Sci. Manuf. 40 (2009) 1777–1784. https://doi.org/10.1016/j.compositesa.2009.08.013.

[185] A.G. Adeniyi, S.A. Abdulkareem, J.O. Ighalo, D.V. Onifade, S.A. Adeoye, A.E. Sampson, Morphological and thermal properties of polystyrene composite reinforced with biochar from elephant grass (Pennisetum purpureum), (2020). https://doi.org/10.1177/0892705720939169.

[186] S.M.B.N. Ã, G.S. Cerveira, S.M.L. Rosa, ARTICLE IN PRESS POLYMER New polymeric-coupling agent for polypropylene / wood-flour composites, 26 (2007) 619–628. https://doi.org/10.1016/j.polymertesting.2007.03.007.

[187] H. Demir, U. Atikler, D. Balko, The effect of fiber surface treatments on the tensile and water sorption properties of polypropylene – luffa fiber composites, 37 (2006) 447–456. https://doi.org/10.1016/j.compositesa.2005.05.036.

[188] Hammiche, D., Boukerrou, A., Djidjelli, H., Kervoëlen, A., & Grohens, Y. (2015). Etude des Propriétés Physico-chimiques, Thermiques et Mécaniques des Fibres d'Alfa Grasses. Revue des Composites et des Matériaux avancés. J. compost. Adv. Mat, 25, 7-24.

[189] D. Bachtiar, S.M. Sapuan, A. Khalina, E.S. Zainudin, K.Z.M. Dahlan, The flexural, impact and thermal properties of untreated short sugar palm fibre reinforced high impact polystyrene (HIPS) composites, Polym. Polym. Compos. 20 (2012) 493–502. https://doi.org/10.1177/096739111202000510.

[190] T. Krishnan, S. Jayabal, V.N. Krishna, Tensile, flexural, impact, and hardness properties of alkaline-treated Sunnhemp fiber reinforced polyester composites, J. Nat. Fibers 00 (2018) 1–11. https://doi.org/10.1080/15440478.2018.1492488.

[191] M. Chikhi, Young's modulus and thermophysical performances of bio-sourced materials based on date palm fibers, Energy Build. 129 (2016) 589–597. https://doi.org/10.1016/j.enbuild.2016.08.034.

[192] I.S.M.A. Tawakkal, M.J. Cran, S.W. Bigger, Effect of kenaf fibre loading and thymol concentration on the mechanical and thermal properties of PLA/kenaf/thymol composites, Ind. Crops Prod. 61 (2014) 74–83. https://doi.org/10.1016/j.indcrop.2014.06.032.

[193] R. Siakeng, M. Jawaid, H. Ariffin, M.S. Salit, Effects of Surface Treatments on Tensile, Thermal and Fibre-matrix Bond Strength of Coir and Pineapple Leaf Fibres with Poly Lactic Acid, J. Bionic Eng. 15 (2018) 1035–1046. https://doi.org/10.1007/s42235-018-0091-z.

[194] M. Das, D. Chakraborty, Evaluation of Improvement of Physical and Mechanical Properties of Bamboo Fibers Due to Alkali Treatment, (2007). https://doi.org/10.1002/app.

[195] K.C. Manikandan Nair, S.M. Diwan, S. Thomas, Tensile properties of short sisal fiber reinforced polystyrene composites, J. Appl. Polym. Sci. 60 (1996) 1483–1497. https://doi.org/10.1002/(sici)1097-4628(19960531)60:9<1483::aid-app23>3.0.co;2-1.

[196] K. Panyasart, N. Chaiyut, T. Amornsakchai, O. Santawitee, Effect of surface treatment on the properties of pineapple leaf fibers reinforced polyamide 6

composites, Energy Procedia 56 (2014) 406–413. https://doi.org/10.1016/j.egypro.2014.07.173.

[197] H.N. Dhakal, Z.Y. Zhang, M.O.W. Richardson, Effect of water absorption on the mechanical properties of hemp fibre reinforced unsaturated polyester composites, Compos. Sci. Technol. 67 (2007) 1674–1683. https://doi.org/10.1016/j.compscitech.2006.06.019.

[198] M. Rokbi, H. Osmani, A. Imad, N. Benseddiq, Effect of chemical treatment on flexure properties of natural fiber-reinforced polyester composite, Procedia Eng. 10 (2011) 2092–2097. https://doi.org/10.1016/j.proeng.2011.04.346.

[199] G.A. rzo RAO, Mechanical and thermal properties of date palm/kenaf fiber-reinforced epoxy hybrid composites, Polym. Compos. 42 (2021) 2217–2224. https://doi.org/10.1002/pc.25971.

[200] N. Kotelnikova-weiler, J. Caron, N. Kotelnikova-weiler, J.C. Etude, Etude expérimentale et phénoménologique de la rupture différée de composites pultrudés UD sous chargements permanents To cite this version : HAL Id : hal-00597512, (2011).

[201] B. Abu-Jdayil, M.S. Barkhad, A.H.I. Mourad, M.Z. Iqbal, Date palm wood waste-based composites for green thermal insulation boards, J. Build. Eng. 43 (2021) 103224. https://doi.org/10.1016/j.jobe.2021.103224.

[202] G. Wu, Y. Wang, K. Wang, A. Feng, The effect of modified AlN on the thermal conductivity, mechanical and thermal properties of AlN/polystyrene composites, RSC Adv. 6 (2016) 102542–102548. https://doi.org/10.1039/c6ra22794e.

[203] A. Al-Khanbashi, K. Al-Kaabi, A. Hammami, Date palm fibers as polymeric matrix reinforcement: Fiber characterization, Polym. Compos. 26 (2005) 486–497. https://doi.org/10.1002/pc.20118.

[204] Midani, M., Saba, N., & Alothman, O. Y. (2020). Date palm fiber composites. composites science and technology). Singapore: Springer Singapore.

[205] L.A. Elseify, M. Midani, L.A. Shihata, H. El-Mously, Review on cellulosic fibers extracted from date palms (Phoenix Dactylifera L.) and their applications, Cellulose 26 (2019) 2209–2232. https://doi.org/10.1007/s10570-019-02259-6.

[206] Y. Liao, J. Fan, R. Li, B. Da, D. Chen, Y. Zhang, Influence of the usage of waste oyster shell powder on mechanical properties and durability of mortar, Adv. Powder Technol. 33 (2022). https://doi.org/10.1016/j.apt.2022.103503.

[207] P. B a, B. P Shetty, S. B, S.P. Singh Yadav, A. L, Physical and mechanical properties, morphological behaviour of pineapple leaf fibre reinforced polyester resin composites, Adv. Mater. Process. Technol. 00 (2020) 1–13. https://doi.org/10.1080/2374068X.2020.1853498.

[208] B. Haba, B. Agoudjil, A. Boudenne, K. Benzarti, Hygric properties and thermal conductivity of a new insulation material for building based on date palm concrete, Constr. Build. Mater. 154 (2017) 963–971. https://doi.org/10.1016/j.conbuildmat.2017.08.025.

[209] H. Al, B. Abu-jdayil, M.Z. Iqbal, Improvement of mechanical properties and water resistance of bio-based thermal insulation material via silane treatment, J. Clean. Prod. 346 (2022) 131242. https://doi.org/10.1016/j.jclepro.2022.131242.

[210] Agoudjil, B., Benchabane, A., Boudenne, A., Ibos, L., & Fois, M. (2011). Caractérisation thermophysique du bois de palmier dattier en vue de son utilisation en isolation thermique dans l'habitat. In Congrès Français de Thermique (pp. 171-176).

[211] J.O. Ighalo, A.G. Adeniyi, O.O. Owolabi, S.A. Abdulkareem, Moisture absorption, thermal and microstructural properties of polymer composites developed from rice husk and polystyrene wastes, Int. J. Sustain. Eng. 14 (2021) 1049–1058. https://doi.org/10.1080/19397038.2021.1892234.

[212] M. Haddadi, B. Agoudjil, N. Benmansour, A. Boudenne, B. Garnier, Experimental and Modeling Study of Effective Thermal Conductivity of Polymer Filled With Date Palm Fibers, (2015) 1–8. https://doi.org/10.1002/pc.

[213] M. Boumhaout, L. Boukhattem, H. Hamdi, B. Benhamou, F. Ait Nouh, Thermomechanical characterization of a bio-composite building material: Mortar reinforced with date palm fibers mesh, Constr. Build. Mater. 135 (2017) 241–250. https://doi.org/10.1016/j.conbuildmat.2016.12.217.

[214] L. Bai, X. Zhao, R. Bao, Z. Liu, M. Yang, W. Yang, Effect of temperature , crystallinity and molecular chain orientation on the thermal conductivity of polymers :

a case study of PLLA, J. Mater. Sci. 53 (2018) 10543–10553. https://doi.org/10.1007/s10853-018-2306-4.

[215] K. Al-malah, B. Abu-jdayil, Clay-based heat insulator composites : Thermal and water retention properties, 37 (2007) 90–96. https://doi.org/10.1016/j.clay.2007.01.001.

[216] H.A. Moghadam, A. Mirzaei, Comparing the effects of a retarder and accelerator on properties of gypsum building plaster, J. Build. Eng. (2019) 101075. https://doi.org/10.1016/j.jobe.2019.101075.

[217] P. Gunavathi, D. Janaki, P. Balasubramaniam, A. Alagesan, S. Geethanjali, Characterization and identification of elemental sulphur , iron pyrite , mineral gypsum , Phospho gypsum and marine gypsum by using ATR-FTIR, 10 (2021) 80–86.

[218] F.S.A. Hassani, W. Ouarhim, M. El Achaby, Y. Tamraoui, M. Bensalah, D. Rodrigue, R. Bouhfid, Recycled tires shreds based polyurethane binder: Production and characterization, Mech. Mater. (2020) 103351. https://doi.org/10.1016/j.mechmat.2020.103351.

[219] L. Tian, Q. Chen, W. Jiang, L. Wang, H. Xie, N. Kalogerakis, Y. Ma, R. Ji, A carbon-14 radiotracer-based study on the phototransformation of polystyrene nanoplastics in water: Versus in air, Environ. Sci. Nano 6 (2019) 2907–2917. https://doi.org/10.1039/c9en00662a.

[220] A.K. Chaudhary, R.P. Vijayakumar, Studies on biological degradation of polystyrene by pure fungal cultures, Environ. Dev. Sustain. 22 (2020) 4495–4508. https://doi.org/10.1007/s10668-019-00394-5.

[221] A. El, M. Charai, S. Channouf, Application analysis and environmental impact of straw reinforced gypsum plaster for improving the energy efficiency in buildings in the six climate zones of Morocco, J. Build. Eng. 74 (2023) 106829. https://doi.org/10.1016/j.jobe.2023.106829.

[222] R.A. Ilyas, S.M. Sapuan, R. Ibrahim, H. Abral, M.R. Ishak, E.S. Zainudin, M.S.N. Atikah, N. Mohd Nurazzi, A. Atiqah, M.N.M. Ansari, E. Syafri, M. Asrofi, N.H. Sari, R. Jumaidin, Effect of sugar palm nanofibrillated cellulose concentrations on morphological, mechanical and physical properties of biodegradable films based on agro-waste sugar palm (Arenga pinnata (Wurmb.) Merr) starch, J. Mater. Res.

Technol. 8 (2019) 4819–4830. https://doi.org/10.1016/j.jmrt.2019.08.028.

[223] T. Lu, S. Liu, M. Jiang, X. Xu, Y. Wang, Z. Wang, J. Gou, D. Hui, Z. Zhou, Effects of modifications of bamboo cellulose fibers on the improved mechanical properties of cellulose reinforced poly(lactic acid) composites, Compos. Part B Eng. 62 (2014) 191–197. https://doi.org/10.1016/j.compositesb.2014.02.030.

[224] A.M. Al-sabagh, Y.M. Moustafa, A. Hamdy, H.M. Killa, R.T.M. Ghanem, R.E. Morsi, Preparation and characterization of sulfonated polystyrene / magnetite nanocomposites for organic dye adsorption, 27 (2018) 403–413.

[225] Huang, G., Xu, J., Geng, P., & Li, J. (2020). Carrier flotation of low-rank coal with polystyrene. Minerals, 10(5), 452.

[226] F.Z. Semlali Aouragh Hassani, W. Ouarhim, M.O. Bensalah, H. Essabir, D. Rodrigue, R. Bouhfid, A. el K. Qaiss, Mechanical properties prediction of polypropylene/short coir fibers composites using a self-consistent approach, Polym. Compos. 40 (2019) 1919–1929. https://doi.org/10.1002/pc.24967.

[227] L.D. Hung Anh, Z. Pásztory, An overview of factors influencing thermal conductivity of building insulation materials, J. Build. Eng. 44 (2021). https://doi.org/10.1016/j.jobe.2021.102604.

[228] Ayşe, The Thermal Analysis of Plaster with Waste Expanded Polystyrene Gypsum and Resin, Int. J. Innov. Eng. Appl. 7 (2023). https://doi.org/10.46460/ijiea.1212678.

[229] M. Boumaaza, A. Belaadi, M. Bourchak, The Effect of Alkaline Treatment on Mechanical Performance of Natural Fibers-reinforced Plaster: Optimization Using RSM, J. Nat. Fibers 18 (2021) 2220–2240. https://doi.org/10.1080/15440478.2020.1724236.

[230] S. Hamza, H. Saad, B. Charrier, N. Ayed, F. Charrier-El Bouhtoury, Physico-chemical characterization of Tunisian plant fibers and its utilization as reinforcement for plaster based composites, Ind. Crops Prod. 49 (2013) 357–365. https://doi.org/10.1016/j.indcrop.2013.04.052.

[231] S. Balti, A. Boudenne, N. Hamdi, Characterization and optimization of eco-friendly gypsum materials using response surface methodology, J. Build. Eng. 69 (2023) 106219. https://doi.org/10.1016/j.jobe.2023.106219.

[232] M. Chikhi, B. Agoudjil, M. Haddadi, A. Boudenne, Numerical modelling of the effective thermal conductivity of heterogeneous materials, J. Thermoplast. Compos. Mater. 26 (2013) 336–345. https://doi.org/10.1177/0892705711424921.

[233] Á. Lakatos, F. Kalmár, Investigation of thickness and density dependence of thermal conductivity of expanded polystyrene insulation materials, Mater. Struct. Constr. 46 (2013) 1101–1105. https://doi.org/10.1617/s11527-012-9956-5.

[234] B. Ismail, N. Belayachi, D. Hoxha, Optimizing performance of insulation materials based on wheat straw, lime and gypsum plaster composites using natural additives, Constr. Build. Mater. 254 (2020) 118959. https://doi.org/10.1016/j.conbuildmat.2020.118959.

[235] Y. Chihab, N. Laaroussi, M. Garoum, Thermal performance and energy efficiency of the composite clay and hemp fibers, J. Build. Eng. 73 (2023). https://doi.org/10.1016/j.jobe.2023.106810.

[236] M. Charai, A. Mezrhab, L. Moga, M. Karkri, Hygrothermal, mechanical and durability assessment of vegetable concrete mixes made with Alfa fibers for structural and thermal insulating applications, Constr. Build. Mater. 335 (2022). https://doi.org/10.1016/j.conbuildmat.2022.127518.

[237] F.M. Al-Oqla, S.M. Sapuan, Natural fiber reinforced polymer composites in industrial applications: Feasibility of date palm fibers for sustainable automotive industry, J. Clean. Prod. 66 (2014) 347–354. https://doi.org/10.1016/j.jclepro.2013.10.050.

APPENDICES

APPENDICES

Published Papers

1. A published research paper entitled: "Experimental Evaluation of New Environmentally Friendly Insulating Materials Based on Date Palm Fibers and Polystyrene" (2023) in Building Engineering Journal (class A)

Journal of Building Engineering 65 (2023) 105751

Contents lists available at ScienceDirect

Journal of Building Engineering

journal homepage: www.elsevier.com/locate/jobe

An experimental evaluation of a new eco-friendly insulating material based on date palm fibers and polystyrene

Houssam Eddine Benchouia [a,*], Belhi Guerira [a], Mourad Chikhi [b], Hamida Boussehel [a], Cristina Tedeschi [c]

[a] Laboratoire de Génie Mécanique (LGM), Université de Biskra, BP 145, Biskra, 07000, Algeria
[b] Unité de Développement des Equipements Solaires, UDES/Centre de Développement des Energies Renouvelables, CDER, Bou Ismail, 42415, W. Tipasa, Algeria
[c] Laboratoire de diagnostic et d'investigation sur les matériaux du patrimoine bâti, Politecnico di Milano, Milan, Italy

ARTICLE INFO

Keywords:
Insulating materials
Date palm fibers
Polystyrene
Composites
Alkalisation
Benzoylation
Mechanical properties
Thermal conductivity

ABSTRACT

The purpose of this study is to minimize the environmental impact and to reduce the cost of petroleum-derived polystyrene by the use of date palm leaves remnants in the production of polystyrene/date palm fiber composite materials (PS-DPF). Moreover, this new material must have mechanical properties and thermal insulation comparable or superior to those of virgin polystyrene (VPS) or other insulating materials. Three types of fibers are used to make samples with fillers of 10%, 20%, and 30% (by weight), namely untreated fiber (UDPF), fiber treated by alkalinisation (ADPF), and fiber treated by benzoylation (BDPF). The melt-mixing method and hot compression molding were used for the production of the composites. Various morphological, mechanical, and thermophysical tests were carried out on the produced composites. From scanning electron microscopy (SEM) micrographs, it was determined that the dispersion of filler and its interfacial in-

2. A published research paper entitled: "An experimental evaluation of a hybrid bio-composite based on date palm petiole fibers, expanded polystyrene waste, and gypsum plaster as a sustainable insulating building material" (2024) in Construction and Building Materials Journal (class A+).

Construction and Building Materials 422 (2024) 135735

Contents lists available at ScienceDirect

Construction and Building Materials

journal homepage: www.elsevier.com/locate/conbuildmat

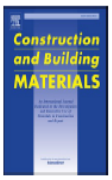

An experimental evaluation of a hybrid bio-composite based on date palm petiole fibers, expanded polystyrene waste, and gypsum plaster as a sustainable insulating building material

Houssam Eddine Benchouia [a,*], Hamida Boussehel [a], Belhi Guerira [a], Lakhdar Sedira [a], Cristina Tedeschi [b], Hossam Eddine Becha [a], Marco Cucchi [c]

[a] Laboratory of Mechanical Engineering (LGM), University Mohamed Khider of Biskra, B.P. 145, Biskra RP 07000, Algeria
[b] Diagnostic and Investigation laboratory on Building Materials, Dept. of Civil and Environmental Engineering, Politecnico di Milano, Milan, Italy
[c] Materials testing laboratory (LPM), Politecnico di Milano, Milan, Italy

ARTICLE INFO

Keywords:
Hybrid biocomposites
Gypsum plaster
Date palm petiole fibers
Expanded polystyrene waste
Thermal insulator
Mechanical properties
Thermophysical properties

ABSTRACT

Gypsum plaster is essential in construction as a thermal insulator and decorative material. This study aims to protect the environment by valorizing two commonly found wastes in Algeria, namely date palm petiole fibers (DPP) and expanded polystyrene waste (EPS), to produce a gypsum plaster hybrid biocomposite material comparable to, or better than, neat gypsum plaster (NGP). Hand-made samples with different DPP mass loadings (0; 5; 10; and 15%), EPS mass ratios (0.3%), or both were used. Different morphological, mechanical, and thermophysical tests were performed on the produced hybrid composites. FTIR shows the characteristic peaks for gypsum, polystyrene, and fibers. XRD shows that NGP, EPS, and DPP are 71.58, 29.91, and 52.93% crystallinity, respectively. Compression strengths, flexural strengths, and young modulus show that EPS, DPP, or both significantly reduce all mechanical properties of prepared samples. The biocomposites produced had lower thermal conductivity (λ) (0.265–0.414 W/(m.K) at 24∘C) and bulk density (ρ) (852–925 kg/m^3) than reference NGP samples witch have 0.425 W/(m.K) in thermal conductivity and 977 kg/m^3 in therm of bulk density. Based on a comparative study, gypsum plaster reinforced with DPP, EPS, or both exhibits potential as a viable alternative to insulation materials, thereby offering a sustainable solution for construction purposes.